International PhD Programme in Cardiovascular Pathophysiology and Therapeutics - 36° cycle

Current challenges in management of cardiac arrhythmias.

PhD thesis

Davide Fabbricatore, MD

2020-2023

Current challenges in management of cardiac arrhythmias

Ph.D. Thesis

Davide Fabbricatore, MD

18/9/1989, Nocera Inferiore (Italy)

Promotor: Prof. G. Iaccarino

Department of Advanced Biomedical Science

Federico II, University of Naples, Italy

Co-promotor: Dr. T. De Potter

Cardiovascular Centre Aalst, OLV Clinic, Aalst, Belgium

Naples, 6/2024

UNIVERSITY FEDERICO II OF NAPLES

FACULTY OF MEDICINE

VIA PANSINI N. 5, 80131 NAPLES, ITALY

Index:

CHAPTER 1

Chapter 1 of the thesis focuses on managing atrial fibrillation (AF), a common heart rhythm disorder. In this chapter, the author delves into their transformative journey at the Cardiovascular Research Centre of Aalst in Belgium, guided by the esteemed Professor Tom De Potter. Immersed in the realm of electrophysiology, their focus gravitated towards pioneering innovations and emerging technologies in the realm of atrial fibrillation. This period, integral to their PhD program, proved to be truly life-changing. Within this innovative environment, characterized by a prolific volume of procedures and research endeavours, the author's understanding of electrophysiology blossomed progressively. They found themselves invigorated by the exposure to cutting-edge practices, fostering a sense of self-assurance that would resonate throughout their career trajectory.

The chapter begins with an overview of AF and its treatment, with a special emphasis on strategies for controlling heart rhythm, improving the efficiency of treatment processes and stroke prevention. The chapter then presents papers authored or co-authored by the researcher, with a highlight on the ProPVI paper. This paper, conducted during the researcher's fellowship, stands out for its in-depth analysis and insights into pulmonary vein management optimization. Another significant aspect is the BIO-PVI study, conceived, executed, and developed during the PhD program. This paper endeavours to elucidate the role of biomarkers during the periprocedural period of pulmonary vein isolation (PVI) concerning the recurrence of atrial fibrillation. Through meticulous examination, it aims to shed light on the potential predictive value of biomarkers in predicting the outcomes for AF patients undergoing PVI procedures. One paper is dedicated to the use of the new technology “Ultralow temperature cryoablation” to perform long lasting PVI. The end of this chapter brings forth a study on the optimization of left atrial appendage closure as a stroke preventive strategy. This paper targets patients at high risk of stroke, either due to resistance to anticoagulant therapy or an inability to tolerate it. Through meticulous examination and analysis, the authors sheds light on novel approaches to enhancing patient care and outcomes in this critical area of cardiovascular medicine.

Atrial fibrillation

Atrial fibrillation (AF) is the predominant sustained arrhythmia afflicting adults, with projections suggesting a tripling of its prevalence over the next three decades, leading experts to term it an "AF epidemic." Given these concerning epidemiological shifts and the advancements in both prevention and treatment, it's imperative for all clinicians to possess a thorough understanding of AF management. The therapeutic landscape for AF, whether focusing on rate control or rhythm

management, has undergone significant evolution, from the decision-making process surrounding stroke prevention, with the advent of the new anticoagulant agents and left atrial appendage closure, to invasive strategies for rhythm control such as catheter ablation.

Epidemiology

In 1909, employing Einthoven's string galvanometer, Lewis and Rothberger independently utilized electrocardiography to ascertain that "auricular fibrillation" led to "pulsus irregularis perpetuus," a phenomenon previously observed by Sir James Mackenzie, a Scottish cardiologist who noted the absence of the jugular A wave on his ink-writing polygraph.[1-3] Initially dismissed as an insignificant condition, AF is now acknowledged to exert a substantial impact on both morbidity and mortality, further straining healthcare resources and costs. [4-5] AF stands as the most prevalent clinically significant arrhythmia, with a recent global estimate surpassing 33.5 million patients, a figure that does not even encompass those with clinically silent disease, thus underscoring its emergence as a global epidemic.[6] Age represents a significant risk factor for AF, with the likelihood of developing the condition doubling with each passing decade of life.[7]For instance, among individuals aged over 85 years in the Framingham population, the annual incidence of AF per 1000 persons markedly exceeds that of those under 65 years.[8] Moreover, both men and women older than 40 years exhibit a lifetime risk of AF estimated to be approximately 25%.[9] A Medicare database review, showed that the incidence of AF has remained approximately stable in the US population older than 65 years over the past decade, ranging from 27.8 to 28.3 per 1000 person-year.[10] Whites exhibit a higher risk of incident AF compared to African Americans, Hispanics, and Asians.[11] Despite African Americans possessing a higher prevalence of risk factors for AF, studies such as the Cardiovascular Health Study and the Analysis of the Atherosclerosis Risk in Communities (ARIC) study have revealed a lower risk of AF among African Americans compared to whites, suggesting a protective effect.[12] Sex also plays a role in both the incidence and consequences of AF. Women tend to experience lower incidence of AF. [10,12] However, they face a heightened risk of stroke compared to men and an independent 2.5-fold increased risk of cardiovascular mortality related to AF among women compared to men.[13,14] AF progression involves stages where triggered activity initiates transient AF episodes, evolving into persistent or permanent forms with ongoing structural and electrical changes.[15] Established risk factors including hypertension, cardiovascular disease, obesity, and diabetes mellitus predispose individuals to AF by inducing atrial histological remodelling and electrical changes.[16] The multifactorial nature of AF involves susceptibility related to comorbidities, atrial enlargement, fibrosis, inflammation, ion channel abnormalities, and autonomic remodelling.[17] Therapeutic approaches targeting neuromodulation are actively investigated for reducing AF occurrence and

maintenance, including ganglionated plexus ablation, renal sympathetic denervation, and biological therapies.

References

1. Lewis T. Report CXIX. Auricular fibrillation: a common clinical condition. Br Med J. 1909; 2: 1528
2. Rothberger C. Winterberg H. Vorhofflimmern und arrhythmia perpetua. Wien Klin Wochenschr. 1909; 22: 839-844
3. Mackenzie J. Observations on the process which relsults in auricular fibrillation. Br Med J. 1922; 2: 71-73
4. Marijon E., Le Heuzey J.Y., Connolly S. et al. RE-LY Investigators. Causes of death and influencing factors in patients with atrial fibrillation: a competing-risk analysis from the randomized evaluation of long-term anticoagulant therapy study. Circulation. 2013; 128: 2192-2201
5. Thrall G., Lane D., Carroll D., Lip G.Y. Quality of life in patients with atrial fibrillation: a systematic review. Am J Med. 2006; 119: 448e1-448e19
6. Chugh S.S., Havmoeller R., Narayanan K., et al. Worldwide epidemiology of atrial fibrillation: a Global Burden of Disease 2010 Study. Circulation. 2014; 129: 837-847
7. Benjamin E.J., Levy D., Vaziri S.M., D'Agostino R.B., Belanger A.J., Wolf P.A. Independent risk factors for atrial fibrillation in a population-based cohort: the Framingham Heart Study. JAMA. 1994; 271: 840-844
8. Kannel W.B., Benjamin E.J. Status of the epidemiology of atrial fibrillation. Med Clin North Am. 2008; 92 (ix): 17-40
9. Lloyd-Jones D.M., Wang T.J., Leip E.P., et al. Lifetime risk for development of atrial fibrillation: the Framingham Heart Study. Circulation. 2004; 110: 1042-1046
10. Piccini J.P., Hammill B.G., Sinner M.F., et al. Incidence and prevalence of atrial fibrillation and associated mortality among Medicare beneficiaries, 1993-2007. Circ Cardiovasc Qual Outcomes. 2012; 5: 85-93
11. Dewland T.A., Olgin J.E., Vittinghoff E., Marcus G.M. Incident atrial fibrillation among Asians, Hispanics, blacks, and whites. Circulation. 2013; 128: 2470-2477
12. Alonso A., Agarwal S.K., Soliman E.Z. et al. Incidence of atrial fibrillation in whites and African-Americans: the Atherosclerosis Risk in Communities (ARIC) study. Am Heart J. 2009; 158: 111-117
13. Wang T.J., Massaro J.M., Levy D. et al. A risk score for predicting stroke or death in individuals with new-onset atrial fibrillation in the community: the Framingham Heart Study. JAMA. 2003; 290: 1049-1056
14. Friberg J., Scharling H., Gadsbøll N., Truelsen T., Jensen G.B., Copenhagen City Heart Study Comparison of the impact of atrial fibrillation on the risk of stroke and cardiovascular death in women versus men (The Copenhagen City Heart Study). Am J Cardiol. 2004; 94: 889-894
15. January C.T., Wann L.S., Alpert J.S. et al. American College of Cardiology/American Heart Association Task Force on Practice Guidelines 2014 AHA/ACC/HRS guideline for the management of patients with atrial fibrillation: a report of the American College of Cardiology/American Heart Association Task Force on Practice Guidelines and the Heart Rhythm Society. J Am Coll Cardiol. 2014; 64 ([published correction appears in J Am Coll Cardiol. 2014;64(21):2305-2307]): e1-e76

16. Menezes A.R., Lavie C.J., De Schutter A., et al. Lifestyle modification in the prevention and treatment of atrial fibrillation. Prog Cardiovasc Dis. 2015; 58: 117-125
17. Narayan S.M., Krummen D.E., Shivkumar K., Clopton P., Rappel W.J., Miller J.M. Treatment of atrial fibrillation by the ablation of localized sources: CONFIRM (Conventional Ablation for Atrial Fibrillation with or Without Focal Impulse and Rotor Modulation) trial. J Am Coll Cardiol. 2012; 60: 628-636
18. Chen P.S., Chen L.S., Fishbein M.C., Lin S.F., Nattel S. Role of the autonomic nervous system in atrial fibrillation: pathophysiology and therapy. Circ Res. 2014; 114: 1500-1515
19. Nguyen B.L., Fishbein M.C., Chen L.S., Chen P.S., Masroor S. Histopathological substrate for chronic atrial fibrillation in humans. Heart Rhythm. 2009; 6: 454-460

Rate vs rhythm control

The management of AF involves a choice between rhythm control and rate control strategies. Rate control primarily uses medications like beta-blockers, calcium channel blockers, and digitalis to manage the heart rate. Achieving adequate ventricular rate control is crucial to prevent complications like tachycardia-mediated cardiomyopathy and heart failure symptoms.[1] Studies have shown that lenient rate control (resting heart rate <110 beats/min) is as effective as strict rate control (resting heart rate <80 beats/min) in terms of clinical outcomes, with fewer clinical visits associated with lenient control.[2] Once rate control is achieved, the decision must be made whether to continue rate control alone or pursue rhythm control. Rhythm control involves restoring and maintaining sinus rhythm through medications, electrical cardioversion, or invasive procedures like catheter ablation or surgery.[3,4] Patient-specific factors like AF stage, symptoms, age, and comorbidities should guide this decision.[5] Various studies have previously compared outcomes between rate control and rhythm control strategies for AF treatment. The Atrial Fibrillation Follow-Up Investigation of Rhythm Management (AFFIRM) Study found no survival benefit with rhythm control, nor difference in stroke incidence compared to rate control.[6] Recent research, including the EAST AFNET 4 trial, showed improved outcomes with early rhythm control, using catheter ablation alongside antiarrhythmic drugs. Subgroup analyses of the EAST AFNET 4 trial demonstrated benefits across different patient groups, regardless of heart failure symptoms, comorbidity burden, or AF pattern.[7] The current European Society of Cardiology (ESC) guidelines recommend rhythm control for patients with symptomatic AF.[8] This recommendation is primarily based on previous studies that showed no significant benefit from rhythm control compared to rate control. However, a sub-analysis of the EAST AFNET 4 trial revealed that the primary outcome did not differ between asymptomatic and symptomatic patients.[9] This suggests that early rhythm control should be considered for all AF patients, irrespective of their symptom status.[10] Real-world data from Korea, UK, and Europe further support the efficacy and safety of early rhythm control, showing reduced risk of cardiovascular events

compared to rate control. Meta-analyses of observational studies also confirm the superiority of early rhythm control strategy. Overall, recent evidence favours early rhythm control over rate control, unlike previous trials.[11-15]

References

1. January C.T., Wann L.S., Alpert J.S. et al. American College of Cardiology/American Heart Association Task Force on Practice Guidelines 2014 AHA/ACC/HRS guideline for the management of patients with atrial fibrillation: a report of the American College of Cardiology/American Heart Association Task Force on Practice Guidelines and the Heart Rhythm Society. J Am Coll Cardiol. 2014; 64 ([published correction appears in J Am Coll Cardiol. 2014;64(21):2305-2307]): e1-e76
2. Van Gelder I.C., Groenveld H.F., Crijns H.J., et al., RACE II Investigators. Lenient versus strict rate control in patients with atrial fibrillation. N Engl J Med. 2010; 362: 1363-1373
3. Lee A.M., Melby S.J., Damiano Jr., R.J. The surgical treatment of atrial fibrillation. Surg Clin North Am. 2009; 89 (x-xi): 1001-1020
4. Calkins H, Hindricks G, Cappato R, Kim YH, Saad EB, Aguinaga L, Akar JG, Badhwar V, Brugada J, Camm J, Chen PS, Chen SA, Chung MK, Nielsen JC, Curtis AB, Davies DW, Day JD, d'Avila A, de Groot NMSN, Di Biase L, Duytschaever M, Edgerton JR, Ellenbogen KA, Ellinor PT, Ernst S, Fenelon G, Gerstenfeld EP, Haines DE, Haissaguerre M, Helm RH, Hylek E, Jackman WM, Jalife J, Kalman JM, Kautzner J, Kottkamp H, Kuck KH, Kumagai K, Lee R, Lewalter T, Lindsay BD, Macle L, Mansour M, Marchlinski FE, Michaud GF, Nakagawa H, Natale A, Nattel S, Okumura K, Packer D, Pokushalov E, Reynolds MR, Sanders P, Scanavacca M, Schilling R, Tondo C, Tsao HM, Verma A, Wilber DJ, Yamane T. 2017 HRS/EHRA/ECAS/APHRS/SOLAECE expert consensus statement on catheter and surgical ablation of atrial fibrillation. Heart Rhythm. 2017 Oct;14(10):e275-e444. doi: 10.1016/j.hrthm.2017.05.012. Epub 2017 May 12. PMID: 28506916; PMCID: PMC6019327.
5. Calkins H, Hindricks G, Cappato R, Kim YH, Saad EB, Aguinaga L, Akar JG, Badhwar V, Brugada J, Camm J, Chen PS, Chen SA, Chung MK, Nielsen JC, Curtis AB, Davies DW, Day JD, d'Avila A, de Groot NMSN, Di Biase L, Duytschaever M, Edgerton JR, Ellenbogen KA, Ellinor PT, Ernst S, Fenelon G, Gerstenfeld EP, Haines DE, Haissaguerre M, Helm RH, Hylek E, Jackman WM, Jalife J, Kalman JM, Kautzner J, Kottkamp H, Kuck KH, Kumagai K, Lee R, Lewalter T, Lindsay BD, Macle L, Mansour M, Marchlinski FE, Michaud GF, Nakagawa H, Natale A, Nattel S, Okumura K, Packer D, Pokushalov E, Reynolds MR, Sanders P, Scanavacca M, Schilling R, Tondo C, Tsao HM, Verma A, Wilber DJ, Yamane T. 2017 HRS/EHRA/ECAS/APHRS/SOLAECE expert consensus statement on catheter and surgical ablation of atrial fibrillation. Heart Rhythm. 2017 Oct;14(10):e275-e444. doi: 10.1016/j.hrthm.2017.05.012. Epub 2017 May 12. PMID: 28506916; PMCID: PMC6019327.
6. Corley S.D., Epstein A.E., DiMarco J.P. et al. AFFIRM Investigators. Relationships between sinus rhythm, treatment, and survival in the Atrial Fibrillation Follow-Up Investigation of Rhythm Management (AFFIRM) Study. Circulation. 2004; 109: 1509-1513
7. P Kirchhof, AJ Camm, A Goette, et al. Early Rhythm-Control Therapy in Patients with Atrial Fibrillation. N Engl J Med [Internet], 383 (2020), pp. 1305-1316
8. G Hindricks, T Potpara, P Kirchhof, et al. 2020 ESC Guidelines for the diagnosis and management of atrial fibrillation developed in collaboration with the European Association for Cardio-Thoracic Surgery (EACTS): The Task Force for the diagnosis and management of atrial fibrillation of the European Society of Cardiology (ESC) Developed with the special contribution

of the European Heart Rhythm Association (EHRA) of the ESC . Eur Heart J, 42 (2021), pp. 373-498, 10.1093/eurheartj/ehaa612
9. Systematic, early rhythm control strategy for atrial fibrillation in patients with or without symptoms: The EAST-AFNET 4 trial. Eur Heart J, 43 (2022), pp. 1219-1230
10. J Dickow, P Kirchhof, HK Van Houten, *et al.* Generalizability of the EAST-AFNET 4 Trial: Assessing Outcomes of Early RhythmControl Therapy in Patients With Atrial Fibrillation J Am Heart Assoc (2022), p. 11
11. GI Yu, D Kim, JH Sung, et al. Impact of frailty on early rhythm control outcomes in older adults with atrial fibrillation: A nationwide cohort study Front Cardiovasc Med, 9 (2023)
12. DS Kang, D Kim, E Jang, et al. Sex Difference in Effectiveness of Early Rhythm- over Rate-Control in Patients with Atrial Fibrillation J Clin Med (2022),
13. S Kany, VR Cardoso, L Bravo, et al. Eligibility for early rhythm control in patients with atrial fibrillation in the UK Biobank Heart, 108 (2022), pp. 1873-1880
14. M Proietti, M Vitolo, SL Harrison, et al.Real-world applicability and impact of early rhythm control for European patients with atrial fibrillation: a report from the ESC-EHRA EORP-AF Long-Term General Registry Clin Res Cardiol, 111 (2022), pp. 70-84
15. J Dickow, P Kirchhof, HK Van Houten, et al. Generalizability of the EAST-AFNET 4 Trial: Assessing Outcomes of Early RhythmControl Therapy in Patients With Atrial Fibrillation J Am Heart Assoc (2022), p. 11

Ambulatory pulmonary vein isolation workflow using the Perclose ProglideTM suture-mediated vascular closure device: the PRO-PVI study

Davide Fabbricatore, Dimitri Buytaert, Chiara Valeriano, Niya Mileva, Pasquale Paolisso, Sakura Nagumo, Daniel Munhoz, Carlos Collet, and Tom De Potter

Europace. 2023 Apr; 25(4): 1361–1368.

Published online 2023 Feb 16. doi: 10.1093/europace/euad022

PMCID: PMC10105833

PMID: 36793243

Abstract

Aims: The leading reason for delayed discharge after pulmonary vein isolation (PVI) is vascular complications. This study aimed to evaluate feasibility, safety, and efficacy of the Perclose Proglide™ suture-mediated vascular closure in ambulatory PVI, report complications, patient satisfaction, and cost of this approach.

Methods and results: Patients scheduled for PVI were enrolled prospectively in an observational design. Feasibility was assessed as % discharged the day of procedure. Efficacy was analysed as acute access site closure rate, time to reach haemostasis, time to ambulate, and time to discharge. Safety analysis consisted of vascular complications at 30 days. Cost analysis was reported using direct and indirect cost analysis. A 1:1 propensity matched control cohort was used for comparing time to discharge to usual workflow. Of 50 enrolled patients, 96% were discharged on the same day. 100% of devices were successfully deployed. Immediate (<1 min) haemostasis was reached in 30 patients (62.5%). Mean time to discharge was 5:48 ± 1:03 h (vs. 10:16 ± 1:21 h in the matched cohort, $P < 0.0001$). Patients reported high level of satisfaction with the post-operative time. No major vascular complication occurred. Cost analysis showed a neutral impact compared to the standard of care.

Conclusion: The use of the closure device for femoral venous access after PVI led to safe discharge of patients within 6 h from the intervention in 96% of the population. This approach could minimize the overcrowding of healthcare facilities. The gain in post-operative recovery time improved patients' satisfaction and balanced the economic cost of the device.

Keywords: Atrial fibrillation, Pulmonary vein isolation, Femoral access, Perclose ProGlide™, Ambulatory management, Rapid discharge

Graphical Abstract

Ambulatory Pulmonary Vein Isolation workflow using a suture-mediated vascular closure devices: a prospective observational cohort study - The PROPVI study

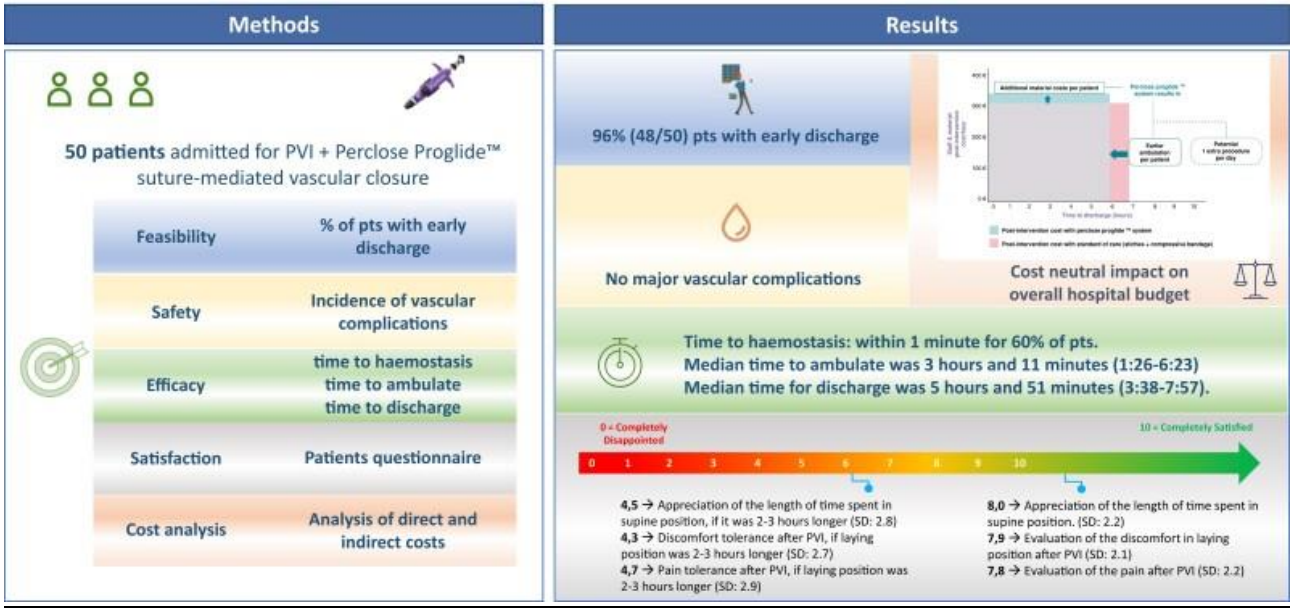

What's new?

- There is still lack of knowledge on the use of vascular devices in the EP field; this paper provides evidence supporting the use of Perclose ProGlide™ suture-mediated vascular closure in PVI procedures.
- A shorter post-operative supine position was preferred by patients.
- Analysis of costs showed a neutral economical impact of vascular closure device use in PVI.

Introduction

Pulmonary vein isolation (PVI) for the treatment of atrial fibrillation (AF) is an increasingly performed procedure worldwide.[1] The procedure workflow has been improving quickly through both the implementation of new ablative technologies and peri-procedural management, so that PVI is now routinely performed within 120 min.[2] Although procedure time has been shortened significantly, the post-operative management of patients undergoing PVI has remained almost unchanged.[3] Thus, the possibility to perform these procedures in a same day discharge setting presents an interesting prospect in the electrophysiology (EP) field. To date, the possibility of a rapid discharge after PVI is limited by post-procedural adverse events, driven mainly by vascular complications.[1,3] The incidence of serious complications such as femoral pseudoaneurysm, arteriovenous fistula, and retroperitoneal bleeding are approximately 1.5% and increase with the number and size of sheaths used.[1,3] In addition, the intensive peri-procedural anticoagulative regimen recommended at the time of PVI procedures aggravates the incidence of minor complication such as bleeding or haematomas.[4] In order to reduce complications related to the venous puncture, an ultrasound approach for venous accesses has been adopted, resulting in a drastic decline in puncture-related complications.[5–7] As for the post-

operative management, a figure-of-eight suture and/or manual compression (MC), followed by post-operative bedrest (up to 8 h) is still the standard approach in many centres.[5–7] Hence, the application of devices that can reduce the bedrest time after EP procedure is an interesting clinical opportunity.[8–10] The aim of this study was to evaluate the feasibility, safety, and efficacy of using Perclose ProGlide™ suture-mediated vascular closure in percutaneous PVI procedures for the purpose of enabling a workflow without any bedrest after recovery from anesthesia. We evaluated the feasibility of this method to achieve early mobilization of patients undergoing PVI. We also investigated patients' clinical symptoms and satisfaction. Incidence of vascular complication at Days 1, 7, and 30 following the intervention were analysed. Hospital costs compared to the standard of care (SOC) in our hospital was assessed considering direct and indirect costs.

Methods

Study design

We performed an observational prospective single-centre cohort study of patients admitted for PVI with Perclose ProGlide™ system use, from January 2020 to May 2021.

Data were prospectively collected; an electronic case report form (e-CRF) was promptly completed. Source data and database quality control was performed by investigators. A detailed description of the study design had been previously accepted by the local ethical committee. A Clinical Events Committee was recruited for the follow-up clinical events evaluation.

Variables and definitions

The primary endpoint (feasibility of an ambulatory PVI strategy) was assessed as the percentage of patients being able to be discharged the same day of the procedure. The secondary endpoints were analysed only for patients who met the primary endpoint. Acute vascular device closure performance was evaluated as the number of successful deployments out of total number of devices utilized (two for single PVI). Immediate haemostasis (< 1 min from device deployment) rate was recorded as a proportion of the total number of procedures. Post-procedural time to reach haemostasis was measured as the time from the delivery of the closure device to confirmed venous haemostasis in those patients needing further manual compression after device deployment. Time to ambulation was analysed as time from the removal of closure device to patients' ability to walk. Time to be deemed suitable for discharge was calculated as the time from the removal of closure device to the medical assessment that deemed discharge possible. Time to discharge was considered as the effective time from the removal of closure device to patient discharge. Patient satisfaction was evaluated using the

Post Ablation Procedure Patient Survey (see Supplementary material online). Minor and major vascular complications were calculated as the number of patients with venous access-related issues both requiring or not investigation, medical management, or surgical intervention out of the total number of patients enrolled.

Inclusion/exclusion criteria

All patients scheduled for elective PVI were considered eligible for study participation. All patients participating accepted to be enrolled in the study and signed the informed consent after detailed discussion. Exclusion criteria were: age <18 years, previous adverse event after vascular access resulting in prolonged hospitalization, previous vascular surgery in either leg or in the aorto-iliac axis, nonstandard ablation (i.e. need for more than two femoral punctures), known history of bleeding diathesis, coagulopathy, hypercoagulability or platelet count < 100 000 cells/mm^3, history of deep vein thrombosis (DVT), pulmonary embolism or thrombophlebitis, significant anaemia or renal insufficiency, haemodynamic or electrical instability, body mass index (BMI) > 45 kg/m^2 or < 20 kg/m^2, active liver disease or hepatic dysfunction, severe renal dysfunction, defined as an estimated global filtration rate (eGFR) < 30 mL/min/1.73 m^2 unless the patient is in renal support therapy.

Procedure

All subjects provided written informed consent prior to the PVI procedure. Patients were admitted to the hospital at the same day of the intervention. All procedures were performed under uninterrupted anticoagulation, if indicated, and heparin was administered during the procedure in order to get an activated clotting time (ACT) of 300 s or greater.[1] No anticoagulation was given on the morning of the procedure itself. All procedures were performed under general anaesthesia. Two sheaths with 8 and 8.5 French diameter, respectively, were placed in the right common femoral vein via an US-guided approach. No local anaesthetic was given at any site during any phase of the procedure. At the end of the procedure, a Perclose Proglide^{TM}-closure system was used for each sheath. After discharge from the anaesthesiology recovery unit, patients were kept in observation in an ambulatory recovery room, in a sedentary position without further bedrest, until discharge was deemed possible by the attending physician. A transthoracic ultrasound to exclude pericardial effusion was part of the pre-discharge assessment as per the standard of care for all patients in our institution.

Endpoint

The primary endpoint was the rate of patients discharged the same day of the procedure. Secondary endpoints were: (i) acute vascular device closure performance, (ii) post-procedural time to reach haemostasis, (iii) time to ambulation, (iv) time to possibility of discharge, (v) time to discharge, and

(vi) patient satisfaction. Prior to discharge, all patients were asked to complete the Post Ablation Procedure Patient Survey questionnaire (see Supplementary material online) in which scores from zero (very unsatisfied) to 10 (very satisfied) were assigned. Level of pain, need for analgesic medications, and patient's satisfaction were also evaluated using the 'Post Ablation Procedure Patient Survey' questionnaire (see Supplementary material online). The secondary safety endpoint was the incidence of minor and major vascular complications within 30 days after the procedure and according to the Clinical Event Committee (CEC) analysis.

Analysis of costs

Cost comparison considered direct and indirect costs including time and staff allocation spent in the EP lab and the ward. Procedure timings and relative costs were provided by the cardiology department of OLV Aalst. Costs related to nursing staff salaries are in accordance with the mandatory barema scales and expert opinion was sought for clinician staff costs. A detailed description of the process and methodology of the cost comparison is provided as a Supplementary material online to the manuscript.

Follow-up

Patients were followed-up for a period of 30 days after the procedure. Photographs of the puncture site were collected from the patients or their caregivers at Day 1 and/or Day 7 after the procedure. Patients were instructed to inform the investigators at any time with new cases of symptoms. A CEC consisting of three independent members evaluated the occurrence of adverse events.

Statistical analysis

For descriptive analysis, categorical variables are presented as absolute numbers and their relative percentages, continuous variables are presented as mean ± standard deviation (SD) and/or median and interquartile range (IQR) according to normal or non-normal distribution. Baseline characteristics are presented as numbers (%) for categorical variables and as means ± standard deviation for continuous variables. Differences between groups were analysed using the Student's *t*-test or the Mann–Whitney *U* test for continuous variables, and the χ^2 test or Fisher's exact test for categorical variables, as appropriate. Propensity score (PS)-matching was used to reduce selection bias between the PROPVI group and the general population and to adjust for significant differences in the patients' baseline characteristics. The propensity score was computed by a logistic regression model, and the matching was performed using the nearest neighbour method with a 1:1 ratio.

Matching criteria were age, sex, BMI, hypertension, diabetes, smoking habit, peripheral arteriopathy (PAD), and creatinine clearance. Analyses were performed with R version 3.5.2 (R Foundation for Statistical Computing, Vienna, Austria). A *P*-value of 0.05 was considered statistically significant.

Results

A predefined number of 50 patients were enrolled (*Table 1*). All patients underwent PVI with radiofrequency (RF) ablation. No intra-procedural complications occurred. At the end of the procedure, two Perclose Proglide™ systems were placed—one for each vein. In total 48/50 (96%) patients were discharged on the day of the procedure (*Table 2*). 49 patients (98%) were deemed to be suitable for discharge, but one patient requested to prolong the admission for non-medical reasons. One patient was kept supine due to discomfort until an ultrasound evaluation was carried the day after which excluded severe complications. Successful Proglide deployment was observed in all 48 patients that met the primary endpoint (96/96 devices, 100% success rate). After the procedure, anticoagulation was reversed by protamine administration in two patients (4%). Immediate haemostasis was reached in 30 patients (60%), with 20 subjects (40%) requiring short additional manual compression. In this last group, the mean and median time to achieve haemostasis were 4 min and 34 s (± 3:27) and 3 min (2–15), respectively. During the post-operative stay, two patients (4.2%) experienced minor bleeding, stopped after additional short manual compressions. Mean and median time to ambulation was 3 h and 18 min (± 1:05) and 3 h and 11 min (1:26–6:23), respectively. The mean and median time to discharge in the 48 patients was 5 h and 48 min (± 1:03) and 5 h and 51 min (3:38–7:57) (*Figure 1* and *Table 2*). By using the 'Post Ablation Procedure Patient Survey,' patients reported high levels of satisfaction for the total duration of the supine position, as well as for discomfort and access-related pain during the post-operative supine position. The mean score assigned to 'satisfaction about the total duration of lying position after PVI' was 7.8/10, vs. a score of 4.7/10 that was assigned had a hypothetical supine position lasted 2–3 h longer. Similar results were observed regarding the discomfort and access-related pain during the post-operative supine position (*Figure 2* and *Table 3*). Post-operative pain required management in only three patients, consisting of two single doses of salicylic acid or paracetamol and one repeated administration of paracetamol. There was no need for local analgesia or long-term analgesia prescription (*Table 2*). All patients concluded the 30-day follow-up period. They all received phone calls at Days 1, 7, and 30. No major vascular complications as well as necessity of any invasive intervention were described in the overall population (*Table 2*). Post-procedural haematomas bigger than 6 cm occurred in three patients (6.25%) which spontaneously resolved during the follow-up time with no further assessment or management needed. In 15 (31%) patient,s an asymptomatic superficial haematoma <6 cm occurred, and in one patient (2.08%) a transient access site-related nerve injury was reported

(*Table 2*). For the analysis of cost, this workflow was compared to the figure-of-eight approach that represents the standard of care in our centre. With respect to the figure-of-eight method, the use of Perclose ProGlide™ increased the overall cost of the procedure (device and staff costs included) by 259,15€ favouring figure of eight closure. However, considering the time spent in the ward after the ablation, the use of Perclose ProGlide™ reduced the time to discharge by 60 min. This reduction potentially increases the cost effectiveness of the PVI unit by improving efficiency and flow-through of patients with the potential to increase the number of procedures being carried out (for example diuretic administration for treatment of heart failure). The above staff and procedure efficiencies offset the cost of the Perclose ProGlide™ system, resulting in a neutral economic impact for the hospital for a single patient (*Figure 3*).

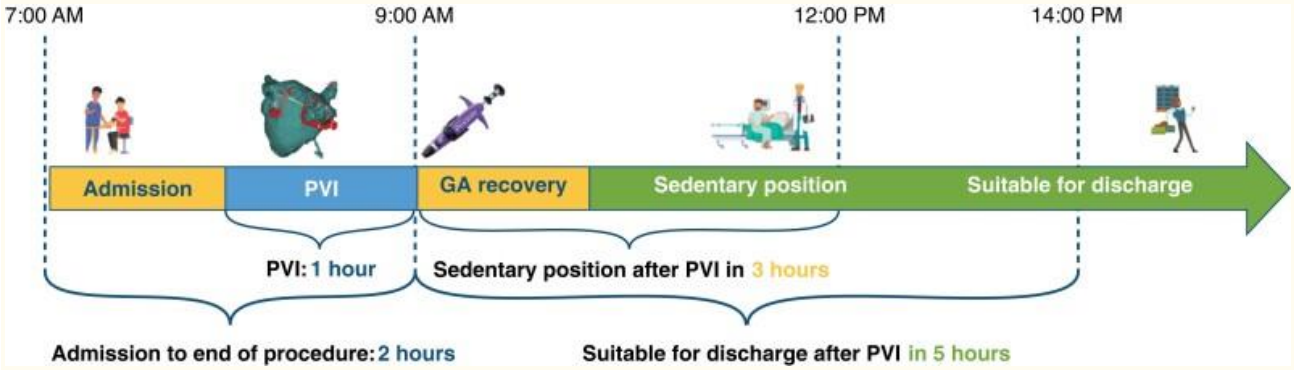

Figure 1

Patients' flow in the PROPVI study. The timeline exposed in the figure is realized according to data from the population that reached the primary endpoint; to: admission in hospital; yellow arrow: waiting (pre and post) times, blue arrow: operative time; green arrow: endpoint GA = general anesthesia.

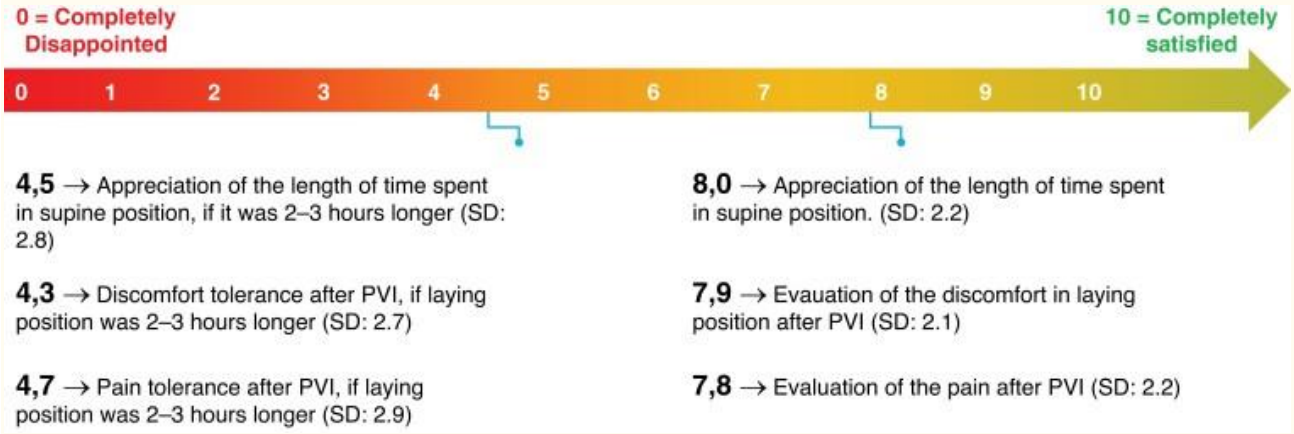

Figure 2

Visual extract from the post ablation procedure patient survey. Patient's preference for shorter supine position, less discomfort, and less pain. All three parameters can be achieved by using Perclose Proglide™ system.

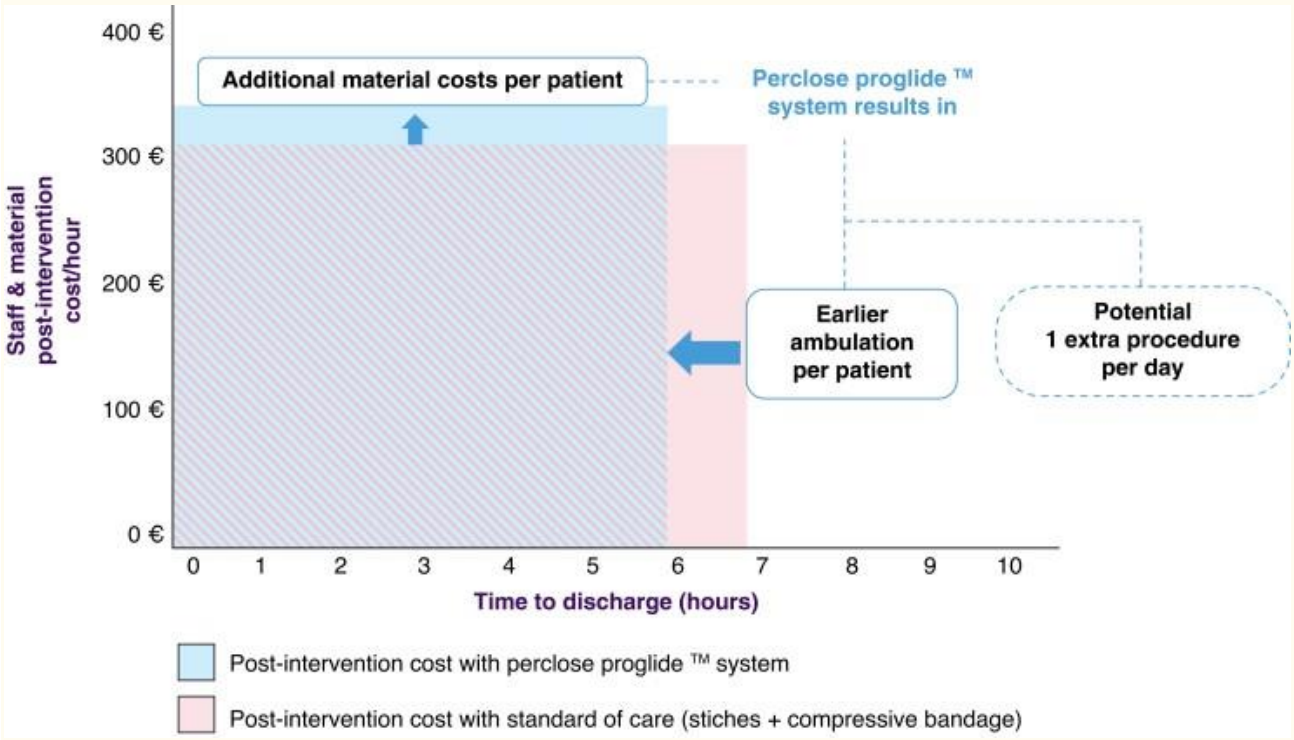

Figure 3

Hospital efficiency gain. The increased efficiency gain when using Perclose Proglide™ system. Shaded are shows shared costs between both approaches. Despite the upfront incremental cost for Proglide (solid blue box), the system allows to mobilize the patient earlier (solid pink box), thus reducing the cost for the hospital.

Table 1. Patient demographic, clinical and procedural characteristics

Patient demographic, clinical and procedural characteristics	
Total population, *n* (%)	50 (100)
Median age (IQr)	64 (28–80)
Male sex, *n* (%)	38 (76)
Median BMI (IQr)	26.3 (21–42)
Hypertension, *n* (%)	20 (40)

Patient demographic, clinical and procedural characteristics	
DM, *n* (%)	11 (22)
Smokers, *n* (%)	4 (8)
Necessity of protamine administration (%)	2 (4)
Median ACT (s)	318 (225–355)

Table 2. Endpoints and outcomes

Total population, *n* (%)	50 (100%)
Primary endpoint	
Discharge in the same day, *n* (%)	48 (96)[a]
Outcomes	
Success of device deployment, *n* (%)	96 (100)
Necessity of post-deployment manual compression > 1 min, *n* (%)	20 (41.7)
Late recurrence of bleeding, *n* (%)	2 (4.16)
Mean/median time to reach haemostasis (mm:ss)[b]	4:35 (± 3:27)/3:00 (2:00–15:00)
Mean/median time to ambulation (hh:mm)—IQR	3:18 (± 1:05)/3:11 (1:26–6:23)
Mean and median time to be deemed suitable for discharge	4:55 (±00:54)/4:48 (2:50–7:30)
Mean/median post-procedural time to be discharged (hh:mm)—IQR	5:48 (± 1:03)/5:51 (3:38–7:57)
Major vascular complications needing surgical intervention, *n* (%)	0 (0)
Major vascular complications needing further medical evaluation/investigation, *n* (%)	0 (0)
âHematoma > 6 cm, *n* (%)	3 (6.25)
âAsymptomatic superficial bruising ≤ 6 cm, *n* (%)	15 (31.25)
Necessity of pain medication, *n* (%)	3 (6.25)
âParacetamol, *n* (%)	2 (4.16)
ââSingle administration, *n* (%)	1 (2.08)
ââRepeated administration, *n* (%)	1 (2.08)
âSalicylic acid, *n* (%)	1 (2.08)

49 patients (98%) were deemed to be suitable for discharge. One of them wanted to prolong the hospital stay for non-medical reasons.
Described only for patients in which haemostasis within 1 min was not achieved.

Table 3. Patients' reported satisfactions after PVI

Parameters of satisfaction	***n***	**Mean**	**SD**
Appreciation of the length of time spent in supine position	47	8.0	2.2

Parameters of satisfaction	*n*	Mean	SD
Discomfort laying position after PVI	47	7.9	2.1
Pain after PVI	46	7.8	2.2
Appreciation of the length of time spent in supine position if it was 2–3 h longer	45	4.5	2.8
Discomfort, if laying position was 2–3 h longer	45	4.3	2.7
Pain after PVI, if laying position was 2–3 h longer	45	4.7	2.9

Patients were asked to assess satisfaction for each parameter in a range from 0 (very dissatisfied) to 10 (very satisfied).
SD, standard deviation; PVI, pulmonary vein isolation.

From the contemporary cohort of patients undergoing PVI with standard-of-care treatment including figure of 8 suture, 166 patients were matched in a 1:1 ratio with the PROPVI study group. No differences were observed across baseline characteristics of the matched population (*Table 4*). Details of the propensity score matching are reported in Supplementary material online, *Figures S1* and *S2*. Mean time to discharge for the control cohort was 10:16 ± 1:21 h ($P < 0.0001$ for comparison to the study group). Time to ambulation was not available for the control group as it does not apply to our standard figure of eight workflow.

Table 4. Propensity matched population comparison

	Matched population (*n* = 50)	PROPVI population (*n* = 50)	Total population (*n* = 100)	*P* value
Age mean (SD)	59.9 (11.46)	61.06 (11.71)	60.48 (11.54)	0.618
Gender male *n* (%)	38 (76%)	38 (76%)	76 (76%)	1.000
BMI mean (SD)	27.70 (4.05)	27.56 (4.95)	27.63 (4.50)	0.875
Hypertension *n* (%)	18 (36.0%)	20 (40.0%)	38 (38.0%)	0.680
Diabetes *n* (%)	11 (22.0%)	11 (22.0%)	22(22.0%)	1.000
Smoke habit *n* (%)	4 (8%)	4 (8%)	8 (8%)	1.000
PAD *n* (%)	1 (2%)	2 (4%)	3 (3%)	0.558
Creatinine clearance Mean (SD)	74 (25.7)	81 (27.05)	77(26.5)	0.236
hours for discharge Mean (SD)	10.16 (1.21)	5.48 (1.03)	7.98 (1.12)	<0.001
conversion to in hospital management *n* (%)	4 (8%)	1 (2%)	5 (10%)	0.1

Discussion

Although the PVI procedures have been shortened significantly over the last years, the post-operative management of patients undergoing PVI has remained almost unchanged normally requiring a post-operative bedrest up to 6 h and an intra-hospital observation up to 24 h.[1,11] As a consequence, the number of PVI procedures performed is limited by the available bed capacity which was particularly affected in the era of restrictive rules applied for the COVID-19 pandemic containment.[12] Thus, the possibility to perform PVI, and in general advanced procedures, in a day care setting, represents an

interestingly prospect in the electrophysiology (EP) field, and emerging data support feasibility of same day discharge approaches using several ablation modalities.[13,14] Existing data also support a potential for cost saving driven by a reduction in hospital costs, although there are little prospective controlled data available on this topic.[15,16] The advantages of using devices for vascular closure have already been assessed in the context of arterial procedures.[17] In particular, they were shown to reduce the rate of complication and the necessity of bedrest, shortening the total hospital stay.[17] Despite the use of large femoral sheaths (up to 12 French) in the EP field, there is still a lack of knowledge about vascular closure devices. However, based on the low-pressure of the venous circulation, the effect of these systems can be even more advantageous than for arterial procedures. Recently, in a multicentre retrospective study investigating the usefulness of vascular closure devices after catheter ablation, a significant reduction of access-site complications, and ambulation time were observed.[8] In another randomized multi-centre trial that assessed the use of the VASCADE MVP Venous Vascular Closure System, improvements were demonstrated with time to ambulation, total post-procedure time, time to discharge eligibility, time to haemostasis, and patient satisfaction.[9] Our study demonstrates that an ambulatory strategy for pulmonary vein isolation procedure is feasible considering time to achieve haemostasis, time to ambulation, and time to discharge. This is of considerable importance for such increasingly rapid procedures, performed during intense anticoagulation and in an era favouring day case management. Since the majority of complications leading to prolonged hospitalization are related to the vascular approach, the use of a system able to properly close the femoral access is of critical importance to improve the femoral access management after the procedure. Furthermore, patient satisfaction with post-operative time was considerably higher than in the case of a postoperative stay longer than 2–3 h. In a time of shortage of healthcare workers and stress on hospital resources, the efficiency gain from medical technology innovations can be extremely beneficial. In our study, the Perclose ProGlide™ system, despite bringing an upfront incremental cost than the standard treatment, improves hospital efficiency and patient satisfaction. Reducing the ward stay and the staff costs, the Perclose Proglide™ closure approach offsets the cost of the Perclose ProGlide™ system, resulting in a final neutral impact for the hospital per single patient.

Limitations

There are several limitations in this study. The main limitation is the observational nature of the study design, making definitive comparisons with other established workflows impossible. However, to provide a basis for comparison, we performed a retrospective comparison with a propensity-matched cohort that can serve as a reference point for the time to discharge. Similarly, the analysis of costs for the comparator treatment is based on the price of the materials at the time the data were collected without setting a case control study. Also, patients were all managed with the Perclose

Proglide™ closure device; thus, satisfaction analysis was based on a comparison on an only 'virtual' experience for patients.

We have chosen to only study uncomplicated PVI procedures in a first stage, excluding patients with higher probability of access related complications. Nevertheless, the stated exclusion criteria appear uncommon in straightforward PVI as zero patients scheduled for such procedures were ineligible for the study protocol.

Finally, the time to discharge in our study group is obviously the outcome of a micromanaged patient population and may very well represent the best achievable scenario. When comparing the time to discharge in the study group with the propensity-matched control group, it is important to keep in mind no particular efforts were made to optimize the time to discharge for the latter.

Regarding technical aspects of our workflow, we only assessed safety and feasibility using two venous sheaths with 8F diameter. We cannot extrapolate results to workflows using three or more sheaths. In addition, a two-sheath workflow where one sheath is large bore (e.g. cryoballoon) was not tested either. The authors do report anecdotal experience supporting feasibility of a three-sheath approach, and also report feasibility of large access closure if appropriate device recommendations are followed (specifically for the study device, the use of pre-close rather than post-close and the potential consideration of two devices per access site).

Conclusion

The PROPVI trial demonstrates that the ambulatory management of PVI by using the percutaneous Perclose Proglide™ closure device is safe and effective, appropriately closing venous accesses. The use of the closure device for PVI led to safe discharge of patients within 6 h from the intervention in 96% of the population with no major complications observed in the follow-up period. The ambulatory management described in the article is useful to reduce the post-PVI recovery time leading to a significantly improved patients' experience. The cost of the Perclose ProGlide™ devices is balanced by savings made with the reduced use of day case department and by the decreased nursing time required. Further randomized trials are needed to better demonstrate the benefits of this approach.

BIOPVI Study

Role of BIOmarkers as predictors of effectiveness of the lesion during Pulmonary Vein Isolation procedures: a prospective observational cohort study

Authors:

Davide Fabbricatore, MD1,2, Chiara Valeriano, MD1, Peter Peytchev, MD1, Koen De Schouwer, MD1, Dimitri Buytaert, MSc1, Pasquale Paolisso, MD1,2, Cristina De Colle MD1,2, Louis Verdonckt,MSc1 , Peter Geelen, MD1 and Tom De Potter, MD1.

Affiliations:

1. Cardiovascular Center Aalst, OLV-Clinic, Aalst, Belgium

2. Dept. of Advanced Biomedical Sciences, University of Naples Federico II, Naples, Italy

Corresponding author:

Davide Fabbricatore

Contribution:

TDP and DF conceived the study, designed the protocol, and selected patients. TDP supervised the statistical analysis and the manuscript. TDP, PG, PP, KDS performed the interventions. DF performed the statistical analysis and wrote the manuscript. PP and CDC performed the echocardiogram. CV contributed to data collection and patients' assessment. DB contributed to data collection and contributed to the manuscript. All authors provided critical feedback and helped shape the research, analysis, and manuscript.

BIO-PVI Study

"BIOmarkers as predictors of Pulmonary Vein Isolation efficacy: the BIO-PVI study"

List of abbreviations

AF Atrial fibrillation

PVI Pulmonary vein isolation

PVs Pulmonary vein

ANP Atrial natriuretic peptide

BNP Brain natriuretic peptide

NT-pro-BNP N-terminal pro-brain natriuretic peptide

CRP C-reactive protein

TIMP-2 tissue inhibitor of metalloproteinase-2

RFCA Radiofrequency catheter ablation

RF Radiofrequency

CFAE complex fractionated atrial electrogram

RDW red cell distribution width

HB haemoglobin

AST aspartate aminotransferase

ALT alanine aminotransferase

LDH lactate dehydrogenase

ECG electrocardiogram

LVEF Left ventricular ejection fraction

AHRE Atrial high-rate episode

CRF Case Report Form

REDCap Research Electronic Data Capture

SD standard deviation

IQR interquartile range

COPD Chronic obstructive pulmonary disease

OSAS obstructive sleep apnea

CKD chronic kidney disease

HF heart failure

Introduction

Pulmonary vein isolation (PVI) is an increasingly recognized procedure for managing atrial fibrillation (AF). Despite advancements in technology and innovative strategies, the challenge of AF recurrence persists. In the context of persistent AF, the relapse rate is notably higher. Research indicates that up to 50% of patients treated with PVI may experience recurrence, often necessitating further intervention.[1,2] The primary cause of recurrences is often incomplete isolation of the pulmonary veins (PVs) rather than the emergence of new arrhythmic foci.[4] However, a recent research from the Bern University group in Switzerland, published in the Journal of the American College of Cardiology: Clinical Electrophysiology (JACC EP), observed, on 26 patients undergoing RF ablation and remap 6 months later, more AF recurrence in patients with complete PV isolation compared to those with PV reconnections (33 vs. 9%). The unexpected finding that PV reconnections were associated with a lower AF recurrence rate raises questions about the mechanisms of AF maintenance and the role of PV isolation and makes patients management more complex. For example, the decision to prolong the antiarrhythmic and the anticoagulant therapy after the ablation, particularly in patients with borderline-low CHA_2DS_2-VASc scores, remains a topic of debate among clinicians. Given these uncertainties, identifying reliable markers that can predict AF recurrence post-ablation would be highly beneficial for patient management and follow-up. These markers could aid in tailoring individualized treatment plans, thereby potentially improving clinical outcomes for patients with AF, for example avoiding medications, if not needed, and even interrupting the anticoagulant therapy after the blanking period to reduce the risk of bleeding. While various clinical and imaging factors have been identified as predictors of AF recurrence after PVI, the role of biomarkers, although extensively explored, remains uncertain.[4] In particular, whether the association between biomarkers and AF relapses is attributable to the patient's systemic condition or the quality of PVI lesion itself has not been clarified yet.

In this research we aimed to correlate the level of biomarkers related to inflammation and myocardial damage, in the periprocedural period of the ablation, in order to predict the occurrence of AF relapse.

To have a better understanding of lesion formation, we indexed the changes of the biomarkers by the energy delivered to the tissue. In fact, despite the PVI method is standardised, the amount of energy used during the ablation could vary extensively and the response of the tissue could not follow a linear correlation with it. This observation could serve as a valuable predictor of procedural success.

Methods

Study population

Single-centre, prospective cohort study designed to explore the predictive value of biomarkers to predict AF recurrences following pulmonary vein isolation. Consecutive patients with paroxysmal or persistent AF who provided written informed consent were enrolled from September 1st, 2021 to July 31st, 2022. Patients with i) long-standing persistent and permanent AF; ii) post-operative AF; iii) contra-indication for oral anticoagulation; iv) recent (<30 days) acute coronary syndrome were excluded. The follow-up data collection was concluded in February 2023. The study centre was the Cardiovascular Research Centre OLV in Aalst, Belgium. The study was conducted according to the declaration of Helsinki and Good Clinical Practice guidelines. The study did not add any specific risk for participating patients since they received the standard management of surgical and medical conditions, according to national and international guidelines, during all the study periods. Privacy was ensured by collecting data anonymously. The study was submitted to the local Ethic Committees and informed consent requested from patients.

Laboratory assessment (Blood samples and biomarkers)

The evaluation included various biomarkers and blood parameters related to inflammation, myocardial damage/dysfunction, iron balance, and other haematological parameters. Inflammation biomarkers such as interleukin-6 (IL-6), tissue inhibitor of metalloproteinase-2 (TIMP-2), and C-reactive protein (CRP) were analysed to gauge the inflammatory response. Biomarkers indicative of

myocardial damage or dysfunction, such as high-sensitive Troponin T (hs-TnT) and N-terminal pro-brain natriuretic peptide (NTproBNP), were examined. Iron balance was assessed by measuring iron, ferritin and transferrin levels. Additionally, various blood parameters including red blood cells, white blood cells, red cell distribution width (RDW), haematocrit, haemoglobin, neutrophils, lymphocytes, basophils, eosinophils, monocytes, as well as enzymes like aspartate aminotransferase (AST), alanine aminotransferase (ALT), and lactate dehydrogenase (LDH) were evaluated. After the ablation, changes in the biomarkers were observed at three different times: pre-procedural (time 0), post-procedural (time 1), and at the moment of discharge (time 2). Time 1 and 2 were subsequently corrected by the values at time 0 to extrapolate the delta 1 (biomarkers at time 1 – biomarkers at time 0) and delta 2 (biomarkers at time 2 – biomarkers at time 0).

Post-operative follow-up and data management

Patients were seen regularly according to the usual follow-up or whenever symptoms would occur after the PVI. All patients underwent electrocardiography (ECG) during every visit and 24-h Holter recordings at 3 and/or 6 months. Holter monitoring or event monitor recordings were also performed in case of symptoms of palpitations suggestive of an arrhythmia recurrence. The minimum duration of AF episodes to establish the diagnosis was at least 30 seconds, or entire 12-lead ECG documenting AF. [1]

Outcome and objective

This study proposes that the magnitude of the increase in biomarkers following a PVI procedure may serve as a predictor for AF recurrences. The study's objective was to investigate the impact of biomarker levels and their dynamic changes after ablation on predicting AF relapses.

Statistical analysis

For descriptive analysis, categorical variables were presented as absolute numbers and their relative percentages, continuous variables were presented as mean ± standard deviation (SD) or median and

interquartile range (IQR) according to normal or non-normal distribution. The rate of AF recurrences was calculated using the total number of patients as the denominator and the number of patients experiencing AF recurrences as the numerator. Risk factors for AF recurrences were evaluated in a univariate and multivariate Cox regression model. Laboratory changes and differences within and between groups with and without AF recurrences were assessed using appropriate statistical tests such as chi-square or Fisher exact test for categorical variables and the Mann-Whitney U test for continuous variables, Huynh-Feldt, and Anova for the analysis of the change. Furthermore, the impact of blood markers on AF recurrences was evaluated through both univariate and multivariate Cox regression analyses. The statistical analysis was conducted using SPSS 21.0 software.

Study Timeline

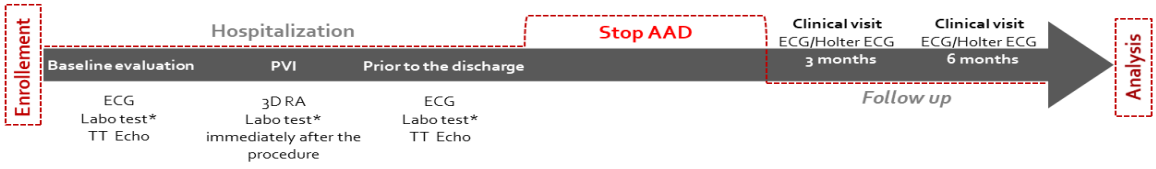

* **Labo test:** hs-TnT, NTproBNP, CRP, IL-6, TIMP2, iron level (sideremia), ferritin, red blood cells, white blood cells, haematocrit, haemoglobin, neutrophils, lymphocytes, basophils, eosinophils, monocytes, aspartate Aminotransferase (AST), Alanine Aminotransferase (ALT), Lactate Dehydrogenase (LDH)

Results

In total 134 patients were enrolled of which 90 (62.1%) male, mean age 64.8 (SD 10.53). The AF was paroxysmal in 93 (64.1%). Baseline characteristics of the overall population stratified by occurrence of relapses are presented in **Table 1**.

	overall population	no recurrences	recurrences	pvalue
	129	95	34	
Age (mean, SD)	64,7 (10,5)	64,14 (10,2)	66,21 (12,00)	0.15
Time in AF	803.6 (1423)	814 (1443)	789.4 (1420)	0.3
Overweight	70 (54.3)	49 (51.6)	21 (61.8)	0.3
Diabetes	12 (9.3)	10 (10.5)	2 (5.9)	0.4
Hypertension	57 (44.2)	42 (44.2)	15 (44.1)	0.9
Heart failure	14 (10.9)	8 (8.4)	6 (17.6)	0.14
IHD	14 (10.9)	10 (10.5)	4 (11.8)	0.8
Betablocker	74 (57.4)	51 (53.7)	23 (67.6)	0.16
Amiodaron	12 (9.3)	8 (8.4)	4 (11.8)	0.6
Class 1C AAD	20 (15.5)	14 (14.7)	6 (17.6)	0.7
Calcium antagonist	6 (4.7)	4 (4.2)	2 (5.9)	0.7
Digoxin	7 (5.4)	6 (6.3)	1 (2.9)	0.5
Sotalol	12 (9.3)	8 (8.4)	4 (11.8)	0.6
ACE inhibitors	31 (24)	23 (24.2)	8 (23.5)	0.9
Height (mean, SD)	173,3 (12,4)	173,54 (13,6)	172,9 (9,3)	0.76
Weight (mean, SD)	85,1 (17,8)	85,72 (18,9)	83,7 (15,3)	0.89
BMI (mean, SD)	29,2 (19,7)	29,9 (23,4)	27,8 (4,3)	0.907
HR (mean, SD)	71,5 (23,4)	73,5 (25,7)	67,2 (17,2)	0.395

LAS_resevoir (mean, SD)	21,9 (11,9)	23,25 (12,5)	18,9 (9,1)	0.199
LAS_conduit_baseline (mean, SD)	14,3 (6,9)	14,9 (6,9)	13,5 (6,6)	0.653
LAS_contraction_baseline (mean, SD)	7,6 (7,7)	8,4 (8,2)	5,4 (5,8)	0.485
LAS_volume_baseline (mean, SD)	55,3 (21,2)	51,1 (18,5)	66,2 (24,2)	0.018*
LVEF	53.2	53.25 (7.7)	53.06 (6.2)	0.349

Table 1: Baseline clinical characteristics and univariate analysis for differences between groups. SD: standard deviation; IHD: ischemic heart disease; AF: atrial fibrillation; AAD: anti arrhythmic drug; BMI: body mass index; HR: heart rate; LAS: left atrial strain. LVEF: left ventricular ejection fraction

Preoperative biomarkers

During the follow-up period, with a median duration of 166 days (37-445 days), 38 patients (28%) experienced a recurrence of atrial arrhythmia. When comparing baseline clinical parameters in patients who experienced relapses or not, the only significant difference observed was in the preprocedural left atrial (LA). Furthermore, differences were found in several baseline biomarkers, such as lactate dehydrogenase (LDH), alanine aminotransferase (ALT), Troponins, neutrophil-to-lymphocyte ratio (NLR), and mean corpuscular haemoglobin (MCH).

0: no recurrences 1: recurrences		N	Mean	standard deviation	mean error std.	F	pvalue
GFR	0	83	73,63	16,145	1,772	1,432	,234
	1	29	69,34	18,615	3,457		
IL6	0	77	3,191873	4,0602012	,4627029	,023	,880
	1	28	2,907412	3,4156773	,6455023		
TIMP2	0	92	67,547077	17,8030137	1,8560925	,000	,988
	1	36	71,986293	16,9925353	2,8320892		

LDH	0	97	177,53	27,711	2,814	7,434	**,007***
	1	38	200,24	41,795	6,780		
AST	0	97	25,02	12,970	1,317	1,865	,174
	1	38	23,37	5,533	,898		
ALT	0	97	20,78	13,539	1,375	4,288	**,040***
	1	38	18,84	8,375	1,359		
Iron ∞	0	96	99,85	34,503	3,521	,329	,567
	1	37	96,41	31,700	5,212		
Ferritine +	0	97	278,64	204,869	20,801	,029	,865
	1	37	269,70	221,217	36,368		
Transferrine °	0	97	2,105979	,3013914	,0306017	2,738	,100
	1	37	2,151081	,3336813	,0548569		
TnT	0	95	13,580000	13,1824158	1,3524873	12,933	**,000***
	1	38	31,868421	82,0048651	13,3029458		
NTproBNP	0	95	551,48	850,990	87,310	2,054	,154
	1	37	922,62	960,409	157,890		
CRP	0	97	3,116495	10,7567777	1,0921853	,044	,833
	1	38	2,992105	7,8001518	1,2653517		
Neutrophils*	0	71	3788,59	1333,813	158,295	,205	,652
	1	32	3705,94	1454,051	257,042		
NLR	0	71	2,898955	1,3507838	,1603085	4,943	**,028***
	1	32	3,058945	2,0496477	,3623299		
RBC	0	71	4,203944	,4867956	,0577720	2,093	,151
	1	32	4,190313	,3900578	,0689531		
HB	0	96	12,984375	1,4122269	,1441348	,701	,404
	1	38	12,926316	1,2898113	,2092350		
HCT	0	96	37,506250	3,9055106	,3986045	,196	,659
	1	38	37,644737	3,6822215	,5973352		
MCV	0	96	90,130208	4,3054951	,4394278	1,860	,175
	1	38	89,057895	3,6978907	,5998771		
MCH	0	96	31,194792	1,7316478	,1767356	5,344	**,022***
	1	38	30,565789	1,2281113	,1992260		
MCHC	0	96	34,610417	,9549295	,0974621	4,687	**,032***
	1	38	34,342105	,7008225	,1136884		
Platelet	0	71	213,73	65,088	7,725	2,086	,152
	1	32	206,13	49,467	8,745		
MPV	0	96	10,705208	,9727194	,0992778	,232	,631
	1	38	10,913158	,9412961	,1526984		

Table 2: baseline biomarkers and univariate analysis for differences between groups.
IL6: Interleukin-6 in pg/mL; TIMP_2: Tissue Inhibitor of Metalloproteinases 2 +; LDH: Lactate Dehydrogenase in U/L; AST: Aspartate Aminotransferase in U/L; ALT: Alanine Aminotransferase in U/L; TnT: Troponin T in ng/mL; NT-proBNP: N-terminal pro b-type natriuretic peptide in pg/mL; CRP: C-reactive protein in mg/L; NLR: Neutrophil to Lymphocyte ratio; RBC: red blood cells in million cells per microliter; HB: haemoglobin in g/dL; HCT: Haematocrit in percentage; MCV: Mean Corpuscular Volume in

femtoliters;MCH: Mean Corpuscular Haemoglobin: in picograms; MCHC: Mean Corpuscular Haemoglobin Concentration in g/dL; MPV: Mean Platelet Volume measured in femtoliters.
∞ µg/dL; + in ng/mL; ° in g/L; *Total number per microliter

Postoperative biomarkers

The linear regression analysis of the biomarkers highlighted that the changes in Troponin levels and mean platelet volume (MPV) immediately following ablation were good predictors of arrhythmia relapses, as indicated by a R^2 value (Nagelkerke R^2) of 0.396. Notably, the influence of these biomarkers varied by gender; as MPV was a more significant predictor in women ($R^2 = 0.29$), while changes in Troponin levels were more predictive in men, with a strong R^2 of 0.6.

Established cut-off values were identified 58.1 for Troponin immediately post-procedure, and 20 for MPV. In both scenarios, smaller increases in these biomarkers post-ablation were associated with a higher probability of experiencing arrhythmia relapse.

Recurrences and delta (immediately after ablation)

		B	S.E.	Wald	gl	Sign.	Exp(B)	95% C.I.per EXP(B)	
								Inferiore	Superiore
Phase 3a	Delta_Transferrine	4,746	2,863	2,747	1	**,097**	115,102	,420	31512,051
	DELTA_TROPO_1	-,032	,014	5,200	1	**,023**	,968	,942	,995
	DELTA_MPV_1	-2,640	1,182	4,994	1	**,025**	,071	,007	,723
	Constant	1,764	,879	4,025	1	**,045**	5,834		

a. Variables considered in phase 3: DELTA_MPV_1.

Classification table

Osservato			Predicted		
			Recurrence		Percentage of accuracy
			no	yes	
Fase 3	Recurrence	no	**43**	**4**	**91,5**
		yes	**10**	**8**	**44,4**
	Global Percentage				**78,5**

Variables in the equation

Gender			B	S.E.	Wald	gl	Sign.	Exp(B)	95% C.I.per EXP(B)	
									Inferior	Superior
female	Phase 1[a]	Delta_MPV_1	-3,821	1,994	3,670	1	**,055**	,022	,000	1,092

		Constant	-1,511	,681	4,921	1	**,027**	,221		
male	Phase 2[b]	Delta Transferrin_1	4,819	3,718	1,680	1	**,195**	123,837	,085	180953,626
		Delta_Troponin_1	-,078	,031	6,459	1	**,011**	,925	,872	,982
		Constant	3,148	1,374	5,251	1	**,022**	23,301		
a. Variables considered in phase 1: DELTA_MPV_1.										
b. Variables considered in phase 2: Delta_Transferrin.										

Classification table[a]

Gender				Previsto		
				Recurrence		Percentuale di correttezza
				no	yes	
female	Phase 1	Recurrence	no	**14**	**3**	**82,4**
			yes	**4**	**3**	**42,9**
		Global Percentage				**70,8**
male	Phase 2	Recurrence	no	**28**	**2**	**93,3**
			yes	**2**	**9**	**81,8**
		Global Percentage				**90,2**

The neutrophil-to-lymphocyte ratio (NLR) and changes in Troponin levels measured at the moment of discharge were predictive of recurrence, with a higher occurrence of relapses when the delta at discharge was below 756 for Troponin and 4.4 for NLR, respectively. Interestingly, when analysing the data by gender, only in males were certain biomarkers predictive of relapses: LDH levels above 233, Troponin levels below 745, lymphocyte counts below 1115, NLR below 7.4, and haematocrit (HCT) below 1.55 showed significant predictive value.

Variables in the equation

		B	S.E.	Wald	gl	Sign.	Exp(B)	95% C.I.per EXP(B)	
								Inferiore	Superiore
Fase 2[a]	DELTA_TROPO_2	-,002	,001	6,890	1	**,009**	,998	,997	1,000
	DELTA_NLR_2"	-,218	,085	6,556	1	**,010**	,804	,681	,950
	Costante	1,125	,658	2,919	1		3,080		
a. Variables considered in phase 2: DELTA_TROPO_2.									

Classification table[a]					
			Predicted		
			Recurrence		Percentuale di correttezza
Osservato			no	yes	
Fase 2	Recurrence	no	**58**	**4**	**93,5**
		yes	**20**	**5**	**20,0**
	Global percentage				**72,4**

Variables in the equation

Gender			B	S.E.	Wald	gl	Sign.	Exp(B)	95% C.I.per EXP(B)	
									Inferior	Superior
female	Fase 1	Constant	-,742	,384	3,729	1	**,053**	,476		
male	Fase 5[a]	DELTA_LDH_2	,035	,012	8,079	1	**,004**	1,036	1,011	1,062
		DELTA_TROPO_3	-,006	,002	9,473	1	**,002**	,994	,990	,998
		DELTA_LIMFO_2	,003	,001	4,412	1	**,036**	1,003	1,000	1,005
		DELTA_NLR_"	-,340	,169	4,072	1	**,044**	,712	,511	,990
		DELTA_HCT_2	-,637	,249	6,566	1	**,010**	,529	,325	,861
		Costant	-4,573	2,587	3,126	1	**,077**	,010		

a. Variables considered in phase 5: DELTA_LIMFO_2.

Classification table[a]						
				Previsto		
				Recurrence		Percentage of accuracy
Gender				no	yes	
female	Fase 1	Recurrence	no	**21**	**0**	**100,0**
			yes	**10**	**0**	**0,0**
		Global percentage				**67,7**
male	Fase 5	Recurrence	no	**37**	**4**	**90,2**
			yes	**2**	**13**	**86,7**
		Global percentage				**89,3**

RECURRENCES in persAF	B	S.E.	Wald	gl	Exp(B)	95% C.I.per EXP(B)		Sign.
						Inferiore	Superiore	
delta_TIMP2_2	,030	,015	3,980	1	1,030	1,001	1,061	**,046**

Ratio power/delta

Following the above findings, a "Power to Release Ratio" (PTRr) was applied. This was calculated by dividing the change in biomarker levels between two-time points (delta 1 and delta 2) by the total amount of energy delivered during the ablation procedure. Specifically, the PTRr for delta LDH (below 0.00018), delta iron (below 0.0002), and delta troponin (below 0.0016) measured immediately after ablation (time 1) showed a moderate correlation with recurrence of arrhythmia ($R^2 = 0.45$). Additionally, the PTRr for the NLR (0.00013) measured at discharge demonstrated a weaker predictive capability ($R^2 = 0.12$) in forecasting arrhythmia recurrences.

Variables in the Equation									
		B	S.E.	Wald	df	Sig.	Exp(B)	95% C.I.for EXP(B)	
								Lower	Upper
Step 3[a]	Ratio_DELTA_LDH_1	-2048,523	957,320	4,579	1	**,032**	0,000	0,000	,000
	Ratio_DELTA_Iron_1	7814,229	3496,256	4,995	1	**,025**			
	Ratio_DELTA_Troponin_1	-1861,372	745,174	6,240	1	**,012**	0,000	0,000	,000
	Constant	1,174	,917	1,639	1	**,200**	3,234		

Classification Table[a]					
			Predicted		
			Recurrence		Percentage Correct
Observed			no	yes	
Step 3	Recurrence	no	**37**	**4**	**90,2**
		yes	**6**	**8**	**57,1**
	Overall Percentage				**81,8**

Variables in the Equation									
		B	S.E.	Wald	df	Sig.	Exp(B)	95% C.I.for EXP(B)	
								Lower	Upper
Step 1[a]	Ratio_DELTA_NLR_"	-7719,535	3818,609	4,087	1	**,043**	0,000	0,000	,000
	Constant	-,728	,341	4,556	1	**,033**	,483		
a. Variable(s) entered on step 1: Ratio_DELTA_NLR_".									

Classification Table[a]	
Observed	Predicted

			Recurrence		
			no	yes	Percentage Correct
Step 1	Recurrence	no	**51**	**0**	**100,0**
		yes	**13**	**3**	**18,8**
	Overall Percentage				**80,6**

Dynamic variation of Biomarkers

The variation of the biomarkers in the perioperative period of the ablation, revealed that all the biomarkers analysed displayed significant changes except for TIMP2 and ALT as observed using the Huynh-Feldt analysis. However, the mixed-design ANOVA to compare these changed in who experienced relapses of atrial arrhythmias or not, showed significant differences between the two groups only in Troponin (Huynh-Feldt Pvalue 0.008) and Haemoglobin levels variations (Huynh-Feldt Pvalue 0.04).

Source			Type III Sum of Squares	df	Mean Square	F	Sig.	Partial Eta Squared	Noncent. Parameter	Observed Power[a]
Tempo	IL6	Huynh-Feldt	6688,026	1,060	6311,804	10,355	**,002**	,163	10,973	,898
	TIMP2	Huynh-Feldt	989,685	1,649	600,296	2,662	,086	,048	4,389	,467
	LDH	Huynh-Feldt	37526,827	1,429	26258,634	16,957	**,000**	,242	24,234	,997
	AST	Huynh-Feldt	9312,235	1,048	8883,163	26,396	**,000**	,332	27,671	,999
	ALT	Huynh-Feldt	890,383	1,032	863,044	2,760	,101	,049	2,847	,377
	Iron	Huynh-Feldt	18456,309	1,102	16741,139	19,837	**,000**	,272	21,870	,995
	Ferritin	Huynh-Feldt	62708,309	1,565	40062,917	30,524	**,000**	,365	47,777	1,000
	Transferrin	Huynh-Feldt	1,743	1,205	1,447	20,427	**,000**	,278	24,606	,998
	TnT	Huynh-Feldt	36191463,848	1,010	35821370,858	155,110	**,000**	,745	156,712	1,000
	NTproBNP	Huynh-Feldt	2362851,348	1,017	2322576,372	5,714	**,020**	,097	5,813	,656
	CRP	Huynh-Feldt	840,587	1,002	838,534	10,914	**,002**	,171	10,941	,901
	NLR	Huynh-Feldt	296,346	1,412	209,823	37,758	**,000**	,416	53,328	1,000
	HB0	Huynh-Feldt	30,741	1,932	15,913	51,790	**,000**	,494	100,045	1,000
	MCV	Huynh-Feldt	4,439	1,426	3,112	1,983	,157	,036	2,828	,336
	PLT	Huynh-Feldt	2593,716	1,877	1381,681	6,274	**,003**	,106	11,778	,873
	MPV	Huynh-Feldt	2,021	1,913	1,056	14,182	**,000**	,211	27,132	,998

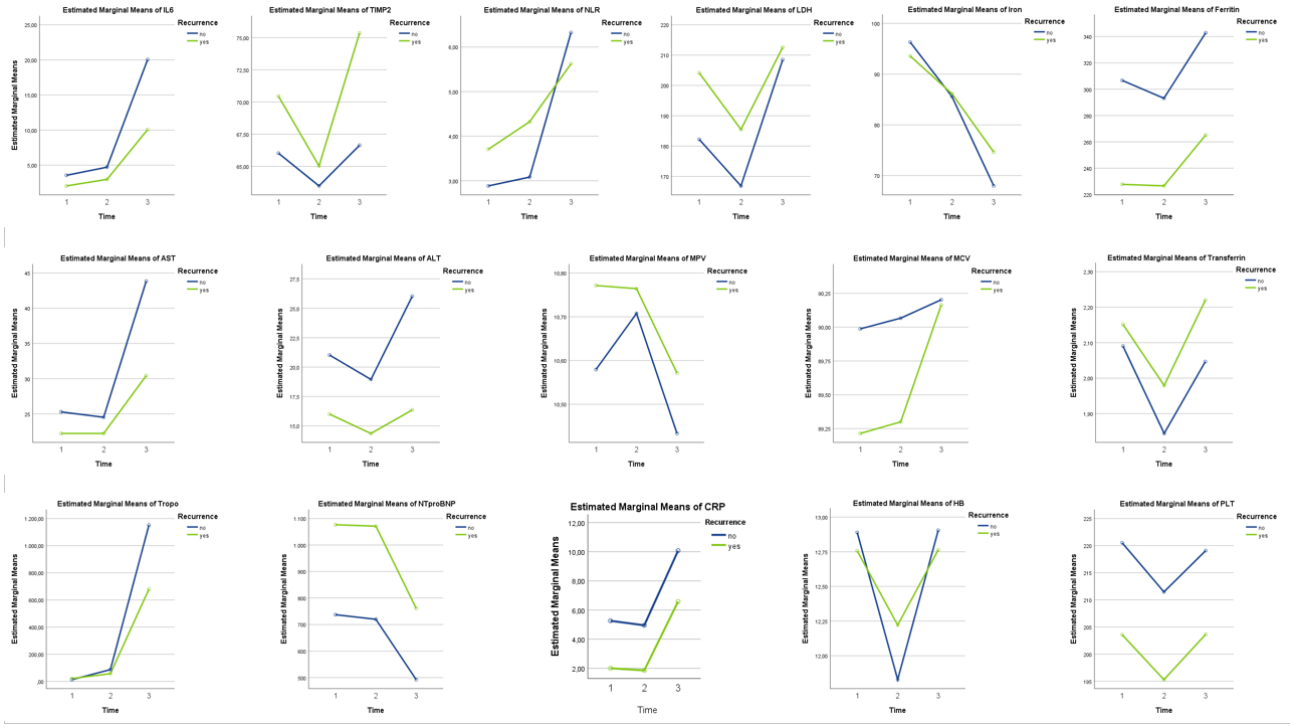

Discussion

Two are the main findings of the study: i) disparities in delta of troponin, mean platelet volume (MPV), neutrophil-to-lymphocyte ratio (NLR), lymphocytes, and lactate dehydrogenase (LDH) have been identified as predictive of AF relapses post-catheter ablation. Particularly, lower increments in troponins and inflammatory markers appear prognostic of relapses. Intriguingly, gender-specific variations in troponin levels and MPV have also been observed with a more predictable behaviour in the male population. Notably, despite not being statistically different, the persistent form of AF exhibits distinct predictive biomarker profiles for relapses, exemplified by TIMP-2 levels at discharge. A persistent question, which also draws on insights from prior research on this topic, is whether the observed change in biomarker levels indicates superior lesion formation or merely reflects the health of the tissue. Specifically, while an effective ablation might lead to a significant increase in biomarker levels, fibrotic tissue, which has fewer viable myocytes (as seen in atrial cardiomyopathy), might release fewer biomarkers even though the energy applied could still create effective lesions. To address this uncertainty, we introduced a new parameter called the “Power to

Release Ratio" (PTRr). This ratio quantifies the behaviour of biomarkers relative to the total amount of energy delivered to the tissue, providing a more nuanced interpretation of biomarker dynamics post-ablation. Our analysis revealed that the release of Troponin immediately post-ablation, along with Iron and LDH, consistently served as a reliable predictor of arrhythmia relapse. Additionally, at the time of discharge, the PTRr for the neutrophil-to-lymphocyte ratio (NLR) also showed an acceptable level of predictability for arrhythmia relapses. Overall, our findings suggest that integrating biomarker analysis with clinical and imaging parameters (LA diameters and strain for example – see supplements materials for details) could enhance the stratification of risk for AF recurrence following PVI. Further research is needed to explore these predictors in other contexts. First of all, larger studies could provide enough data to elaborate a scoring system that could eventually lead to the continuation or discontinuation of antiarrhythmic therapy after the ablation. Most interestingly, however, in the context of other forms of energy applied for ablation, such as pulse field ablation, other parameters could be used as a surrogate of energy administered during RF catheter ablation, and define the "expected response of the tissue". Such studies could help refine the assessment tools available for predicting AF recurrence, leading to more targeted and effective post-operative management.

References:

1. Hindricks G, Potpara T, Dagres N, et al. 2020 ESC Guidelines for the diagnosis and management of atrial fibrillation developed in collaboration with the European Association for Cardio-Thoracic Surgery (EACTS). *Eur Heart J*. 2021;42(5):373-498. doi:10.1093/eurheartj/ehaa612

2. Kirchhof P, Benussi S, Kotecha D, et al. 2016 ESC Guidelines for the management of atrial fibrillation developed in collaboration with EACTS. *Eur Heart J*. 2016;37(38). doi:10.1093/eurheartj/ehw210

3. Calkins H, Hindricks G, Cappato R, et al. 2017 HRS/EHRA/ECAS/APHRS/SOLAECE expert consensus statement on catheter and surgical ablation of atrial fibrillation. *Hear Rhythm*. 2017;14(10):e275-e444. doi:10.1016/j.hrthm.2017.05.012

4. Al-Hijji MA, Deshmukh AJ, Yao X, et al. Trends and predictors of repeat catheter ablation for atrial fibrillation. *Am Heart J*. 2016;171(1):48-55. doi:10.1016/j.ahj.2015.10.015

5. Liang JJ, Elafros MA, Chik WW, et al. Early recurrence of atrial arrhythmias following pulmonary vein antral isolation: Timing and frequency of early recurrences predicts long-term ablation success. *Hear Rhythm*. 2015;12(12):2461-2468. doi:10.1016/j.hrthm.2015.07.015

6. Jiang H, Wang W, Wang C, Xie X, Hou Y. Associationofpre-ablation levelofpotential blood markers with atrial fibrillation recurrence after catheter ablation: A meta-analysis. *Europace*. 2017;19(3):392-400. doi:10.1093/europace/euw088

7. Verma A, Kilicaslan F, Pisano E, et al. Response of atrial fibrillation to pulmonary vein antrum isolation is directly related to resumption and delay of pulmonary vein conduction. *Circulation*. 2005;112(5):627-635. doi:10.1161/CIRCULATIONAHA.104.533190

8. Balk EM, Garlitski AC, Alsheikh-Ali AA, Terasawa T, Chung M, Ip S. Predictors of atrial fibrillation recurrence after radiofrequency catheter ablation: A systematic review. *J Cardiovasc Electrophysiol*. 2010;21(11):1208-1216. doi:10.1111/j.1540-8167.2010.01798.x

9. Carballo D, Noble S, Carballo S, et al. Biomarkers and arrhythmia recurrence following radiofrequency ablation of atrial fibrillation. *J Int Med Res*. 2018;46(12):5183-5194. doi:10.1177/0300060518793807

10. Nakanishi K, Fukuda S, Yamashita H, et al. High-sensitive cardiac troponin Tas a novel predictor for recurrence of atrial fibrillation after radiofrequency catheter ablation. *Europace*. 2017;19(12):1951-1957. doi:10.1093/europace/euw314

11. M K, M H, JY K, et al. Clinical relationship between anemia and atrial fibrillation recurrence after catheter ablation without genetic background. *Int J Cardiol Hear Vasc*. 2020;27. doi:10.1016/J.IJCHA.2020.100507

12. S L-L. Mechanisms of cardiac iron homeostasis and their importance to heart function. *Free Radic Biol Med*. 2019;133:234-237. doi:10.1016/J.FREERADBIOMED.2018.08.010

13. Coppens M, Eikelboom JW, Hart RG, et al. The CHA2DS2-VASc score identifies those patients with atrial fibrillation and a CHADS2 score of 1 who are unlikely to benefit from oral anticoagulant therapy. *Eur Heart J*. 2013;34(3):170-176. doi:10.1093/eurheartj/ehs314

Supplementary materials

Echocardiographic assessment

Comprehensive Transthoracic echocardiography (TTE) was performed as part of routine clinical practice using a high-quality ultrasound system (GE Vivid E9, E95 or S70, GE Healthcare Horten, Norway or Epiq 7C, Philips Healthcare, Eindhoven, The Netherlands). Echocardiographic examinations were performed following the recommendations of the American Society of Echocardiography and the European Association of Cardiovascular Imaging. Multiple acoustic windows including apical five-chamber and three-chamber, right parasternal, and suprasternal views was systematically acquired (1). If patients were in sinus rhythm, 3 cardiac cycles were averaged for

all measures, whereas for those in atrial fibrillation, 5 cardiac cycles were averaged. The recorded images were reviewed by two cardiologists with more than 10-year experience in echocardiography. LVEF was calculated using Simpson's biplane method. LV diastolic function was assessed by E, e' velocities, E/e', left atrial volume index (LAVi), and tricuspid regurgitation velocity. Determination of LV diastolic function was made using the algorithm proposed by the guidelines (2). The left atrial reservoir strain (LARS) was defined as the first peak positive deflection and represented the LA reservoir function. The LARS was calculated as the mean longitudinal strain in 2 apical views (4 and 2 chambers) using R-R gating as the zero-reference point.

Postoperative parameters

Compared to patients who experienced recurrences of atrial arrhythmia, patients who did not show a smaller LA volume and LA strain measurements—reservoir, conduit, and contraction. Linear regression analysis revealed that LA volume and LA strain measurements could predict AF recurrences. This trend was also evident in the analysis of major adverse cardiovascular events (MACE) that occurred during the follow-up period. Cut-off values, determined using the Youden's index, were set at 49.5 mL for LA volume, 25.50% for reservoir strain, -15.50% for conduit strain, and -4.5% for contraction strain.

	Recurrences	No recurrences	P value
LAS reservoir	21.23 (11.02)	25.93 (9.7)	0.4
LAS conduit	14.96 (7.3)	15.93 (6.2)	0.6
LAS contraction	6.73 (6.04)	9.77 (6.6)	0.8
LAS volume	64.73 (27)	52.61 (17.3)	**0.003***
LAS: left atrial strain			

Recurrence		N	Media	Deviazione std.	pvalue
LASreservoirPOST	no	82	25,93	11,016	0.4
	yes	26	21,23	9,668	
LASconduitPOST	no	82	15,93	6,200	0.6

	yes	26	14,96	7,264	
LAScontractionPOST	no	82	9,77	6,570	0.8
	yes	26	6,73	6,044	

RECURRENCES	B	S.E.	Wald	df	Exp(B)	95% C.I.for EXP(B)		Sig.
						Lower	Upper	
LAvolume	,029	,011	6,927	1	1,029	1,007	1,052	**,008***
LASreservoirPOST	-1,370	,571	5,764	1	,254	,083	,778	**,016***
LASconduitPOST	1,390	,574	5,875	1	4,017	1,305	12,364	**,015***
LAScontractionPOST	1,314	,562	5,461	1	3,723	1,236	11,210	**,019***
LavolumePOST	,029	,013	4,704	1	1,029	1,003	1,056	**,030***
Variable(s) entered on step 1: Overweight, diabetes, Hypertension, CongestiveHF, Age, LASreservoirPOST, LASconduitPOST, LAScontractionPOST, LavolumePOST, EchoLADiam, LVEF.								

MACE	B	S.E.	Wald	df	Sig.	Exp(B)	95% C.I.for EXP(B)	
							Lower	Upper
LASreservoirPOST	-1,566	0,65	5,812	1	0,209	0,058	0,746	**0,016**
LASconduitPOST	1,61	0,655	6,046	1	5,001	1,386	18,045	**0,014**
LAScontractionPOST	1,484	0,633	5,492	1	4,411	1,275	15,263	**0,019**
Variable(s) entered: Overweight, diabetes, Hypertension, CongestiveHF, Age, LASreservoirPOST, LASconduitPOST, LAScontractionPOST, LavolumePOST, EchoLADiam, LVEF.								

Ablation procedure

All the procedures were performed under general anaesthesia. Access to the femoral vein was obtained and basal blood samples were collected (T0). Subsequently, the procedure was performed according to the usual practice. Imaging techniques such as 3D rotational angiography or electro-anatomical reconstruction of the left atrium were employed. Pulmonary vein isolation was then performed. PVI consisting in a linear lesion around the ostium of the pulmonary veins (PV) was the standard treatment for all patients. Other sets of ablations, based on the operator's discretion, were allowed. 10 min after last ablation was performed, and isolation reassessed, if no recurrences were noted, the procedure was terminated. Different techniques, including point-by-point and single-shot

methods, were employed. Radiofrequency (RF) used cooled catheters irrigated by a saline flow, using contact force sensing catheters with either Low Power Long Duration (25-35W) or High-Power Short Duration (50 W) setting. Single-Shot Methods included cryo-ablation performed either via a balloon (specifically, the The Arctic Front Cardiac Cryoablation Catheter, Medtronic) or the ultralow temperature cryoablation using near-critical nitrogen (by Adagio Medical Cryoablation System, USA). Laser-ablation was performed with the HeartLight X3 System. Pulse Field Ablation (PFA) was applied in brief electrical pulses to the entrance of each pulmonary vein, utilizing the Varipulse catheter by Biosense. Immediately following the PVI procedure, if the patient remained in AF, a Direct Current Cardioversion (DCCV) was performed. A blood sample was also collected at this time (T1). Before discharge, blood samples were taken within 12 (T2). Additionally, imaging of the left atrium is assessed using a 2D standard transthoracic echocardiogram within 12 hours after the procedure.

Ultralow temperature cryoablation using near-critical nitrogen for cavotricuspid isthmus-ablation, first-in-human results

Martijn N. Klaver MD, Tom J. R. De Potter MD, Konstantinos Iliodromitis MD, PhD, Alexander Babkin PhD, DSc, David Cabrita, Davide Fabbricatore MD, Lucas V. A. Boersma MD, PhD

https://doi.org/10.1111/jce.15142

Abstract

Introduction: Cryoablation has evolved as a safe alternative to radiofrequency ablation in the treatment of several supraventricular arrhythmias and has potential advantages, yet is limited by the properties of the cryogen used. We investigated a novel ultralow temperature cryoablation (ULTC) system using nitrogen near its liquid-vapor critical point as a freezing source, achieving temperatures as low as -196 degrees Celsius in a long linear catheter with a continuous energy release. Initial safety, procedural and efficacy outcomes of ULTC are described in patients undergoing cavotricuspid isthmus (CTI) ablation.

Methods and Results: The Cryocure studies (NCT02355106, NCT02839304) are prospective, single-arm, multi-center, first-in-human clinical studies in 17 patients with atrial flutter (AFL) and 13 patients with atrial fibrillation (AF). A total of 30 patients, mean age 65 ± 8 years old and 67% male, were enrolled and underwent ablation of the CTI. Acute success, defined as the confirmation of stable bidirectional conduction block across the CTI, was achieved in all 30 patients. After 12 months of follow-up, 14 out of 17 AFL patients remained free from any AFL. One (3.3%) procedure-related but not device-related serious adverse event was reported, involving transient inferolateral ST-elevation associated with temporary AV conduction block.

Conclusion: In this first-in-human clinical study the safety and performance results demonstrate the capabilities of ultralow temperature near-critical nitrogen as an effective energy source for CTI ablation. Ongoing, larger, studies should confirm our findings and evaluate the capabilities to create linear and focal transmural lesions in other arrhythmias.

1 INTRODUCTION

Ablation treatment has acquired a prominent role in the treatment of supraventricular arrhythmias, leading to an increasing demand for operating rooms and operator time. New technologies aim to improve the efficacy, speed and durability of ablation treatment. Cryoablation has evolved as a safe alternative to radiofrequency (RF) ablation in the ablation of supraventricular arrhythmias.[1-6] Potential advantages of cryothermal energy are catheter stability due to adherence to myocardial tissue, the ability of reversible cryomapping mitigating the risk of permanent damage to critical structures like the atrioventricular (AV) node, a low risk of thrombus formation and systemic embolization, and a low probability of myocardial perforation due to the preservation of tissue architecture.[1, 2, 5, 7-10] Yet, efficacy of cryoablation using gaseous cryogens may be hampered by physiological reversibility of cellular injury when ablation times are too short or freezing temperatures not low enough, allowing thicker areas of myocardium to recover from freezing injury and recurrence of arrhythmias to occur.[11, 12] he efficiency and speed of cryoablation is first and foremost determined by cryogen that is used in the ablation catheter. Classic cryoablation systems have used gaseous cryogens (predominantly nitrous oxide gas [N_2O]), which have a much lower thermal capacity due to their small density when compared to liquid cryogens. This limits the catheters' overall cooling power, cooling speed, minimum temperature and effective cooling surface, while resulting in a massive gas consumption, mandating multiple applications (freeze-thaw-cycles) of several minutes.[12-15] Although liquid cryogens possess much higher thermal conduction and greater heat capacity than N_2O, they are difficult to handle in endovascular catheters and considered unreliable and unsafe. Nitrogen near its liquid-vapor critical point (near-critical nitrogen) provides a unique solution that can be used in cardiac applications. Owing to its very low viscosity, it can be flowed down tiny channels while providing a freezing capacity that can overcome endovascular heat sinks. This new concept of near-critical cooling makes it possible to maintain an uninterrupted flow of a cryogen close to its critical state along the full catheter length. It also solves issues related to slow “start-stop” times present in liquid cryogen flow systems, limited to larger probe sizes.[12] Recently, Adagio Medical has developed a novel cryoablation system using near-critical nitrogen as a freezing source, achieving temperatures as low as −196°C in a 9F linear catheter with continuous energy release. This could overcome many of the efficiency and speed limitations with prior cryoablation platforms. Preclinical data demonstrated that ultralow temperature cryoablation (ULTC) is highly effective and capable of creating durable, transmural and contiguous atrial and ventricular lesions in an in vivo model in large animals.[16] In this first-in-human study, we describe the initial safety and efficacy outcomes using the Adagio ULTC system to create durable bidirectional cavotricuspid isthmus (CTI) conduction block.

2 METHODS

2.1 Study population

The Cryocure 1 (CC1, NCT02355106) and Cryocure 2 (CC2, NCT02839304) clinical studies are prospective, single-arm, multi-center, first-in-human clinical studies to assess the initial safety and performance of the Adagio Medical Cryoablation System. The treatment population consisted of patients from CC1 and CC2 in which ablation of the CTI was performed. CC1 enrolled patients with a typical atrial flutter (AFL) pattern on ECG to undergo CTI alone. In CC2, patients with atrial fibrillation were enrolled and ablation of the CTI was performed as an adjunct target on top of left atrial ablation targets to obtain freedom of atrial fibrillation (AF), neither of which are the subject of this manuscript. Between January 2015 and May 2015 and between April 2017 and February 2019, all patients were enrolled in the two participating hospitals, "St. Antonius Ziekenhuis," Nieuwegein, The Netherlands and the "Onze-Lieve-Vrouw Ziekenhuis," Aalst, Belgium. The study protocol was approved by the Ethics committee, regulatory authorities and the institutional review board of both hospitals. All patients gave written informed consent. The medical history was reviewed, together with a physical exam to confirm inclusion and exclusion criteria.

2.2 The Adagio atrial flutter cryoablation system

The Adagio Cryoablation System consists of the Cryoablation Console and the Cryoablation Catheter. Treatment is achieved by ablating (or isolating) the arrhythmogenic tissue in contact with a distal freezing element of the catheter. During the treatment, the freezing element is cooled to cryogenic temperatures resulting in necrosis (ablation) of the tissue in contact with the catheter. The Adagio Catheter may create both linear (up to 54 mm) and focal lesions, depending on the length of the freezing element extended outside of the sheath. The Adagio Cryoablation Console (Console) is a stand-alone, electronic device providing the cryoablation energy and control mechanisms for the System. The delivery of thermal energy is created by pressurizing nitrogen to critical pressures (CN_2), cooling it down to approximately -196 degrees Celsius, using a liquid nitrogen heat exchanger and delivering the energy to a freezing element at the distal end of the catheter. This process is created and controlled within the Console.

The Adagio Cryoablation catheter is a single-use, sterile device that connects directly to the console and provides the delivery mechanism of the cryoenergy to the targeted tissue. The circumference of the catheter is 9.0 French. A thermocouple at the distal portion (freezing element) provides temperature readouts for operational status. In addition, the cryoablation catheters include electrodes along the freezing zone to enable verification of tissue contact and fluoroscopic landmarks for correct

positioning of the catheter's freezing element within the right atrium (Figure 1). No mapping system is required. The catheter includes a closed, internal lumen where the non-insulated portions (37–54 mm freezing element) can achieve cryoablation temperatures. An active vacuum channel surrounds the closed, internal lumen insulating the nonfreezing portions from cold temperatures, preventing all surfaces, other than the freezing zone, from developing cold temperatures. The catheter connects to the Adagio Cryoablation Console through a multi-channel locking connector at the proximal end. To gain access to the inner walls of the beating heart, a commercially available guiding sheath was placed within the vasculature via a percutaneous femoral vein puncture as per normal vascular access procedures (Seldinger technique). The guiding sheath provides the conduit for the Cryoablation catheter to be placed near the targeted tissue to be ablated. The size and geometry of the catheter freezing zone (distal tip) can be customized to suit the desired target for ablation using a stylet. The catheter can be used in a linear convex, concave or circular shape, as well as focal. For CTI ablation, using a linear convex or concave approach, it is designed to easily contact and cover the CTI tissue, allowing for a single freeze once appropriate contact is made between the distal tip of the catheter and the CTI. The convex approach may overcome pouches along the CTI. The correct catheter position within the CTI is verified by using both fluoroscopy and the catheter electrodes, which enable verification of tissue contact and correct location of the cryoablation element within the right atrium. This makes its positioning easier, shortens the procedure time, and eliminates the need for an additional diagnostic catheter. The use of an electro anatomical mapping system is possible but not mandatory.

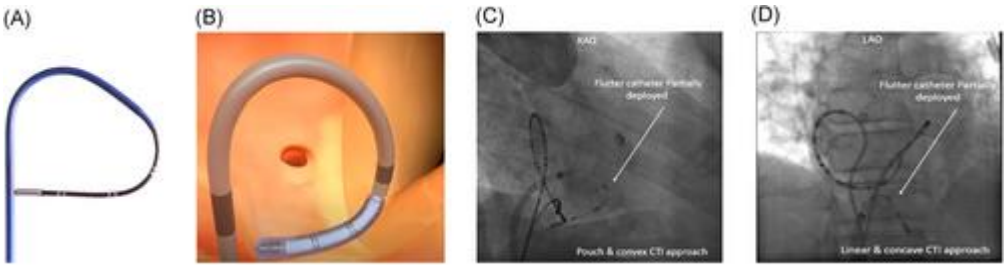

Figure 1: Adagio cryoablation catheter and fluoroscopic images of catheter positioning. (A) Photograph and (B) illustration of the Adagio medical flutter catheter using a convex approach. (C) Fluoroscopic visualization in a right anterior oblique projection of the convex approach and (D) the linear approach is visualized on fluoroscopy in a left anterior oblique projection

2.3 Electrophysiology study and ablation

Subjects were treated under conscious sedation or general anesthesia (GA) and prepared for ablation according to local standard. The procedures were performed under continued oral anticoagulation with vitamin K-antagonists (target international normalized ratio between 2.0 and 3.0) or uninterrupted non-vitamin K oral anticoagulants. All patients were then given an intravenous heparin bolus based on their weight. Once the cryoablation catheter was placed at the target ablation sites, freezes of one minute (limited to two minutes) in duration were performed along the CTI. Applications were continued until there was clear evidence of bidirectional conduction block (BCB). Repeat documentation of BCB was performed at a minimum of 30 min following the last ablation. BCB was confirmed using standard pacing methods and considered stable BCB if no conduction recovered. If conduction recovered, additional ablations were allowed, and the process for BCB verification at 30 min postablation was reinitiated. The use of isoproterenol for additional assessment of isthmus conduction was allowed at the investigators' discretion. At the completion of all ablation and mapping procedures, catheters and sheaths were removed, and hemostasis was obtained following the institutions standard of care. There were no pre-specified requirements for length of stay or resumption of medications including, anticoagulation or antiarrhythmic drug therapy.

2.4 Post-ablation management and follow-up

All patients were monitored in hospital for 24 h. In the follow-up phase of the study, two clinic visits were scheduled, followed by standard of care follow-up until 12 months after the ablation procedure. During the clinic visits, a medical history, physical examination and 12-lead ECGs were examined for an evaluation of patient arrhythmia status and any evidence of adverse events. Holter monitoring or event monitoring was performed when symptoms occurred and was left at the discretion of the treating physician. Additional follow-up was collected up to 12 months after the procedure according to the hospitals' standard of care. All ECGs, continuous ECG monitoring and repeat electrophysiology studies (EPS) were reviewed for recurrent arrhythmias.

2.5 Outcome measures

The primary objective of the study was to provide data on the safety of ULTC using the Adagio medical device for CTI ablation. All safety events were classified by the severity of the event, the relationship of the event to the study device or procedure and whether the event or severity of the event was anticipated or unanticipated. All serious adverse events, unanticipated events and events of an unexpected severity were investigated by the Independent Data Safety Monitoring Board (DSMB) to determine the relationship to the investigational device. Serious adverse events were classified according to the MEDDEV definitions.

The secondary objective of the study was to access the performance of ULTC using the Adagio catheters. Acute success was defined as the confirmation of complete bidirectional conduction block across the cavotricuspid isthmus at the end of the cryoablation procedure after a minimum of 30 min following the last CTI freeze (stable BCB). The procedural characteristics, i.e. total procedure duration, fluoroscopy time and catheter dwell time were only collected for the CC1 patients (AFL). Ablation characteristics, i.e. cumulative freeze duration, number of freezes and length of each freeze, time until block and freezes until block were collected in all CC1 and CC2 patients (AFL and AF). When repeat EPS was performed during follow-up, CTI conduction was evaluated and findings obtained (AFL and AF). Long-term success was defined as the number of patients free from recurrent AFL on ECG at 12 months. Long-term success was only collected in CC1 patients (symptomatic AFL).

2.6 Data collection

Data collected at all visits were entered through a web-based electronic data capture system. The data were monitored following ISO 14155, Good Clinical Practice and in compliance with the Clinical Monitoring Plan. Maintenance of the study database was performed by the sponsor. As needed, data clarification requests were issued to sites and resolved to completion. The data underlying this article were provided by the sponsor. Data will be shared on request to the corresponding author with permission of the sponsor.

2.7 Statistical analysis

Descriptive statistics for all variables were applied. For continuous variables, mean and standard deviation or median and interquartile range, minimum and maximum were reported. For ordinal and categorical variables, counts and percentages were applied.

3 RESULTS

In a total of 30 patients, CTI ablation was performed; 17 from the CC1 cohort and 13 from the CC2 cohort (mean age was 65 ± 8 years old and 67% male). All patient characteristics are shown in Table 1. Procedural data are summarized in Table 2. CC1 patients were the first to be treated with the cryoablation system, while the CC2 patients were all part of a subsequent study.

Table 1. Baseline characteristics

Characteristics	Result
CTI only procedure	17 (56.7%)

Characteristics	Result
CTI adjunct procedure	13 (43.3%)
Mean age	64.5 ± 7.6 years
Male gender	20 (66.7%)
Mean left ventricular ejection fraction	55% ± 6%
Medical history	
Hypertension	16 (53.3%)
Diabetes	4 (13.3%)
Coronary artery disease	5 (16.7%)
Prior stroke/TIA	1 (3.3%)
Congestive heart failure	1 (3.3%)
Significant valvular disease	1 (3.3%)
Cardiomyopathy	4 (13.3%)
Ischemic	1 (3.3%)
Hypertrophic	3 (10.0%)

- Abbreviations: CTI, cavotricuspid isthmus; TIA, transient ischemic attack.

Table 2. Procedural characteristics

Procedure data CC1 (*n* = 17)**a**	Result
Procedure time (incl. 30-minute waiting time) (minutes)**a**	85 ± 16 (54–116)
Fluoroscopy time (minutes)**a**	12 ± 5 (4–20)
Catheter dwell time (minutes)**a**	54 ± 14 (37–84)

Procedure data CC1 (*n* = 17)a	Result
CTI ablation data (*n* = 30)	
Total CTI freeze time (minutes), median (IQR)	4.0 (2.9–5.3) (2.0–12.0)
Number of freezes per patient (incl. bonus freeze), median (IQR)	4 (2–5) (2–12)
Average duration per freeze (minutes), median (IQR)	1.1 (1.0–2.0) (0.55–2.0)
Freeze time until BCB (minutes), median (IQR)	1.7 (0.67–4.0) (0.23–8.7)
Number of freezes until BCB, median (IQR)	3 (1–4) (1–11)
Number of subjects with BCB during first freeze	12 (40%)

- Abbreviations: AFL, atrial flutter; BCB, bidirectional conduction block; CTI, cavotricuspid isthmus; IQR, inter quartile range.
- [a] Data was only available for CryoCure 1 patients.

3.1 Safety

Safety data was available in all patients. There was one serious adverse event reported among 30 patients (Table 3). The event consisted of transient ST-elevation in the inferolateral limb leads of the 12-lead ECG associated with a temporary AV conduction block, during a procedure in which GA was used. No medications were administered, and the ECG changes resolved spontaneously within a minute, including normal AV conduction. At the completion of the procedure, the patient was awake and free of symptoms. The patient was discharged the following morning as per standard hospital protocol postablation. The discharge and follow-up ECGs showed sinus rhythm with normal AV-conduction. The DSMB classified the event as serious, severe in intensity, and related to the procedure but not related to the device. The cause of the event was attributed to vasospasm of the right coronary artery due to a lateral placement of the cryoablation catheter.

Table 3. Adverse events

Event term	SAE	Relationship to procedure	Relationship to device	Severity
Coronary artery spasm	Yes	Yes	No	Severe

- Abbreviation: SAE, severe adverse event.

3.2 Performance

Acute success, defined as the confirmation of complete bidirectional conduction block across the CTI at the end of the cryoablation procedure after a minimum of 30 min waiting time following the last freeze, was achieved in 30 out of 30 patients (100%). No patients showed conduction recovery after the 30-minute waiting time. During follow-up of the CC1 group, three patients presented with recurrence of documented typical AFL after 3, 9 and 12 months respectively (Table 4). Repeat EPS was performed in 2 out of 3 patients, which confirmed recurrence of CTI-conduction and inducible CTI-dependent flutter for which repeat-ablation was performed in both patients. The third patient did not undergo repeat EPS, and recovery of CTI conduction is unknown. Overall, after 12 months of follow-up, 14 out of 17 patients remained free from typical atrial flutter (82.4%). In 10 of 30 patients repeated EPS was performed (8 in the CC1 group, 2 in the CC2 group) for recurrent AF or AFL, allowing reassessment of conduction over the CTI. In 7 out of 10 patients (70.0%) EPS demonstrated durable bidirectional block after a median of 11 [6-12] months. Recurrent conduction was seen in two symptomatic patients with documented return of AFL, both from the CC1 group and in one patient from the CC2 group, where no AFL was documented.

Table 4. Long-term performance

	Discharge AFL free	**3 Months AFL free**	**6 Months AFL free**	**9 Months AFL free**	**12 Months AFL free**	**Repeat EPS**	**Durable CTI block**
CC1 patients (17)	17/17, 100%	16/17, 94.1%	16/17, 94.1%	15/17, 88.2%	14/17, 82.4%	8/17, 47.1%	6/8, 75%
CC2 patients (13)	13/13, 100%					2/13, 15.4%	1/2, 50%

- Abbreviations: AFL, atrial flutter; CTI, cavotricuspid isthmus; EPS, electrophysiology study.

4 Discussion

This is the first-in-human clinical trial evaluating the use of near critical nitrogen as a cryogen for catheter ablation of the CTI in 30 patients. This proof-of-concept study demonstrates that the Adagio cryoablation system is able to safely perform cryoablation of the CTI with encouraging acute and long-term success rates, while showing favorable procedure characteristics and minimal safety concerns.

4.1 Acute success and procedural outcomes

We demonstrated acute efficacy in 30 out of 30 (100%) of patients, without the use of electro-anatomic navigation, while procedure and fluoroscopy times were reduced compared with those reported in literature.14, 17, 18 A median of 3 + 1 bonus freeze was needed to achieve BCB and 40% of the patients showed BCB after the first freeze. In previous studies, acute success, defined as bidirectional conduction block, is reported in 85-97% of procedures and in agreement with our findings.2, 18-21 In general, reported procedure times for cryoablation tend to be longer than procedures using radiofrequency ablation (120–246 min and 99–198 min, respectively).22 Available cryoablation systems use a focal "point by point" energy delivery, requiring several freeze-thaw cycles of many minutes.13, 14 Ablation using RF requires shorter applications and has no additional thaw time due to the lack of catheter adhesion. Using RF ablation, lines are created using a "drag and burn" method across the CTI followed by selective touch-up to complete conduction block. The reduced procedure time (85 ± 16 min) found in our study as compared to both cryoablation and RF ablation may be attributed to the single-shot design, using a large 37–54 mm freezing element, as well as the increased cooling power and cooling speed of near-critical nitrogen, reducing the number and duration of freeze-thaw cycles needed to create consistent ablation lines. For both cryoablation and RF ablation, a larger ablation tip is associated with reduced time to achieve conduction block and shorter overall procedure times.14, 20 Consequently, the small number of freezes needed to acquire conduction block further decreased the use of fluoroscopy.

4.2 Long-term performance and durable conduction block

In our study, 12-month recurrence of typical AFL on ECG was reported in 3 out of 17 AFL patients (17.6%), and in two patients conduction was confirmed during repeat EPS. A meta-analysis performed by Pérez et al., including 9942 patients from randomized and observational studies, found a corrected AFL recurrence rate of 10.9%. Although long-term success rate is slightly lower compared to large studies on well-established techniques, these initial efficacy results are encouraging and demonstrate the feasibility of near-critical nitrogen as an energy source for endocardial ablation. The first-in-human setting, a learning curve for the ULTC system and catheter use, and the small sample size may have hampered creating optimal long-term durability. Although acute success was high in our cohort, the small number of freezes may have affected durable lesion formation, as the thawing phase is a pivotal part of cellular injury and late physiological reversibility may have occurred. In the 10 patients who underwent a repeat EPS in our study, we found three cases of recurrent conduction (30.0%): two symptomatic AFL patients part of the first pilot phase CC1 study, and one AF patient with no history of AFL. A study by Kuniss et al. used a 3-month repeat EPS as

confirmation of BCB in a comparison trial between an RF catheter and an early generation of cryoablation catheter. Of the 191 enrolled patients, 124 (64%) agreed to a repeat procedure. Asymptomatic conduction recurrence in the CTI was seen in 26.3% of patients in the cryoablation group and 15% in the RF group.21 Future, larger trials and ongoing development should demonstrate the efficacy of ultralow temperature near-critical nitrogen as an energy source to complete durable CTI bidirectional block.

4.3 Safety

RF ablation of CTI-dependent AFL is considered a first line therapy due to favorable long-term flutter free survival and safety profile of the procedure. Serious adverse events are reported in 1-3%.2, 23 In 2016, Patel et al. conducted a search of AFL ablations completed in the US from 2000 to 2011. Using ICD-9 codes, they reviewed 89,638 procedures. They reported an overall mortality rate of 0.17% and an overall procedure complication rate of 3.17%. Complications included cardiac events (1.44%) as the most frequent, followed by respiratory (0.88%), vascular (0.78%), and neurologic (0.05%) complications.22 In the 30 subjects treated in our study, one serious adverse event was independently adjudicated as procedure related, that would be categorized in the 1.44% cardiac complication rate noted above and may not be unexpected in an AFL ablation risk analysis. With cryoablation, the effect of freezing in a very stable position may lead to vasospasm more frequently than with RF ablation. Although spasms may occur more often using cryoablation, a lower incidence of permanent damage (e.g., stenosis) is seen compared to RF ablation.24, 25 There were no unexpected procedural safety events reported. While the sample size was small, the absence of serious adverse events requiring intervention may be attributed to the low number of applications and freeze time to achieve the desired endpoint.

4.4 Future perspective for near critical nitrogen ablation

The development of near-critical cooling of nitrogen paves the way for new possibilities to deliver powerful cryotherapy, down to -196 degrees Celsius, along a defined ablation length of small diameter devices, while using lower pressure compared to most N2O gas catheters and consuming much less cryogen. This technology is also very scalable and therefore there are little limitations on catheter designs, freezing lengths and position of diagnostic electrodes along the catheter.12 This introduces new possibilities to deliver powerful cryotherapy, using a highly customizable catheter design for multiple ablation targets.

The present study shows the ability to perform successful ablation of the CTI, but ongoing studies are directed to substantiate these findings and evaluate the capabilities to create linear and focal

transmural lesions of the ablation system in other arrhythmias. Currently, the iCLAS trial (NCT04061603) is a global, single-arm, clinical study designed to collect acute and long-term safety and efficacy data of the 4th generation Adagio AF Cryoablation System in a larger population. 200 patients with persistent AF will be enrolled and will receive PVI and linear lesions (posterior wall and CTI) with the improved version of the ULTC system.

4.5 Study limitations

The main limitation of this first-in-human study is the exploratory nature, with a single-arm, uncontrolled design with a small sample size. Furthermore, the study population consisted of patients suffering from AFL (CC1) and/or AF (CC2). Recurrence of AFL is therefore not a valid endpoint for CC2 patients. Acute success (stable BCB) was seen in all patients, but the protocol did not include systematic repeat EPS after 2–3 months to reassess durable BCB. Albeit multiple study visits were scheduled to investigate possible safety outcomes and symptoms, only limited scheduled repeat monitoring was performed with ECG or Holter, and additional monitoring was only performed in symptomatic patients. This may have overestimated the overall success rate. No serious adverse events leaving sequelae were seen, but larger studies are needed. Finally, results may be influenced by the learning curve of both centers and ongoing trials are needed to confirm safety and long-term efficacy.

5 CONCLUSIONS

In this first-in-human, thirty-patient clinical study, the safety and performance results demonstrate the capabilities of ultralow temperature near-critical nitrogen as an energy source for ablation of the CTI. One transient procedure-related adverse event (coronary artery spasm) was reported. Acute success was achieved in all subjects, while 82.4% remained free of AFL recurrence at 12-month follow-up. The ultralow temperatures achieved, the lower number and shorter duration of freezes compared to other cryoablation technologies suggest a high potential for this novel energy source. Future studies will evaluate the capabilities of the system in larger sample sizes and other arrhythmias.

2.1 Left atrial appendage closure

Left atrial appendage (LAA) occlusion is an alternative or adjunctive therapy for stroke prevention in AF patients who cannot tolerate oral anticoagulation.1,2 The procedure involves sealing off the LAA, where blood clots often form in non-valvular AF. Studies like PROTECT AF and PREVAIL have shown that LAA occlusion, using devices like the Watchman Left Atrial Appendage System, is non-inferior to warfarin therapy in preventing stroke, particularly haemorrhagic strokes, albeit with

higher rates of periprocedural complications. However, the comparison of LAA occlusion with novel oral anticoagulants (NOACs) or in patients with OAC contraindications is lacking in these trials.1-3 The ASAP Study demonstrated that LAA closure with the Watchman device could be a viable option for patients at high stroke risk but with contraindications to oral anticoagulants.4 Overall, percutaneous LAA occlusion may be considered for AF patients at high stroke risk but unable to take long-term OACs, as per ESC guidelines.5

References:

1. DR Holmes, VY Reddy, ZG Turi, et al. Percutaneous closure of the left atrial appendage versus warfarin therapy for prevention of stroke in patients with atrial fibrillation: a randomised non-inferiority trial Lancet

2. VY Reddy, SK Doshi, H Sievert, et al. Percutaneous Left Atrial Appendage Closure for Stroke Prophylaxis in Patients With Atrial Fibrillation Circulation [

3. DR Holmes, S Kar, MJ Price, et al. Prospective Randomized Evaluation of the Watchman Left Atrial Appendage Closure Device in Patients With Atrial Fibrillation Versus Long-Term Warfarin Therapy: The PREVAIL Trial J Am Coll Cardiol, 64 (2014), pp. 1-12

4. VY Reddy, S Möbius-Winkler, MA Miller, et al. Left Atrial Appendage Closure With the Watchman Device in Patients With a Contraindication for Oral Anticoagulation: The ASAP Study (ASA Plavix Feasibility Study With Watchman Left Atrial Appendage Closure Technology) J Am Coll Cardiol, 61 (2013), pp. 2551-2556

5. G Hindricks, T Potpara, P Kirchhof, et al. 2020 ESC Guidelines for the diagnosis and management of atrial fibrillation developed in collaboration with the European Association for Cardio-Thoracic Surgery (EACTS): The Task Force for the diagnosis and management of atrial fibrillation of the European Society of Cardiology (ESC) Developed with the special contribution of the European Heart Rhythm Association (EHRA) of the ESC . Eur Heart J, 42 (2021), pp. 373-498, 10.1093/eurheartj/ehaa612

Pre-cath Laboratory Planning for Left Atrial Appendage Occlusion – Optional or Essential?

Jasneet Devgun, DO, Tom De Potter, MD, Davide Fabbricatore, MD, Dee Dee Wang, MD.

Card Electrophysiol Clin

. 2023 Jun;15(2):141-150. doi: 10.1016/j.ccep.2023.01.009.

DOI:https://doi.org/10.1016/j.ccep.2023.01.009

Introduction

Over the course of the last 2 decades, transcatheter structural interventions have experienced exponential growth and rapid evolution driven by near-Promethean innovation and multi-disciplinary biomedical ingenuity. In the wake of this development, the need for multi-modality imaging for structural heart procedures has been recognized as an important and arguably essential adjunct used in all phases of the procedural process. From preprocedural planning and teaching to guidance within the cath lab, as well as to postprocedural care, structural imaging is proving to be an indispensable asset to ensuring procedural success. Given the inherent complexity of cardiac anatomy, an in-depth understanding of anatomy and physiology is vital for the success of structural heart procedures.

Structural imaging has established its utility in procedures such as transcatheter aortic valve replacement (TAVR), mitral valve interventions such as transcatheter mitral valve replacement (TMVR) and MitraClip (Abbott, Illinois, USA), as well as septal defect repairs. For left atrial appendage occlusion (LAAO), multi-modality imaging is gaining traction and is, likewise, arguably essential in all phases of procedural planning and execution. In the setting of a global pandemic with limited access to personal protection equipment for health care providers, maximizing the efficiency and safety of delivery of health care using modernized imaging technologies has become even more critical. Our review of the literature seeks to synthesize the critical thinking methodologies to investing time in planning for LAAO procedures.

Percutaneous left atrial appendage occlusion

Understanding the Rationale for Periprocedural Evaluation

Common terminology of the left atrial appendage anatomy assumes the orifice of the LAAO landing zone is a circle. With this assumption, 2D transesophageal echocardiogram (TEE) imaging was instituted as the gold standard of imaging the LAA for sizing and device selection. Optimal viewing angles were depicted as 0, 45, 90, and 135°. However, the arrival of multi-detector CT has demonstrated the LAA's landing zone to be elliptical and at times amorphous in shape with multiple angulations that are unique to each patient's anatomy. Traditional 2D TEE and the narrow imaging

field of 2D intracardiac echo (ICE) are unable to visualize the full dimensions of the LAA due to the inability of operators to obtain coaxiality to the true maximal dimensions of the LAA. Hence, modern day LAAO implantation outcomes in the published literature have not achieved 100% procedural success rates. Increasing procedural success and safety outcomes of LAAO technologies requires an in-depth preoperative understanding of each patient's unique LAA anatomy.

Procedure details

In the United States, the WATCHMAN (Boston Scientific, Marlborough, Massachusetts), WATCHMAN FLX (Boston Scientific, Marlborough, Massachusetts) and Amulet (Abbott, Abbott Park, Illinois) have received approval by the Food and Drug Administration for the prevention of stroke in patients with atrial fibrillation (AF).1 The FLX and the Amulet LAAO devices are seated in the LAA, the most common site of intracardiac thrombus formation in AF, to prevent thrombi from forming within it thereby preventing cardio-embolic phenomenon.2 3 4 Due to timing of FDA regulatory approval, currently, the most widely studied LAAO devices in the United States are the WATCHMAN and WATCHMAN FLX LAAO systems. Hence, subsequent procedural details will focus on WATCHMAN FLX delivery systems.

The WATCHMAN FLX LAAO procedure itself begins with obtaining femoral venous access. Transseptal puncture is performed, usually under TEE guidance, to enter into the left atrium (Fig. 1). The optimal transseptal puncture site assessed by TEE is often limited by the fact that we are obtaining 2D images of a 3D structure. Assessing whether one is puncturing too anterior or posterior in the septal plane is difficult. Furthermore, the generation of 3D images, although possible, is limited by the quality of the initial 2D images obtained, which may not render a very precise assessment and execution of this manoeuvre.

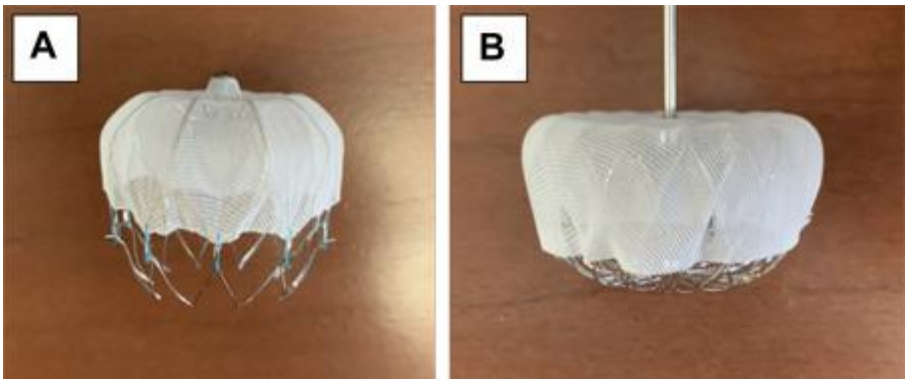

Fig. 1The WATCHMAN (*A*) and WATCHMAN FLX (*B*) devices. The original WATCHMAN is a self-expanding nitinol structure with a porous polyethylene terephthalate (PET) membrane on the proximal face. The WATCHMAN FLX is a modified version with the rearrangement of the nitinol structure at the distal end into a rounded configuration and extension of the PET membrane distally.

Once transseptal puncture is performed, a guidewire is sent to the left atrium and into the left superior pulmonary vein. The WATCHMAN or WATCHMAN FLX access sheath and dilator are advanced over the guidewire into the left atrium. Dilator and guidewire are removed followed by the advancement of the angled pigtail catheter through the WATCHMAN access sheath into the distal portion of the main lobe of the LAA for the contrast visualization of the LAA.[5] Next, the access sheath is advanced into the LAA over the pigtail catheter until the access sheath radiopaque marker band meets the corresponding device size marker band or is just distal to the LAA ostium. Once identified, the pigtail catheter is removed, and the LAA occluder delivery system is advanced through the access sheath. Under fluoroscopic guidance, the delivery system's distal marker band is aligned to the distal marker of the access sheath.[5] Traditionally, confirmation of delivery sheath positioning and coaxiality is verified by TEE. Both fluoroscopic and TEE verification of coaxiality are primarily by 2D images that, by nature, confer an incomplete overall visualization of the LAA ostium and optimal coaxial positioning, which may lead to incomplete seating of the LAA occlude, device leaks, among other complications. The WATCHMAN FLX device is then deployed into the LAA via a combination of passive exposure and advancement of the FLX ball, consisting of retracting the access sheath and delivery system while stabilizing the deployment knob. After the deployment of the device, positioning is evaluated under TEE guidance and contrast fluoroscopy. Specific criteria of appropriate positioning must be met, which includes position, anchor, size, and seal (PASS). Ideally, the LAA occluder would be placed at the level of the circumflex artery with minimal protrusion into the left atrium. A "tug test" is then performed, for which the deployment knob is pulled and the LAAO device is visualized under fluoroscopy, confirming adequate anchoring of the device. Device compression should be at a minimum of 8%, and peridevice flow should be no more than 5 mm at vena contracta on 2D TEE color flow.

Pre-cath Laboratory Planning in Left Atrial Appendage Occlusion

Traditionally, two-dimensional TEE had been the sole imaging modality to guide LAAO procedures until 2011, when computed tomography (CT) began being integrated into cath laboratory planning and postprocedure monitoring.[6] While CT had become standard of care for transcatheter device planning, such as for TAVR and transcatheter mitral replacement therapies, it had not been in use for LAAO until recently. [7] [8] Stand-alone fluoroscopic sizing for LAA in the cardiac catheterization or electrophysiology laboratory without preprocedural imaging has several limitations. Contrast injection with fluoroscopic evaluation in multiple c-arm angle projections provides an overview of the shape of the LAA but is unable to verify maximal coaxial alignment to the true orifice of the LAA landing zone. Off-axis fluoroscopic projections of the LAA may lead to under or oversizing of the LAA landing zone, and the inability to appreciate challenging anatomy. Hence, in patients without

access to intraprocedural TEE or preprocedural CT imaging planning, pure fluoroscopic guidance has a lower device implantation success rate than with standard of care TEE imaging guidance. This may result in aborted LAAO procedures due to inappropriate anatomy for the devices available, or LAA anatomy that may not have been compatible with any commercially available device. However, TEE for LAA closure, although an additive value to fluoroscopic imaging alone, itself also has inherent limitations. Patients undergoing outpatient TEE are usually volume depleted due to necessary fasting nothing by mouth requirements before the procedure. As the LAA volume depends on loading conditions, TEE can certainly underestimate the LAA dimensions.[9] Also, the spatial resolution of TEE is limited and somewhat operator- and image quality dependent, which may lead to the underappreciation of LAA contractility and dimensions changes during the cardiac cycle. [10] Furthermore, in the setting of the 2019 global SARS-CoV-2 pandemic, access to outpatient preprocedural TEE became a barrier to scheduling patients for LAAO procedures. Given the inherent risks of aerosolization procedures and spread of SARS-CoV-2 coupled with a limited global supply of personal protection equipment, echocardiography laboratories across the world decreased their elective TEE procedural volume to ration the supply of personal protection equipment. [11] [12] In some countries, once the supply of personal protection equipment for health care providers became more readily available, mandatory nasopharyngeal swab testing for COVID-19 before any preprocedural TEE became a secondary deterrent for patient's seeking access to LAAO procedures. Hence, a migration away from preprocedural TEE has been accelerated by the global pandemic into alternative additive technologies to support intraprocedural case guidance.

Planning Modalities

Left atrial appendage occlusion is a procedure that has the potential to attain immense gains from not only the integration of CT but also of other imaging modalities as well such as 3D printing, computational modeling (CM), and artificial intelligence (AI).

Computed Tomography

Preprocedural planning for LAAO now consists not only of TEE imaging but also multi-detector ECG-gated, contrast-enhanced cardiac CT. Modern advanced dual-source cardiac CT scanners allow for adequate image acquisition and evaluation of patients with irregular heart rates due to post-scan additive features such as EKG editing.

[13]

The benefits of CT imaging before LAAO are manifold, ranging from the assessment of patient appropriateness (eg, congenitally-absent LAA, prior surgical or transcatheter device, or the presence of LAA thrombus), to the structural characterization of the LAA itself, as well as accurate sizing of

the device and localization of the appropriate landing zones of the LAA occluder with precision (Fig. 2). Furthermore, CT images can be further processed to form 3D print models, which can offer substantial preprocedural planning.

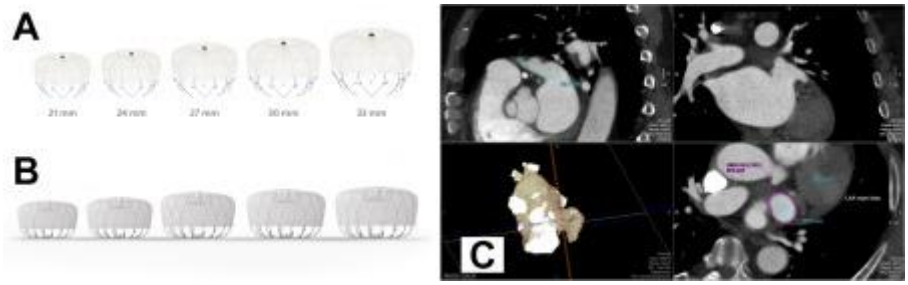

Fig. 2(*A*) The WATCHMAN device is produced in various sizes, as shown above. (*B*) The WATCHMAN FLX comes in the following sizes from left to right: 20 mm, 24 mm, 27 mm, 31 mm, and 35 mm. (*C*) CT-guided LAA sizing to aid in choosing the appropriate device size.

3D printing

Three-dimensional printing is a method of manufacturing three-dimensional physical objects from information derived from digital media (Fig. 3).

[14]

The process of forming three-dimensional physical objects starts with obtaining high-quality imaging data and its conversion to a Digital Imaging and Communication in Medicine (DICOM) format for further image processing. Processing is done through special software to define and build the anatomic body parts of interest in a process called *segmentation*. Subsequently, 3D volume rendering and digital modeling of patient-specific anatomy are constructed. Patient-specific 3D digital anatomic models are then saved in a stereolithography (STL) file format, which contains the surface mesh information of the specific geometries to be used in the 3D printing process, which can be further refined by computer-aided design modeling and computational analysis. Finally, a 3D print model is made by processing and using this digital information to create physical objects by depositing multiple layers of material over digitally defined geometries.

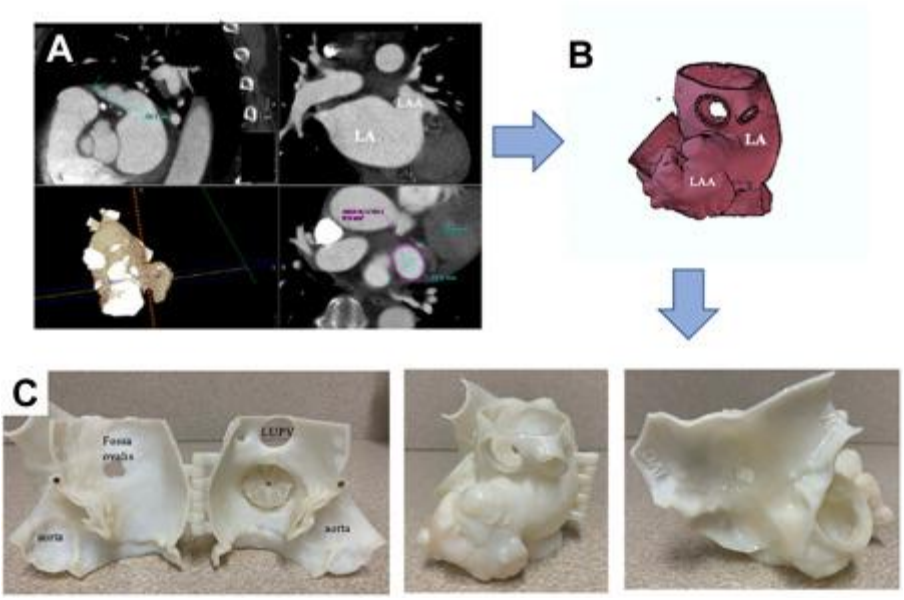

Fig. 3The process of LAA image acquisition and processing is displayed in this figure. (*A*) A series of frames was taken during CT imaging for visualizing the appendage and its landing zone with accurate measuring of the maximum and minimum diameter, LAA orifice area, and length of LAA from the landing zone. The CT images are processed via 3D volume-rendering into a digital format and structure (*B*), which in turn can be used to create 3D print models (*C*) for a more in-depth understanding of LAA anatomy and for the use of preprocedural simulation. The 3D model demonstrates the fossa ovalis (bottom left & bottom right, labeled as FO) between the SVC and IVC, demonstrating optimal transseptal puncture site. The WATCHMAN device is seen well-seated in the LAA orifice. FO: fossa ovalis, IVC: inferior vena cava, LA: left atrium, LAA: left atrial appendage, SVC: superior vena cava.

Three-dimensional print models have demonstrated that patient anatomy is much more complex than what is understood by traditional two dimensional TEE imaging alone (Fig. 4). [14,15] The clinical implications of this is that our knowledge of LAAO device sizing as well as identifying appropriate landing zone and deployment, is far more primitive than what was previously understood, as may have been our clinical decisions using traditional imaging methods. Three-dimensional printing has great implications for improving procedural accuracy, device sizing, and time to reaching the early operator learning curve, among many other benefits.[7,14,15]

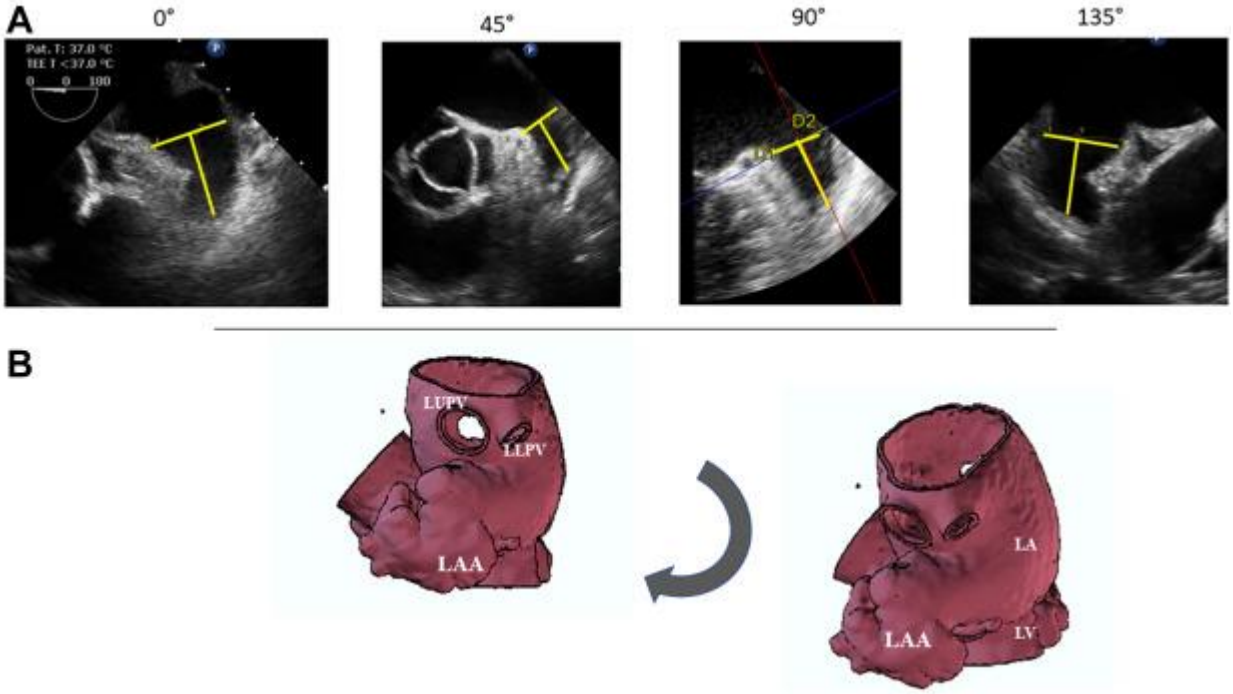

Fig. 4Images of left atrial appendage taken by TEE in various standard views to take measurements of the appendage (*A*). As seen from left to right, these views are taken approximately at 0, 45, 90, and 135°. Transesophageal echocardiography gives us an incomplete understanding of the true complex nature of LAA anatomy (*B*). These are 3D images of the left atrium and LAA taken from the same patient's CT scan images. One can see the complex entry point and curved direction the appendage takes, which would have significant implications on device sizing and deployment. LA: left atrium, LAA: left atrial appendage, LLPV: left lower pulmonary vein, LUPV: left upper pulmonary vein.

Intraprocedural 3D angiography

Rotational angiography or 3D angiography is an imaging modality that allows intraprocedural reconstruction of a 3D model of a chamber of interest such as the LA (including the LAA), yielding datasets much like those derived from cardiac CT. Images can be overlaid on 2D fluoroscopy for anatomic guidance and can be used for LAA sizing and device selection as an alternative to TEE. As the images are acquired on the same table using the same equipment as the 2D fluoroscopy, they can be used to visualize the ideal angulation of the fluoroscopy tube for a particular LAA, eliminating issues of foreshortening. [16] As these images are obtained by contrast injection during apnea and rapid ventricular pacing, a workflow using general anesthesia is typically required for obtaining good image quality.

Dynamic fusion imaging

In day-to-day practice, physicians performing LAA closure have to be able to synthesize and recreate the images obtained by different imaging modalities and techniques into one 3D understanding of the LAA in their mind. However, when initial image acquisition is only performed with 2D TEE or fluoroscopic datasets, a full understanding of the LAA may not be possible. Currently, pre-procedural

CT generated LAA caseplans are not able to be fused onto fluoroscopic displays. Hence, the role of dynamic fusion imaging in LAAO is gaining greater interest in the transcatheter arena.

The dynamic fusion imaging technique has the ability to merge the information obtained from different methods onto one fluoroscopic display. Specifically, for LAA closure, anatomic landmarks identified by TEE or CT are directly overlaid on the real-time fluoroscopy, the latter typically being superior for identifying the closure device itself. Thus, these systems aim to generate a single final real-time hybrid visualization of the aforementioned techniques, improving safety and reducing procedural times. Several vendors offer integrated TEE/fluoroscopy or 3DRA/fluoroscopy modalities (Fig. 5). [17] [18] [19] [20]

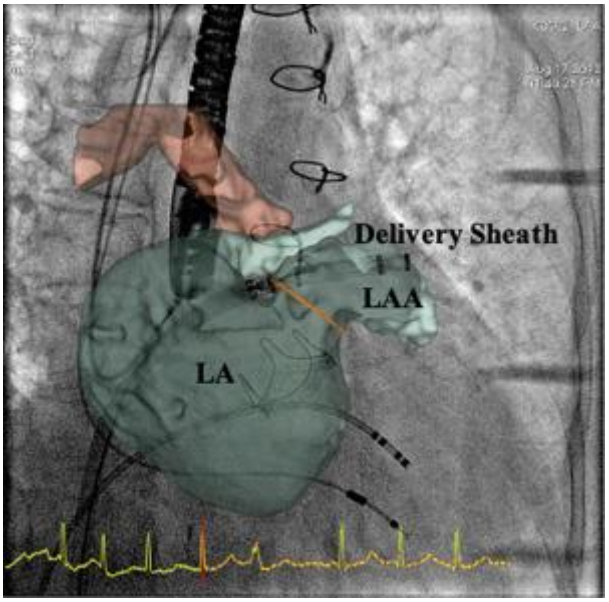

Fig. 5This figure shows a 3D model of the LA, partially cut-away. A Watchman delivery sheath with a loaded Watchman device is positioned in the LAA and is ready for deployment. LA: left atrium, LAA: left atrial appendage.

Computational modelling

CM is a method in which digital 3D reconstructions of any object can be illustrated in a 4D manner over time. [21] Used in biomedical engineering and sciences, CM fills the void that static models have in exemplifying the complex anatomic and physiologic interplay that occurs in real time. About 15 years ago, while in its infancy, computational models were created by simple manual drawings of geometric shapes. Today, the use of multi-modality imaging, such as CT and MRI in the case of cardiac models, is used for more refined and patient-specific modelling. [21]

Through finite element analysis (FEA) and computational fluid dynamics (CFD), computational models can recreate stress and deformation of cardiac tissue, as well as to characterize the blood flow pattern in a patient's heart. [14] [22] The benefits of CM would be manifold, as it would allow for a way to take static cardiac images and bring them to life. This would give operators a greater understanding

and sense of the physiologic environment in which they must operate. As such, CM may offer unique insights and even greater improvement in operator skill as well as procedural success.

Artificial intelligence

AI is defined as the study of algorithms that give machines the ability to reason and perform functions such as problem-solving, object and word recognition, inference of world states, and decision-making.[23] AI has various applications across multiple disciplines, and it has recently found its way into improving precision-medicine and health care. Several procedural specialties have demonstrated the utility and accuracy offered by AI in training and procedure simulation, from general surgery, to anesthesiology, and even to neurosurgery, amongst many more.[23, 24, 25] Bissonnette and colleagues demonstrated the successful use of AI via machine learning algorithms in a surgical laminectomy simulation.[25] They showed that use of AI in their simulation achieved 97.6% accuracy in various metrics including the safety of the procedure, efficiency, motion of the tools, and coordination. Moreover, Engelhardt and colleagues used a deep neural network and recreation of the surgical scene to train operators for minimally invasive mitral valve repair, demonstrating its success in significantly improving their skills, understanding of complex mitral valve anatomy and surgical technique, and therefore, decreasing the time to crossing the learning curve.[26] As such, AI may have great potential in similarly improving accuracy, efficiency, and success in training for structural heart procedures.

Benefits of Pre-Cath Laboratory Planning

Patient selection

Many patients are not appropriate anatomical candidates for LAAO. Some individuals have a congenital absence of the LAA, others may have prior surgical and catheter interventions that preclude entry into the LAA, and lastly some patients may have an LAA thrombus present. Computed tomography is useful in pre-procedural planning to accurately characterize the above possible limitations or patient-specific contraindications to the procedure. Moreover, some patients may not be deemed a candidate for current generation LAAO devices due to LAA size and anatomy that is considered incompatible with their patient specific anatomy. However, in the setting of inadequate pre-procedural imaging, some patients may be deemed not a candidate for LAAO due to incomplete understanding of their patient specific anatomy, when in actuality they may have been anatomically suitable for LAAO by in-depth CT analysis. [27] Alternatively, some patients by pre-procedural 2D TEE or angiography may be deemed a candidate for LAAO, only to find intraprocedurally that the patient anatomy may not truly be amenable to any LAA occluder, rendering the patient with an aborted attempt at LAAO with failed attempt at stroke prevention.

Thrombus visualization

Cardiac CT is a noninvasive modality that offers important information not only of one's LAA anatomy but also of the presence or absence of LAA thrombus. Cardiac CT for LAAO is contrast-enhanced; therefore, a LAA thrombus is immediately visualized as a filling defect that should otherwise not be present. This mitigates the need for invasive tests such as TEE before LAAO for thrombus visualization and therefore mitigates health care spending and multiple medical encounters for the patient.

Device sizing and procedure simulation

It is clear that there exists an early-operator learning curve in LAAO device sizing and implantation.[14] Multi-modality imaging is extremely helpful in the appropriate sizing of the LAA, and accurate selection of the size of the LAAO device to be deployed. In fact, there is a significant difference in device size selection and less change in device size intraprocedurally with a greater success rate of device implantation in those with both CT and TEE guidance compared with TEE alone. [27] As shown in Fig. 2, there are various sizes offered for the WATCHMAN and WATCHMAN FLX devices. In cardiac CT, the LAA landing zone is appropriately sized at maximal LAA diastole or mid-late left ventricular systole (see Fig. 2). This is the moment in the cardiac cycle for which the LAA is at its largest, and therefore, an ideal phase for device sizing to mitigate risks of under-sizing, and therefore, the risk of peridevice leaks and device embolization. [28] Furthermore, CT images can be processed into 3D print models, which can offer finer detail and understanding of a patient's LAA anatomy. This can provide further granularity in sizing and successful mitigation of the above-mentioned risks. There is immense variability in LAA anatomy and structure from patient-to-patient, which is not readily seen in traditional echocardiographic techniques (see Fig. 4). This adds to further complexity in achieving success in LAAO, including device sizing, appropriate transseptal puncture, as well as device deployment. CT imaging and 3D print models are extremely useful, particularly in LAAO procedure simulation. Printed models render a better understanding not only of complex LAA anatomy but also exhibit the visualization of left atrial size and dimensions for improved procedural planning. Accurate identification of the landing zone, simulation of transseptal puncture, appropriate catheter sizing for better deployment, and optimal C-arm angulations can all be determined with 3D print model-based simulation. In fact, one randomized study comparing LAAO guided by 3D-CT and 3D printing versus 2D TEE demonstrated significantly improved accuracy in device sizing (92% vs 27%, $P = .01$), improved procedural efficiency (55 ± 17 min vs 73 ± 24 min, $P < .05$), and fewer C-arm viewing projections (1.3 ± 1.2 vs 3.25 ± 2.52, $P = .05$).[15] Moreover, fewer devices and guide catheters were used in the former group compared with the 2D TEE cohort, namely due to preprocedural planning and simulation. [15] As a result, early operator learning curves may significantly decrease with preprocedural 3D-CT and printed models. [7] Simulation offers the opportunity to teach

trainees and early operators in a more effective way, further decreasing the time to crossing the learning curve. One study demonstrated a 100% success rate of LAAO with 1.245 devices per implantation attempt, compared with the average 1.8 devices per LAAO attempt (82% success rate) in the PROTECT-AF study.[7] [29] Moreover, only 4 out of the 53 patients had peridevice leaks and no device embolization noted in the cohort.[7]Although CT and 3D printing offer a more accurate understanding of the complexities of LAA anatomy, these offer static views without the live mechanics and physiology of a beating heart. Computational modeling opens a window into a more complete understanding of dynamic anatomy. Through computational simulation via methods such as FEA and CFD, these methods would provide further advantages in preprocedural planning. In addition to understanding static anatomy, computational modeling mimics reality with dynamic anatomy, offering a better understanding of real-time tissue deformation blood flow dynamics. Limitations to current widespread medical adaptation of computational modeling, such as FEA and CFD-based tools, include a paucity of easy-to-use medical grade softwares for medical teams in clinical practice, lack of clinical reimbursement, and absence of engineering expertise in integration of these tools to clinical practice. Likewise, AI may even further individualize patient care when used in structural heart procedure planning. When used combination with 3D printing, AI may assist in the manufacturing of patient-specific anatomic replica, as well as real-time procedure simulation tailored to the patient's anatomy and physiology.[14] Through AI, patient-specific anatomy and physiology may be reconstructed to provide a framework for preprocedural planning and practice with instantaneous feedback in a much more realistic setting.

Patient education

The use of 3D print models is effective not only in periprocedural planning but also may be considerably advantageous in patient education. Integration of 3D prints into clinical practice facilitates the shared decision-making between the patient and the physician. 3D print models can be used in the clinic setting to discuss therapeutic options in a much more visual, and therefore, effective way, rendering a much greater level of comprehension by the patient. This has led to further patient engagement in discussion with their physician, and therefore, better-informed decisions, and improved patient satisfaction. Application of 3D prints in clinical visits empowers patients with greater comprehension and knowledge of their disease, personal anatomy, and procedural recommendations for their care. [30] [31] [32]

Limitations of Preprocedural Planning

Preprocedural planning is not critical to the successful development of an LAAO program in all hospitals. Operators and Interventional Imaging physician teams with significant preexisting

expertise in LAAO procedures may not experience a significant additive value of periprocedural planning to their case outcomes. Additionally, depending on the size of the population served by the local health system, not all hospitals will have the same anticipated annual volume of LAAO procedures. Smaller sized LAAO programs may not have the financial reservoir necessary for the purchase of dedicated cardiac computed tomographic scanners for structural procedures. Additionally, in an era whereby reimbursement for cardiac coronary CT scanning is already challenging, reimbursement for the professional time necessary for performing intra or periprocedural structural heart CT planning is lacking. Modern intraprocedural techniques such as 3D angiography require training and experience, and both 3D angiography, as well as TEE fusion imaging, require capital equipment investments. Lastly, disparities in access to health care and reimbursement to new technologies vary by county and country delivering patient care and hence may limit Implanting Team's access to change their delivery of care.

Summary

Preprocedure planning for LAAO is critical to ensuring patient safety, procedural success, and optimal device outcomes for patient care. Pre-cath laboratory planning for LAAO can significantly improve procedural efficiency, accuracy, success, and therefore cost-effectiveness. In addition to multi-modality imaging, various modes of recreating cardiac anatomy and physiology, namely via 3D printing, computational modeling, and AI, can aid in significant improvements in achieving greater understanding of unique patient-specific anatomic and physiologic considerations in the procedural setting. The scalability of periprocedural planning in transcatheter interventions remains a discussion limited by regional practice patterns and solvent reimbursement strategies. As the LAAO procedure becomes more available globally, education on the importance of preprocedural LAAO planning is lagging. To ensure optimal safety and procedural success between the hands of experienced operators and new operators with new devices, preprocedural LAAO planning is invaluable.

References

1. Sharma SP, Park P, Lakkireddy D. Left Atrial Appendages Occlusion: Current Status and Prospective. Korean Circ J 2018;48:692–704. Available at: http://www.ncbi.nlm.nih.gov/pubmed/30073807.

2. Blackshear JL, Odell JA. Appendage obliteration to reduce stroke in cardiac surgical patients with atrial fibrillation. Ann Thorac Surg 1996;61:755–9. Available at: http://www.ncbi.nlm.nih.gov/pubmed/8572814.

3. Reddy VY, Holmes D, Doshi SK, et al. Safety of percutaneous left atrial appendage closure: results from the Watchman Left Atrial Appendage System for Embolic Protection in Patients with AF

(PROTECT AF) clinical trial and the Continued Access Registry. Circulation 2011;123:417–24. Available at: http:// www.ncbi.nlm.nih.gov/pubmed/21242484.

4. Holmes DR, Kar S, Price MJ, et al. Prospective randomized evaluation of the Watchman Left Atrial Current data support the use of preprocedural CT as additive value for improving accuracy of LAA device sizing and procedural success. For any new LAAO implanter, incorporation of pre-procedural CT derived 3D printing and computational modeling decreases early operator learning curves associated with learning new devices and cardiac anatomies. Establishment of preprocedural imaging support protocols and pathways require institutional and societal investment in educational and reimbursment pathways for interventional imaging physicians to assist the Heart Team approach to LAAO procedures. 148 Devgun et al Appendage Closure device in patients with atrial fibrillation versus long-term warfarin therapy: the PREVAIL trial. J Am Coll Cardiol 2014;64:1–12. Available at: http://www.ncbi.nlm.nih.gov/pubmed/ 24998121.

5. Boston Scientific. WATCHMAN Device Directions For Use. 2015. Available at: https://www.watchman. com/content/dam/watchman/downloads/dtr/ watchman-matters-resources/WATCHMAN_Device_ DFU_US.pdf.

6. Lockwood SM, Alison JF, Obeyesekere MN, et al. Imaging the left atrial appendage prior to, during, and after occlusion. JACC Cardiovasc Imaging 2011;4:303–6. Available at: http://www.ncbi.nlm.nih. gov/pubmed/21414580.

7. Wang DD, Eng M, Kupsky D, et al. Application of 3- Dimensional Computed Tomographic Image Guidance to WATCHMAN Implantation and Impact on Early Operator Learning Curve: Single-Center Experience. JACC Cardiovasc Interv 2016;9:2329–40. Available at: http://www.ncbi.nlm.nih.gov/pubmed/ 27884358.

8. Glikson M, Wolff R, Hindricks G, et al, ESC Scientific Document Group. EHRA/EAPCI expert consensus statement on catheter-based left atrial appendage occlusion - an update. EP Europace 2020;22(2): 184. https://doi.org/10.1093/europace/euz258.

9. Spencer RJ, DeJong P, Fahmy P, et al. Changes in Left Atrial Appendage Dimensions Following Volume Loading During Percutaneous Left Atrial Appendage Closure. JACC Cardiovasc Interv 2015; 8:1935–41. Available at: http://www.ncbi.nlm.nih. gov/pubmed/26738661.

10. Patel AR, Fatemi O, Norton PT, et al. Cardiac cycledependent left atrial dynamics: implications for catheter ablation of atrial fibrillation. Hear Rhythm 2008; 5:787–93. Available at: http://www.ncbi.nlm.nih. gov/pubmed/18486563.

11. Shah PB, FGP Welt, Mahmud E, et al. Triage considerations for patients referred for structural heart disease intervention during the COVID-19 pandemic: An ACC/SCAI position statement. Catheter Cardiovasc Interv 2020;96:659–63. Available at: http://www.ncbi.nlm.nih.gov/pubmed/32251546.

12. Einstein AJ, Shaw LJ, Hirschfeld C, et al, INCAPS COVID Investigators Group. International Impact of COVID-19 on the Diagnosis of Heart Disease. J Am Coll Cardiol 2021;77:173–85. Available from: http://www.ncbi.nlm.nih.gov/pubmed/ 33446311.

13. Kaafarani M, Saw J, Daniels M, et al. Role of CT imaging in left atrial appendage occlusion for the WATCHMANTM device. Cardiovasc Diagn Ther 2020;10:45–58.

14. Wang DD, Qian Z, Vukicevic M, et al. 3D printing, computational modeling, and artificial intelligence for structural heart disease. JACC Cardiovasc Imaging 2020;14(1):41–60. https://doi.org/10.1016/ j.jcmg.2019.12.022.

15. Eng MH, Wang DD, Greenbaum AB, et al. Prospective, randomized comparison of 3-dimensional computed tomography guidance versus TEE data for left atrial appendage occlusion (PRO3DLAAO).

Catheter Cardiovasc Interv 2018;92:401–7.

16. De Potter T, Chatzikyriakou S, Silva E, et al. A Pilot Study for Left Atrial Appendage Occlusion Guided by 3-Dimensional Rotational Angiography Alone. JACC Cardiovasc Interv 2018;11:223–4. Available at: http://www.ncbi.nlm.nih.gov/pubmed/29348017. 17. Balzer J, Zeus T, Hellhammer K, et al. Initial clinical experience using the EchoNavigator()-system during structural heart disease interventions. World J Cardiol 2015;7:562–70. Available at: http://www. ncbi.nlm.nih.gov/pubmed/26413233.

18. Ebelt H, Domagala T, Offhaus A, et al. Fusion Imaging of X-ray and Transesophageal Echocardiography Improves the Procedure of Left Atrial Appendage Closure. Cardiovasc Drugs Ther 2020; 34:781–7. Available at: http://www.ncbi.nlm.nih.gov/ pubmed/32761486.

19. Thaden JJ, Sanon S, Geske JB, et al. Echocardiographic and Fluoroscopic Fusion Imaging for Procedural Guidance: An Overview and Early Clinical Experience. J Am Soc Echocardiogr 2016;29:

503–12. Available at: http://www.ncbi.nlm.nih.gov/ pubmed/27021355.

20. Mo B-F, Wan Y, Alimu A, et al. Image fusion of integrating fluoroscopy into 3D computed tomography in guidance of left atrial appendage closure. Eur Hear Journal Cardiovasc Imaging 2021;22:92–101. Available at: http://www.ncbi.nlm.nih.gov/pubmed/ 31764982.

21. Lopez-Perez A, Sebastian R, Ferrero JM. Threedimensional cardiac computational modelling: methods, features and applications. Biomed Eng 2015;14:35. Available at: http://www.ncbi.nlm.nih. gov/pubmed/25928297. 22. Aguado AM, Olivares AL, Yagu¨e C, et al. In silico Optimization of Left Atrial Appendage Occluder Implantation Using Interactive and Modeling Tools. Front Physiol 2019;10:237. Available at: http://www. ncbi.nlm.nih.gov/pubmed/30967786.

23. Hashimoto DA, Witkowski E, Gao L, et al. Artificial Intelligence in Anesthesiology: Current Techniques, Clinical Applications, and Limitations. Anesthesiology 2020;132:379–94. Available at: http://www. ncbi.nlm.nih.gov/pubmed/31939856.

24. Hashimoto DA, Rosman G, Rus D, et al. Artificial Intelligence in Surgery: Promises and Perils. Ann Surg 2018;268:70–6. Available at: http://www.ncbi. nlm.nih.gov/pubmed/29389679.

25. Bissonnette V, Mirchi N, Ledwos N, et al. Neurosurgical Simulation & Artificial Intelligence Learning Centre. Artificial Intelligence Distinguishes Surgical Left Atrial Appendage Occlusion 149 Training Levels in a Virtual Reality Spinal Task. J Bone Joint Surg Am 2019;101:e127. Available at: http://www.ncbi.nlm.nih.gov/pubmed/31800431.

26. Engelhardt S, Sauerzapf S, Brci c A, et al. Replicated mitral valve models from real patients offer training opportunities for minimally invasive mitral valve repair. Interact Cardiovasc Thorac Surg 2019;29: 43–50. Available at: http://www.ncbi.nlm.nih.gov/ pubmed/30783681.

27. So C-Y, Kang G, Villablanca PA, et al. Additive Value of Preprocedural Computed Tomography Planning Versus Stand-Alone Transesophageal Echocardiogram Guidance to Left Atrial Appendage

Occlusion: Comparison of Real-World Practice. J Am Heart Assoc 2021;e020615. Available at: http://www.ncbi. nlm.nih.gov/pubmed/34398676.

28. Korsholm K, Berti S, Iriart X, et al. Expert Recommendations on Cardiac Computed Tomography for Planning Transcatheter Left Atrial Appendage Occlusion. JACC Cardiovasc Interv 2020;13:277–92.

29. Reddy VY, Sievert H, Halperin J, et al. PROTECT AF Steering Committee and Investigators. Percutaneous left atrial appendage closure vs warfarin for atrial fibrillation: a randomized clinical trial. JAMA 2014;312:1988–98. Available at: http://www.ncbi. nlm.nih.gov/pubmed/25399274.

30. Stewart JA, Wood L, Wiener J, et al. Visual teaching aids improve patient understanding and reduce anxiety prior to a colectomy. Am J Surg 2021; 222(4):780–5. https://doi.org/10.1016/j.amjsurg. 2021.01.029.

31. Kliot T, Zygourakis CC, Imershein S, et al. The impact of a patient education bundle on neurosurgery patient satisfaction. Surg Neurol Int 2015;6: S567–72. Available at: http://www.ncbi.nlm.nih.gov/ pubmed/26664909.

32. Oudkerk Pool MD, Hooglugt J-LQ, Schijven MP, et al. Review of Digitalized Patient Education in Cardiology: A Future Ahead? Cardiology 2021;1–9. Available at: http://www.ncbi.nlm.nih.gov/pubmed/ 33550295

Chapter 2

Chapter 2 delves into the intricate realm of ventricular tachycardia, showcasing the culmination of a dedicated study conducted during the researcher's tenure in London at St. George's Hospital. This investigation unfolded within the esteemed AVATAR (Advanced Ventricular Arrhythmia Training and Research) program, led by the esteemed Dr. Magdi Saba. Within this program, the researcher underwent a interesting journey, honing and refining their skills across the spectrum of electrophysiology. Engaging in diverse patient contexts, from outpatient clinics to preoperative assessments and intra-procedural care, they gained invaluable experience under the close guidance of Dr. Saba. Gradually assuming greater autonomy, they adeptly navigated therapeutic strategies tailored to individual patient needs, all while fostering collaborative relationships with colleagues and junior doctors. A pivotal focus of this fellowship centred on the intricacies of electrophysiology procedures within the cath lab. With burgeoning independence, the researcher delved into complex procedures, particularly within the realm of ventricular arrhythmias (VA). Actively immersed in clinical cases and research endeavors pertaining to VA, they encountered novel methodologies and technologies, enriching their understanding and expertise. The culmination of this journey not only resulted in the dissemination of significant findings but also paved the way for future endeavors. Through the insights garnered, the researcher secured a prestigious position as a Locum Consultant in Electrophysiology at Brompton Hospital. Central to the study presented within this chapter is the need to tailor cutoff parameters to effectively delineate scar tissue within the ventricle during catheter ablation—a critical stride toward enhancing patient outcomes and advancing the field of electrophysiology.

Correlation between Bipolar and Unipolar Electrograms with a High-Density Grid catheter and MRI-Identified Scar in Patients Undergoing VT Ablation

Contribution:

MS and AL conceived the study, designed the protocol, selected patients, and performed all the interventions, supervised the statistical analysis and the manuscript. MW analysed the MRI data, the EAVM acquisition. DF performed the statistical analysis and wrote the manuscript. MS, MW promptly offered feedback and helped in refining the manuscript. All authors provided critical feedback and helped shape the research, analysis, and manuscript.

BACKGROUND: Bipolar and unipolar voltage mapping serve as the primary tools used to identify scar during catheter ablation for ventricular tachycardia (VT). However, the commonly used cut-off values were obtained from small cohorts and typically acquired using single-tip ablation catheters. Optimal cut-off values for bipolar and unipolar voltage thresholds for scar detection are unknown when using multielectrode catheters.

OBJECTIVE: To correlate left ventricular (LV) endocardial bipolar and unipolar voltages, as well as other surrogate parameters, gathered using the High-Density (HD) Grid mapping catheter, with 3D late-gadolinium enhanced (LGE)-MRI-detected scar in patients undergoing catheter ablation for VT.

METHODS: Twelve consecutive patients who underwent endocardial and/or epicardial LV mapping ablation were studied. Each patient had pre-ablation late gadolinium-enhanced cardiac magnetic resonance imaging to localize and quantify the scar. Electroanatomic mapping was performed using an HD-Grid catheter and the Ensite X mapping system.

RESULTS: Both bipolar voltage (BV) and unipolar voltage (UV), as well as bipolar electrogram (EGM) area demonstrated a linear relationship with wall thickness, and an inverse regression curve with the presence of scar. Average values from MRI-identified scarred and healthy regions exhibited significant differences in all evaluated parameters except the unipolar EGM duration. ROC curve analysis demonstrated good scar predictivity using unipolar voltage, bipolar voltage, and bipolar EGM area. The optimal cut-off was 9.3mV for UV, 2.3 mV for BV and 20.13 mV*ms for BV area with this catheter. Further analysis was conducted to predict the MRI-detected scar using the new cutoff and parameters described above, and these results correlated better with the scar when compared with those obtained using the classical cutoff.

CONCLUSIONS: The cut-off values for scar definition using contact mapping catheters should be adapted to the specific catheter being used to create the map. Optimal correlation between MRI-defined scar and electro-anatomical mapping-defined scar using the HD-Grid mapping catheter was

obtained using a threshold of 2.3 mV and 9.3 mV for bipolar and unipolar voltage, respectively. The bipolar EGM area may be a useful additional parameter to enhance scar detection.

Keywords:

- Ventricular tachycardia
- Catheter ablation
- Ischemic cardiomyopathy
- Magnetic resonance

List of abbreviations

EAM = electroanatomic mapping

EGM = electrogram

LV = left ventricular

VT = ventricular tachycardia

BV = bipolar voltage

UV = unipolar voltage

HD = high-density

MRI = magnetic resonance imaging

FWHM = full-width-half-maximum

LGE-MRI = late gadolinium enhanced cardiac magnetic resonance imaging

CMRI = Cardiac MRI

SSFP = steady state free precession sequences

TSE = turbo spin echo

Gd-BT-DO3A = Gadobutrol

SPIR = spectral pre-saturation with inversion recovery

TFE = turbo field echo

SD = standard deviation

IQR = interquartile range

IHD = ischemic heart disease

Ethical approval: The study was approved by the institutional ethics committee and informed consent was obtained from patients.

Consent for publication: all patients provided written informed consent to participate in the study.

Availability of data and materials: The data that support the findings of this study are available from the corresponding author upon reasonable request.

What is Known?

- **Traditional unipolar and bipolar voltage thresholds to define abnormal low voltage areas are dependent on recording electrode size, inter-electrode distance, and, in the case of bipolar recording, the angle of incidence between the recording bipole and the wavefront of activation.**

What's new?

- **The optimal unipolar and bipolar voltage thresholds to discriminate scar from healthy tissue using an HD Grid catheter are defined in patients undergoing ventricular tachycardia ablation.**
- **The MRI data used to validate the EAM was acquired using a high-resolution 3D LGE sequence, prior to device implantation and < 6 months from the time of the ablation procedure. This would minimise artifact and registration errors, thereby providing a clinically robust, albeit indirect, 'truth' against which to measure the EAM data.**
- **Bipolar EGM area can help improve the detection of scar tissue during VT mapping and ablation procedure.**

INTRODUCTION

Electroanatomic mapping (EAM) of the ventricular myocardium remains a cornerstone of catheter ablation of ventricular tachycardia (VT) in patients with scar-related VT.[1] One of the main goals of EAM is to discriminate VT substrate from healthy tissue. This is currently done by applying uniform bipolar voltage (BV) cut-offs, most commonly > 1.5 mV for healthy ventricular myocardium and ≤ 0.5 mV for dense scar, with voltage levels in between delineating 'border zone' tissue. For unipolar voltages (UV), the corresponding thresholds for left ventricular (LV) healthy myocardium and scar have been reported as 8.27 mV and 5.5 mV, respectively.[2] However, these cut-off values were derived either from voltage mapping in people without structural heart disease using statistical thresholds and have been historically derived from point by point mapping instead of multielectrode mapping catheters.[2-3] Recent evidence suggests that variations in recording electrode size and inter-electrode distance with multielectrode catheters can improve mapping resolution and improve the overall accuracy of scar detection. However, it's important to note that this approach may yield different voltage values[4-5] Additionally, neighbouring tissue characteristics and pathologic factors like LV remodelling have demonstrated a need for customised cut-offs to more accurately predict regions of scar.[6-8] The Advisor^{TM} high-density (HD) Grid (Abbott Labs, Abbott Park, Il, USA) is a multielectrode mapping catheter with fixed 3mm inter-electrode spacing, 1mm electrode length and surface area of 3.14mm^2 and allows the use of multiple bipolar configurations to increase mapping accuracy. There is currently limited human data on the optimal voltage thresholds to discriminate scar using this catheter, with only data from an animal model to guide the optimal thresholds.[9] The true gold-standard to validate scar is histology but there is a paucity of human histological validation data available.[10] Most studies have therefore used two indirect methods, Magnetic Resonance Imaging (MRI) and EAM, to validate each other.[7-8] However, there are a number of limitations of previous studies using MRI to define the presence of scar.[11] In clinical imaging, the spatial resolution of LGE-MRI is frequently >1.5mm in-plane with a slice thickness between 5-10mm - in these scenarios, the partial volume effect can lead to substantial inaccuracies in identifying the true scar area.[11]

Furthermore, the threshold that is used to classify scar with MRI (e.g. full-width-half-maximum [FWHM], nSD technique or manual quantification) can result in markedly different estimates of scar location and size.[12-16] Moreover, patients with implantable-cardioverter defibrillators in situ (which is present in the overwhelming majority of patients undergoing VT ablation), frequently have device-related image artifacts even with the use of wideband LGE techniques, as well as respiratory motion and arrhythmia-related artifact, limiting whole-heart scar assessment.[17] There is therefore a need to determine optimal voltage thresholds specific to multielectrode catheters used in VT ablation using the best available techniques and processes for scar detection. These findings must remain reliable even in situations where MRI data is inaccessible or hampered by the factors mentioned above..

Objectives

In this study, we investigated whether the HD Grid mapping catheter could provide reliable information for scar detection. The primary objective was to discern the relationship between LV endocardial bipolar and unipolar voltages and the scar distribution noted on high-resolution 3D late gadolinium enhancement cardiac magnetic resonance imaging (LGE-MRI), acquired free of device-related artifacts and close to the time of VT ablation. Moreover, we aimed to determine whether additional EAM parameters could improve the accuracy of scar detection and compare their sensitivity and specificity to traditional voltage cut-offs with this catheter.

METHODS

Study population

The study prospectively enrolled patients presenting with sustained, monomorphic VT with MRI identified scar, scheduled for catheter ablation for VT. All patients underwent a 3D LGE-MRI before receiving an implanted cardiac device, to minimise artifact and within 6 months before catheter ablation. After a comprehensive discussion, all participants provided informed consent. Ethical approval was obtained from the institutional ethics committee.

Inclusion/Exclusion criteria

Consecutive patients scheduled for elective scar-dependent VT mapping and ablation were eligible for the study. Exclusion criteria included: age under 18 years, suboptimal image quality, significant MRI artifact, and unwillingness to join the study.

Cardiac Magnetic Resonance and image analysis:

- **Device and Timing:** Cardiac 3D LGE-MRI was performed on all patients, prior to implantation of an implantable cardioverter-defibrillator within the six months prior to the ablation procedure. MR Imaging was performed using a 3T Philips Achieva magnet (Philips Healthcare, Best, Netherlands) and a 32-channel coil.
- **Image Acquisition:**
- Standard sequences were obtained during breath-holds using white blood steady state free precession sequences (SSFP) and black blood turbo spin echo (TSE), with ECG signal gating. In addition, a 3D late gadolinium-enhanced sequence was obtained following the standard images. Images were obtained 10-15 minutes following the administration of a 0.15mmol/kg intravenous bolus of Gadobutrol (Gd-BT-DO3A) (Gadovist). Free-breathing images were acquired using Spectral

Pre-saturation with Inversion Recovery (SPIR) turbo field echo (TFE) sequence with respiratory navigator motion correction, a 12-degree flip angle and a 360 x 360mm field of view. Acquired voxel resolution was 1.8 x 1.8 x 3.6mm^2, which was reconstructed to 1.3 x 1.3 x 1.8mm^2. Images were analysed and exported using cvi42 version 5.14 (Circle Cardiovascular Imaging Inc, Calgary, Canada).

- **Image Processing:** The exported MRI images are used to generate a patient-specific model which incorporates the geometry and thickness of the scar. The myocardial boundaries are contoured, and the 3D geometry of the myocardial walls reconstructed using previously validated methodology.[8] Signal thresholding using a modified full-width half-maximum (FWHM) approach was used to classify each myocardial region into healthy tissue or infarct. The FWHM maximum approach has been shown to be superior to alternate methods of LGE quantification.[12] The infarct area was subdivided into border-zone or dense scar using a previously validated approach. Dense scar was defined as areas with a pixel signal intensity (PSI) of >50% the maximal signal intensity.[18] Border-zone was classified as a PSI of 35-50% and healthy tissue a PSI of < 35%. For each region in the geometry, the thickness of the myocardial wall as well as the transmurality of the scar (if present) was derived.

Electroanatomic mapping & CMR data merging: Endocardial mapping of the LV was performed with the Advisor™ HD Grid Sensor Enabled™ mapping catheter (Abbott Labs, Abbott Park, Il, USA), during stable right ventricular pacing at 600ms. BV, UV, bipolar EGM area and duration, and unipolar EGM area and duration were collected with the Ensite X mapping system (Abbott Labs, Abbott Park, Il, USA). Once mapping was complete, the MRI-derived LV model was merged with the voltage map. Rigid registration was applied using the aortic sinuses and the apex as consistent fiducial points, which were manually aligned. Furthermore, co-registration of the LVOT and proximal ascending aorta allowed for minimisation of rotational errors in all three axes, to maximise the fidelity

of the merge. The merged EAM and scar model were subsequently exported and analysed with a custom-made MATLAB Runtime. [Figure 2]

Electrogram analysis

Each EGM was reviewed and assessed for quality. EGMs showing artifact, not showing beat-beat uniformity, or inconsistent with neighbouring points, were excluded. Points within MRI-defined border zone and points at the mitral anulus, identified as displaying near-field atrial signals were excluded. Therefore, only near-field ventricular components, EGM were used for analysis. Given the potential for error in image merging, leading to positional mismatches of up to five millimetres, the analysis was confined to areas of scar and healthy tissue, intentionally avoiding the border-zone. Each point on the EAM was projected to the closest point on the MRI-derived ventricular geometry, which allowed visual representation of the local wall thickness, presence of scar, scar transmurality, local voltage data including BV, UV, BV and UV EGM duration as well as BV and UV EGM area. The EGM duration has been shown to correlate with areas of conduction slowing and vulnerability to reentry.[19] The longest EGM duration during VT is also predictive of an isthmus during mapping.[19] Both a prolonged EGM duration and an increased EGM area have been linked to areas of slow conduction, as observed in areas of increased fibrosis in experimental models.[19-20] The EGM area is derived from the EGM curve obtained during mapping. This approach is grounded in the fact that healthy tissue exhibits higher EGM voltage amplitude.[20] To simplify and to automate this process, we utilized MATLAB Runtime, which automatically calculates the EGM area. It is calculated by integrating the total area of the bipolar or unipolar EGM within the clinically specified window of interest on Ensite. All deflections (positive and negative) above a threshold of 0.05mV were included in the calculation.

Statistical analysis

Continuous variables are presented as either mean ± SD or median with interquartile range (IQR), based on their distribution normality, and were assessed using the T-test or the Mann-Whitney U test. Categorical data were analysed using the chi-square test or Fisher's exact test, as appropriate. Linear regression and Pearson's correlation were used to analyse the relationship between continuous variables. All statistical analyses were conducted using SPSS (IBM SPSS Statistics 20) and Prism (version 9.5.1-528). A p-value of <0.05 was deemed statistically significant. A ROC curve analysis determined the balance between clinical sensitivity and specificity for each parameter. Only parameters with a ROC area above 0.80 underwent further analysis to identify optimal cut-offs using Youden's index.

RESULTS

The study included 12 consecutive patients. Most had ischemic heart disease (IHD), with only two exhibiting a non-ischemic aetiology. The mean registration error between the EAM and the MRI was 4.2mm (± 0.7mm). A total of 14,886 data points were collected to create high density electroanatomic maps. Following the analysis of EGM quality, 4,058 high-quality points remained for analysis. These comprised a median of 321 (171-468) points per patient. Both bipolar and unipolar voltage showed a positive linear Pearson's correlation with wall thickness, when analysing both the totality of points and when restricting the analysis to healthy myocardium. A negative correlation was observed with scar thickness (figure 1). When comparing average EGM values within the MRI-defined scar to those in the healthy tissue, there was a statistically significant difference in both the bipolar and unipolar EGM voltage amplitudes [table 1, figure 2]. When analysing EGMs solely from dense scar (a region of points with > 50% maximal pixel intensity[18]), the degree of LGE transmurality revealed statistically significant differences in both BV and UV across the four groups, categorized as: less than 25% transmurality, 25-50% transmurality, 50-75% transmurality, and over 75% transmurality [Table 2, figure 3]. The same results were obtained by the analysis of the EGM duration and area (table 4, figure 4). Furthermore, ROC curve analysis revealed good sensitivity and specificity for scar identification using UV [Area under the ROC curve (AUC) 0.89], BV values (AUC 0.86) and BV-

area (AUC 0.88) [figure 5]. The application of the Youden index identified optimal cut-offs of 9.3 mV for UV (sensitivity 85%), 2.33 mV for BV (sensitivity 70%), and 20.13 mV.ms for BV area (sensitivity 65%). In this cohort, the mean transmurality within the dense scar was 0.86, with a median of 1.0. Therefore, these cut-off values, derived from regions of confluent MRI-defined scar, reflect voltages overlying nearly full thickness scar. Additional analysis was undertaken to compare the MRI-detected scar with the newly derive established cutoff. A comparative examination was then conducted against results obtained using the traditionally employed cutoff, revealing a superior correlation in scar detection. [table 5, and figure 6].

DISCUSSION

Despite the routine clinical application of voltage mapping to characterize myocardial tissue, customised voltage thresholds using different mapping catheters are needed for the accurate identification of scar. The classic cut-off values of BV 1.5 mV and UV 8.27 mV were derived from small study cohorts predominantly utilizing 3.5-4 mm tip ablation catheters and were formulated without the robust validation through with cardiac imaging to define scar in patients undergoing VT ablation. Specifically, the study by Hutchinson et al. included MRI data from only two patients, while that by Dinov et al. did not include any MRI data.[2-3]Subsequent studies where scar data from LGE-MRI were integrated into EAM systems used standard 2D LGE sequences or sequences with a lower spatial resolution or images acquired distant from the VT ablation procedure.[11] There was also significant variation in the thresholding techniques used to classify MRI based scar.[11-18] Recent advancements in MR imaging have been pivotal in elucidating anatomy and pathologic substrate extension and characteristics, thereby becoming a pre-requisite, for the planning of VT ablation. Unfortunately, several factors can hinder MRI utilization and compromise image quality (i.e. the presence of ICDs, respiration artifacts). Despite technological advancements, MRI images may still fall short of perfection due to large voxel sizes, which can obscure subtle myocardial structural changes.[23] Hence, there's a demand for more reliable data from EAV using multipolar catheters,

providing faster and tailored results compared to those obtained with classical single-tip catheters. The use of multi-electrode mapping catheters coupled with mapping systems that can better differentiate between near-field and far-field potentials has improved the accuracy of electro-anatomic mapping. Tung et al. demonstrated, through the application of a duodecapolar catheter, that a lower unipolar voltage cut-off more accurately discerned authentic scars compared to the classical 8.27 mV.[4] That is even though excellent contact throughout the length of a duodecapolar catheter cannot be guaranteed. Recently Ene et al. defined scar based on regions of myocardial thinning on cardiac CT and a Pentaray^{TM} catheter, used only in 10% of patients (Biosense Webster, inc., Irvine, CA, USA) for endocardial bipolar voltage mapping. They found a cut-off value of 0.2mV demonstrated the best correlation with scar areas defined by 2mm of thickness on CT whilst a cut-off of <1.0 mV best correlated with 5mm wall thickeness.[21] Additionally, the BV cut-off voltages that best identified scar and border zone based on the presence of late potentials were 0.32mV and 1.84mVb. Unfortunately, in the field of electrophysiology, particularly in ventricular mapping, there is an understanding that the rays of catheters can trigger arrhythmias. This risk may be reduced with smoother mapping catheters like the HD Grid. The present study is the first to report on human left ventricular voltage mapping data acquired with the HD Grid catheter corroborated with 3D LGE-MRI scar data. To the best of our knowledge, there is only one animal study assessing EAM data acquired with the HD Grid (Abbott Labs, Abbott Park, Il, USA) multielectrode catheter, together with LGE-MRI to define optimal scar thresholds, in an ovine model of ischaemic cardiomyopathy.[9] There are important differences between the animal model and clinical VT ablation procedures - the infarct produced in the animal model is more homogenous whilst the scar present in patients with both ischaemic and non-ischaemic cardiomyopathy is more variable. This limits the applicability of the cut-off values derived in the ovine model with this mapping catheter.[8] In our study, we sought to define dense scar, wall thickness and scar transmurality based on high-resolution 3D LGE-MRI, free from device artifacts, acquired close to the time of VT ablation, thereby minimising the impact of partial volume effects, and possible changes in loading conditions and/or rhythm that could have

occurred between the time of imaging and the time of mapping. Furthermore, we applied the FWHM threshold to classify scar which is the most reproducible method for scar quantification and similar to manual quantification.[12] This allowed our comparator for EAM to be as robust as possible within the context of a clinical study. The EGM points used in this analysis were confined to areas of confluent scar and healthy tissue, avoiding the border zones between the scar and the healthy tissue. Although this strategy may seem arbitrary and might overlook the highly arrhythmogenic substrate of VT found in the border zone, it was chosen because the primary goal of the study was to establish a useable cut-off for identifying scar within the LV musculature using a multi-electrode catheter Moreover, given the spatial resolution of MRI is still far from optimal, and potential discrepancies when merging it with EAM, steering clear of the border zone ensured using points safely distanced from potentially misleading data. Additionally, this could remove the "penumbra effect" that has been shown in the border zone in previous studies and could lead to misleading findings.[22] The main finding of this analysis was that endocardial voltage collection using a multielectrode catheter yields reliable information regarding scar presence, with pronounced differences between healthy and diseased tissues. A second finding is that unipolar voltage acquired with the HD Grid catheter has good sensitivity and specificity for scar detection. In addition, bipolar EGM area measured with this catheter and mapping system have moderate sensitivity for scar delineation. Cut-offs for these parameters, in our population with this mapping catheter, are 9.3 mV for UV, 2.3 mV for BV and 20.13 mV*ms for BV EGM area. Figure 3

Limitations

This study has some limitations. The exclusive analysis of healthy and diseased tissues, avoiding the border zone, while establishing cut-off values for scar versus healthy tissue, does not provide insight into border zone characteristics. Equally important, despite the advances in MRI data quality in recent years, pinpointing differences in minuscule regions of interest remains a challenge. The integration of structural MRI information with electrical, and potentially functional-, data from the EAM can

result in slight displacements, which could influence results particularly in the border zone. To mitigate against this, our analysis strategically focused on areas where slight misalignments are unlikely to compromise data accuracy (confluent scar and healthy tissues).

Conclusions

LV mapping utilizing the HD Grid mapping catheter yields trustworthy scar detection data. However, cut-off values need adjustment for improved scar identification. The bipolar EGM area had a moderate sensitivity for scar detection.

References

1. Zeppenfeld K, Tfelt-Hansen J, Riva M De, Winkel BG, Behr ER, Blom NA, *et al.* 2022 ESC Guidelines for the management of patients with ventricular arrhythmias and the prevention of sudden cardiac death. *Eur Heart J* Eur Heart J; 2022;**43**:3997–4126.
2. Dinov B, Schratter A, Schirripa V, Fiedler L, Bollmann A, Rolf S, Sommer P, Hindricks G, Arya A. Procedural Outcomes and Survival After Catheter Ablation of Ventricular Tachycardia in Relation to Electroanatomical Substrate in Patients With Nonischemic-Dilated Cardiomyopathy: The Role of Unipolar Voltage Mapping. J Cardiovasc Electrophysiol. 2015 Sep;26(9):985-993. doi: 10.1111/jce.12715. Epub 2015 Jul 28. PMID: 25996358.)
3. Hutchinson MD, Gerstenfeld EP, Desjardins B, Bala R, Riley MP, Garcia FC, *et al.* Endocardial unipolar voltage mapping to detect epicardial ventricular tachycardia substrate in patients with nonischemic left ventricular cardiomyopathy. *Circ Arrhythm Electrophysiol* Circ Arrhythm Electrophysiol; 2011;**4**:49–55.
4. Tung R, Kim S, Yagishita D, Vaseghi M, Ennis DB, Ouadah S, *et al.* Scar voltage threshold determination using ex vivo magnetic resonance imaging integration in a porcine infarct model: Influence of interelectrode distances and three-dimensional spatial effects of scar. *Heart Rhythm* Heart Rhythm; 2016;**13**:1993–2002.
5. Tschabrunn CM, Roujol S, Dorman NC, Nezafat R, Josephson ME, Anter E. High-resolution mapping of ventricular scar: comparison between single and multielectrode catheters. Circulation: Arrhythmia and Electrophysiology 2016: 9; e003841.
6. Sramko M, Abdel-Kafi S, Geest RJ van der, Riva M de, Glashan CA, Lamb HJ, *et al.* New Adjusted Cutoffs for 'Normal' Endocardial Voltages in Patients With Post-Infarct LV Remodeling. *JACC Clin Electrophysiol* JACC Clin Electrophysiol; 2019;**5**:1115–26.
7. Desjardins B, Crawford T, Good E, Oral H, Chugh A, Pelosi F, *et al.* Infarct architecture and characteristics on delayed enhanced magnetic resonance imaging and electroanatomic mapping in patients with postinfarction ventricular arrhythmia. *Heart Rhythm* Heart Rhythm; 2009;**6**:644–51.
8. Codreanu A, Odille F, Aliot E, Marie PY, Magnin-Poull I, Andronache M, *et al.* Electroanatomic characterization of post-infarct scars comparison with 3-dimensional myocardial scar reconstruction based on magnetic resonance imaging. *J Am Coll Cardiol* J Am Coll Cardiol; 2008;**52**:839–42.
9. Takigawa M, Relan J, Kitamura T, Martin CA, Kim S, Martin R et al. Impact of spacing and orientation on the scar threshold with a High-Density Grid catheter. Circulation: Arrhythmia and Electrophysiology 2019: 12; e007158
10. Glashan CA, Androulakis AFA, Tao Q, Glashan RN, Wisse LJ, Ebert M et al. Whole human heart histology to validate electroanatomical voltage mapping in patients with non-ischaemic cardiomyopathy and ventricular tachycardia. European Heart Journal 2018: 39; 2867-2875.
11. Mukherjee RK, Whitaker J, Williams SE, Razavi R, O'Neill MD. Magnetic resonance imaging guidance for the optimization of ventricular tachycardia ablation. Europace. 2018 Nov 1;20(11):1721-1732. doi: 10.1093/europace/euy040. PMID: 29584897; PMCID: PMC6212773.
12. Flett AS, Hasleton JM, Quarta G, Hausenloy D, Muthurangu V, Moon JC: The Full Width Half Maximum technique is superior for LGE quantification regardless of its aetiology. Journal of Cardiovascular Magnetic Resonance, 2010; 12:1–4.
13. Schmidt A, Azevedo CF, Cheng A, et al.: Infarct Tissue Heterogeneity by Magnetic Resonance Imaging Identifies Enhanced Cardiac Arrhythmia Susceptibility in Patients With Left Ventricular Dysfunction. Circulation, 2007; 115:2006–2014.

14. Sramko M, Hoogendoorn JC, Glashan CA, Zeppenfeld K. Advancement in cardiac imaging for treatment of ventricular arrhythmias in structural heart disease. Europace 2019; 21: 383-403.
15. Schelbert EB, Hsu LY, Anderson SA, Mohanty BD, Karim SM, Kellman P et al. Late gadolinium-enhancement cardiac magnetic resonance identifies postinfarction myocardial fibrosis and the borderzone at the near cellular level in the ex vivo rat heart. Circulation: Cardiovascular Imaging 2010: 3; 743-52.
16. Flett A, Hasleton J, Cook C, Hausenloy D, Quarta G, Ariti C et al. Evaluation of techniques for the quantification of myocardial scar of differing Etiology using cardiac magnetic resonance. JACC: Cardiovascular Imaging 2011; 4; 150-6.
17. Rashid S, Rapacchi S, Shivkumar K, Plotnik A, Finn JP, Hu P. Modified wideband three-dimensional late gadolinium enhancement MRI for patients with implantable cardiac devices. Magn Reson Med. 2016 Feb;75(2):572-84. doi: 10.1002/mrm.25601. Epub 2015 Mar 13. PMID: 25772155; PMCID: PMC4661130.
18. Schmidt A, Azevedo CF, Cheng A, Gupta SN, Bluemke DA, Foo TK, Gerstenblith G, Weiss RG, Marbán E, Tomaselli GF, Lima JA, Wu KC. Infarct tissue heterogeneity by magnetic resonance imaging identifies enhanced cardiac arrhythmia susceptibility in patients with left ventricular dysfunction. Circulation. 2007 Apr 17;115(15):2006-14. doi: 10.1161/CIRCULATIONAHA.106.653568. Epub 2007 Mar 26. PMID: 17389270; PMCID: PMC2442229.
19. Rossi P, Cauti FM, Niscola M, Calore F, Fanti V, Polselli M, *et al.* A novel Ventricular map of Electrograms DUration as a Method to identify areas of slow conduction for ventricular tachycardia ablation: The VEDUM pilot study. *Heart Rhythm* Heart Rhythm; 2021;**18**:1253–60.
20. Mendonca Costa C, Anderson GC, Meijborg VMF, O'Shea C, Shattock MJ, Kirchhof P, et al. The Amplitude-Normalized Area of a Bipolar Electrogram as a Measure of Local Conduction Delay in the Heart. Front Physiol Front Physiol; 2020;11
21. Ene E, Halbfa P, Nentwich K, Sonne K, Berkovitz A, Cochet H et al. Optimal cut-off value for endocardial bipolar voltage mapping using a multipoint mapping catheter to characterise the scar regions described in cardiac CT with myocardial thinning. Journal of Cardiovascular Electrophysiology 2022: 33; 2174-2180.
22. Tsiachris D, Silberbauer J, Maccabelli G, Oloriz T, Baratto F, Mizuno H, Bisceglia C, Vergara P, Marzi A, Sora N, Guarracini F, Radinovic A, Cireddu M, Sala S, Gulletta S, Paglino G, Mazzone P, Trevisi N, Della Bella P. Electroanatomical voltage and morphology characteristics in postinfarction patients undergoing ventricular tachycardia ablation: pragmatic approach favoring late potentials abolition. Circ Arrhythm Electrophysiol. 2015 Aug;8(4):863-73. doi: 10.1161/CIRCEP.114.002551. Epub 2015 May 28. PMID: 26022186.
23. Bijvoet GP, Nies HMJM, Holtackers RJ, Linz D, Adriaans BP, Nijveldt R, Wildberger JE, Vernooy K, Chaldoupi SM, Mihl C. Correlation between Cardiac MRI and Voltage Mapping in Evaluating Atrial Fibrosis: A Systematic Review. Radiol Cardiothorac Imaging. 2022 Oct 13;4(5):e220061. doi: 10.1148/ryct.220061. PMID: 36339060; PMCID: PMC9627236.

FIGURES

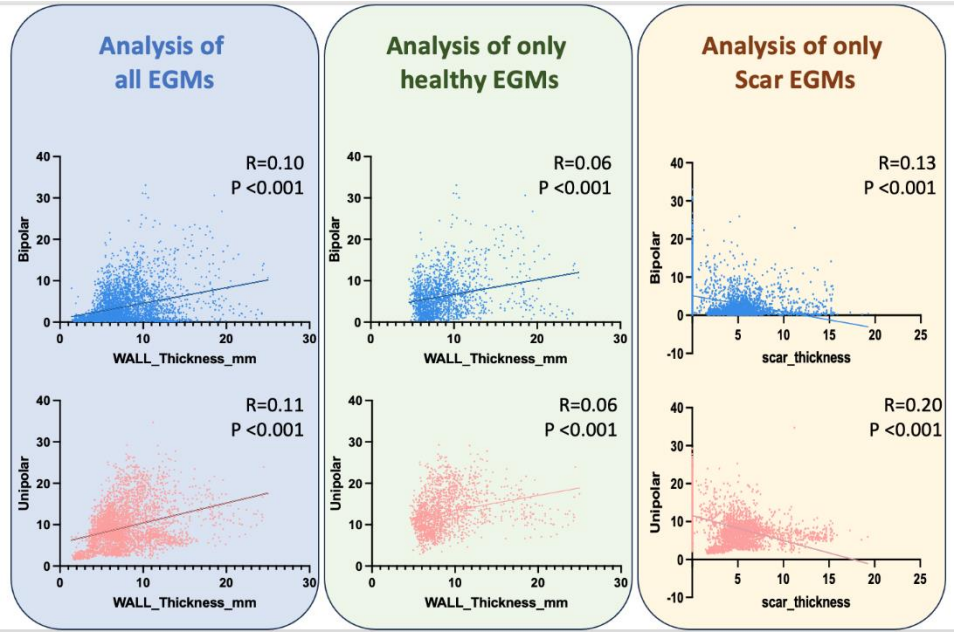

Figure 1: Simple linear regression between bipolar (blue) and unipolar signals (pink) and wall thickness considering every EGM (blue box), only healthy tissue's EGM (green box) and scar's EGM (yellow box).

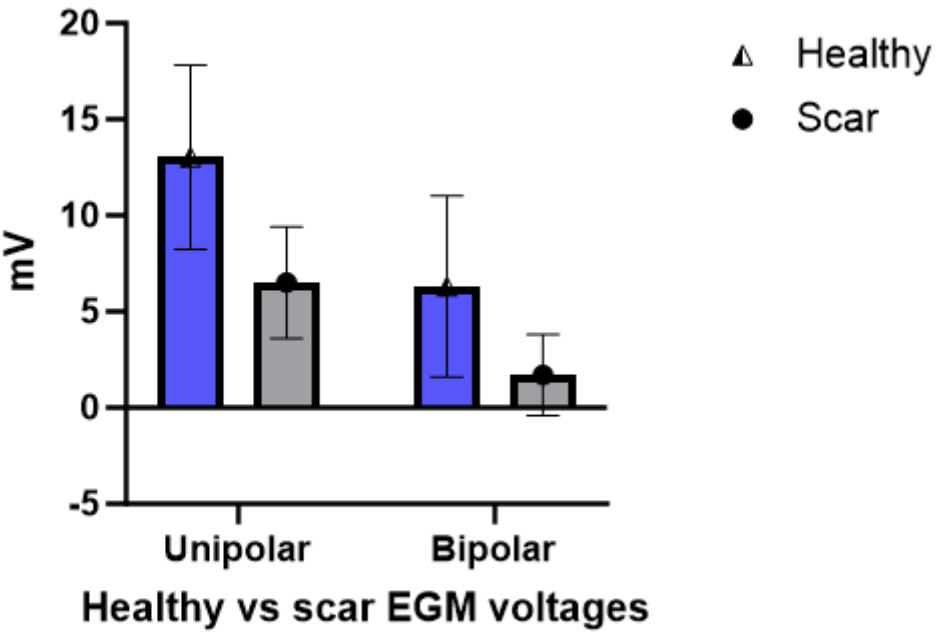

Figure 2. Unipolar and bipolar voltage in healthy (blue columns) and scar (grey columns) tissue.

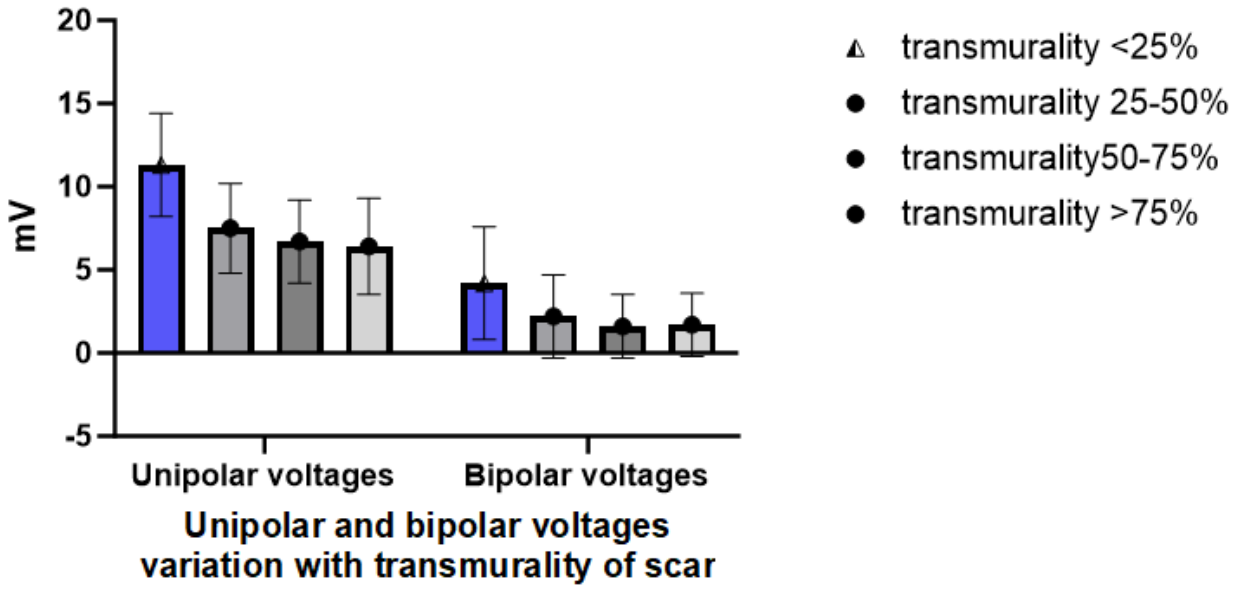

Figure 3. Bipolar and unipolar voltages in different scar transmurality.

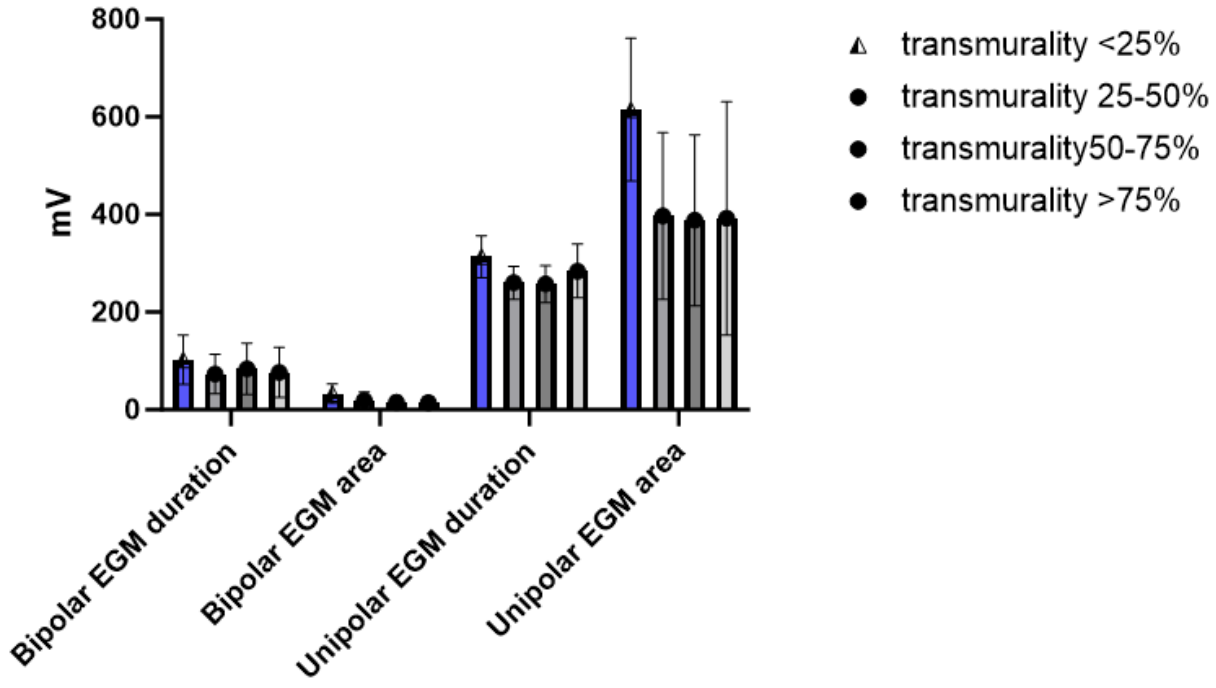

Figure 5. Bipolar and unipolar EGM duration and area in different scar transmurality.

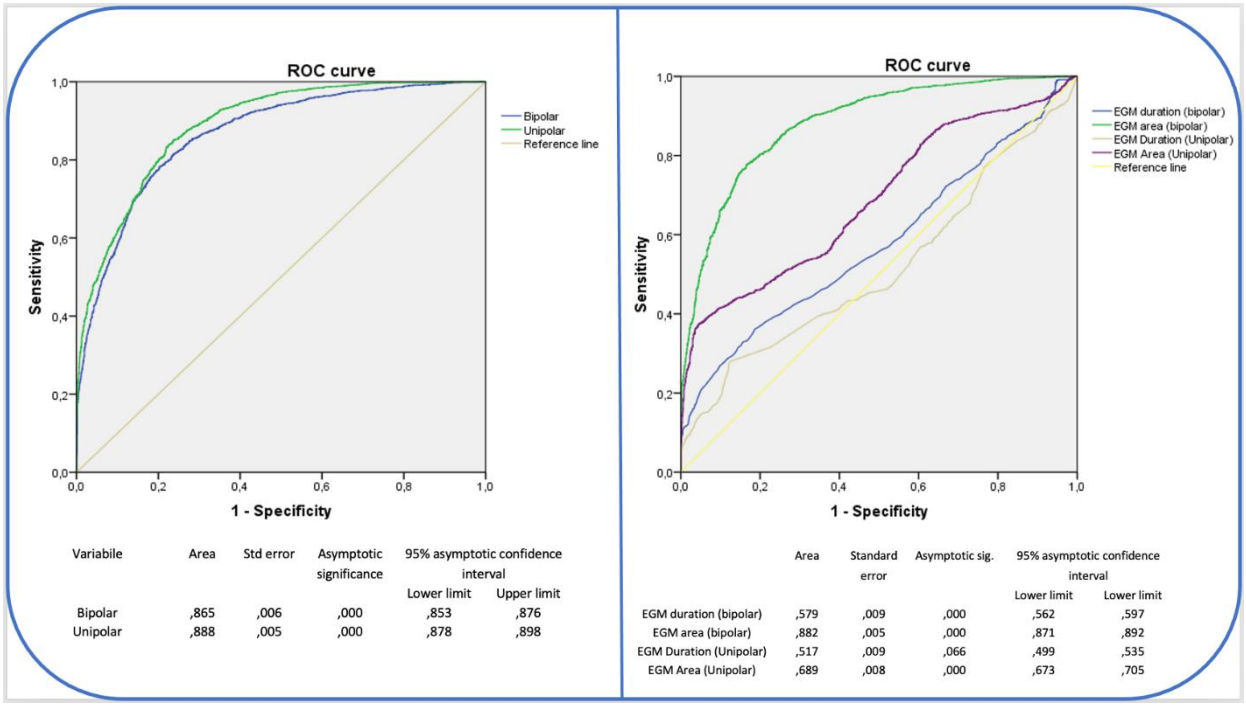

Variabile	Area	Std error	Asymptotic significance	95% asymptotic confidence interval	
				Lower limit	Upper limit
Bipolar	,865	,006	,000	,853	,876
Unipolar	,888	,005	,000	,878	,898

	Area	Standard error	Asymptotic sig.	95% asymptotic confidence interval	
				Lower limit	Lower limit
EGM duration (bipolar)	,579	,009	,000	,562	,597
EGM area (bipolar)	,882	,005	,000	,871	,892
EGM Duration (Unipolar)	,517	,009	,066	,499	,535
EGM Area (Unipolar)	,689	,008	,000	,673	,705

Figure 5: ROC curves for bipolar and unipolar EGMs (left box) and bipolar and unipolar EGMs' areas and durations (right box).

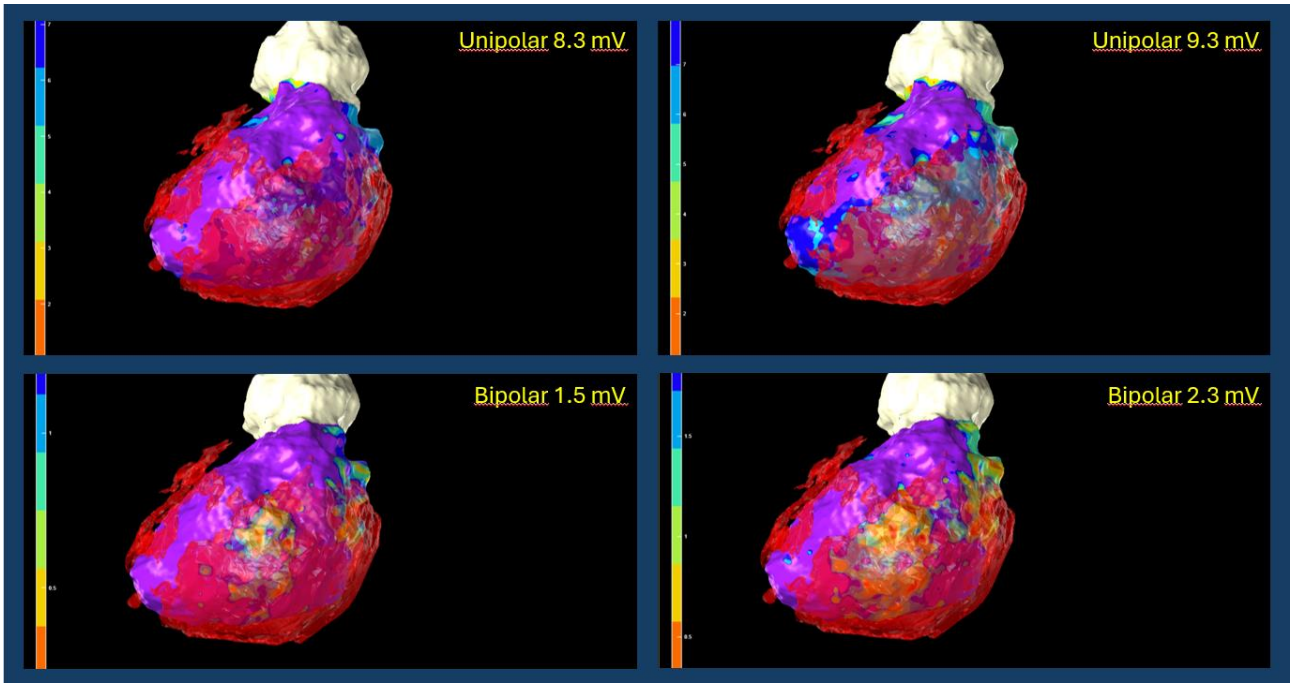

Figure 6: MRI scar and EAM merging. Left panels: Electroanatomic map (using standard voltage cut offs >1.5 mV (BV) and > 8.3 mV (UV) for healthy myocardium. Right Panels: Electroanatomic map (using newly recognised cut offs >2.3 mV (BV) and > 9.3 mV (UV) for healthy myocardium

	Overall	Healthy area	Dense scar	Pvalue
Bipolar voltages, mean (SD)	3,7 (4,1)	6,3 (4,7)	1,7 (2,1)	<0.005
Unipolar voltages, mean (SD)	9,3 (5)	13,03 (4,8)	6,5 (2,9)	<0.005

Table1: Differences between voltages parameters in healthy tissue and dense scar.

Transmurality		**Bipolar**	**Unipolar**
<25%	Mean (SD)	4,21(3,4)	11,3(3,1)
25-50%	Mean (SD)	2,2 (2,5)	7,5 (2,7)
50-75%	Mean (SD)	1,6 (1,9)	6,7 (2,5)
75-100%	Mean (SD)	1,7 (1,9)	6,4 (2,9)
pvalue		<0.005	<0.005

Table 2: Within scar electroanatomic voltage variation depending on transmurality of scar

	Overall	Healthy area	Dense scar	Pvalue
Bipolar EGM duration, mean (SD)	82 (52,9)	88,7 (54,9)	77 (50,9)	<0.005
Bipolar EGM area, mean (SD)	27,8 (24,9)	45,1 (27,1)	15 (12,5)	<0.005
Unipolar EGM duration, mean (SD)	278,1 (48,8)	279,5 (42,2)	535,9 (202,4)	0,07
Unipolar EGM area, mean (SD)	452,5 (227,9)	277,1 (53,1)	390,9 (226,2)	<0.005

Table 3: Differences between EGMs parameters in healthy tissue and dense scar.

Transmurality		BV EGM duration	BV EGM area	UV EGM Duration	UV EGM Area
<25%	Mean (SD)	102 (50,2)	32,8 (19,7)	313,4 (42,8)	614,5 (146,5)
25-50%	Mean (SD)	73 (40,9)	19,1 (16,3)	260,1 (33,8)	396,9 (170,8)
50-75%	Mean (SD)	83,9 (52,7)	14,8 (12,8)	258,5 (37,7)	388 (175,2)
75-100%	Mean (SD)	76,3 (51,4)	14,6 (11,6)	283,9 (55,2)	392,2 (239,1)
pvalue		<0.005	<0.005	<0.005	<0.005

Table 4: Within scar electroanatomic voltage variation depending on transmurality of scar

Patient number	MRI LGE area	Bipolar low voltage area (1.5mV cutoff)	Difference bi 1.5 and LGE area	Bipolar low voltage area 2.3mv cutoff	Difference LGE area and bipolar 2.3mV	Unipolar low voltage area cutoff 8.3	Difference LGE area and unipolar 8.3mV	Unipolar low voltage area cutoff 9.3	Difference LGE area and unipolar 9.3mV	Bipolar area 20.13	Difference area 20.13 and LGE
1	37,3	24,15	41,5%	42,56	-14,10%	57,3	-53,62%	61,4	-64,61%	59,68	-60,00%
2	43,8	33,93	9,0%	51,5	-17,58%	49,2	-12,33%	55,9	-27,63%	57,6	-31,51%
3	34,4	24,5	44,1%	38,5	-11,92%	10,22	70,29%	19,38	43,66%	27,91	18,87%
4	54,2	17,97	47,8%	42,05	22,42%	22,5	58,49%	45,08	16,83%	63,91	-17,92%
5	88,2	79,2	-46,1%	105,11	-19,17%	110,9	-25,74%	127,9	-45,01%	104,53	-18,51%
6	59,9	23,43	73,4%	31,87	46,79%	69,46	-15,96%	85,77	-43,19%	62,79	-4,82%
7	83,7	29,5	50,8%	53,5	36,08%	57,53	31,27%	74,23	11,31%	60,2	28,08%
8	41,3	18,99	77,3%	26,84	35,01%	1,7	95,88%	7,1	82,81%	23,59	42,88%
9	61,4	43,61	-8,8%	56,72	7,62%	41,99	31,61%	54,64	11,01%	51,62	15,93%
10	29,4	22,2	42,8%	40,71	-38,47%	1,67	94,32%	10,13	65,54%	28,7	2,38%
11	29,8	26,29	10,6%	31,59	-6,01%	33,85	-13,59%	41,49	-39,23%	67,17	-125,40%
12	59,8	38,8	-30,2%	61,59	-2,99%	66	-10,37%	82	-37,12%	71,72	-19,93%
Mean			26,01%		3,14%		20,85%		-2,14%		-14,16%
StDev			39,21%		26,46%		49,95%		47,94%		44,96%

Table 5 : EAM detected scar with classical cutoff and newly recognised cutoff (yellow columns) and comparison to the MRI recognised scar.

Chapter 3

In this chapter, the author dives into the dynamic realm of cardiac implantable electronic devices (CIED). Here, the author unveils a fascinating exploration into an uncommon complication stemming from ICD malfunction, to infections associated with CIED unveiling insights from a multicenter study. This study delves into the intricate landscape of infections associated with implantable devices, with a keen focus on the diagnostic prowess of PET scans in identifying gram-negative device infections.

Arrhythmic Storm Due to ICD Atrial Lead Malfunction

Davide Fabbricatore, MD,[a,b,*] Ward Heggermont, MD, PhD,[a] Dimitri Buytaert, MEng,[a] Koen Van Bockstal, RN,[a] and Tom De Potter, MD[a]

JACC Case Rep. 2022 Apr 6; 4(7): 438–442.
Published online 2022 Apr 6. doi: 10.1016/j.jaccas.2021.12.013

PMCID: PMC9175138

PMID: 35693896

Key Words: cardiac pacemaker, genetic disorders, ventricular tachycardia

Abbreviations and Acronyms: AAI, atrial-pacing atrial-sensing inhibited-response; DDD, dual-pacing dual-sensing dual-response; EGM, electrogram; ICD, implantable cardioverter-defibrillator; LQTS, long QT syndrome; VP, ventricular paced (beat); VVI, ventricular-pacing ventricular-sensing inhibited-response

Central illustration

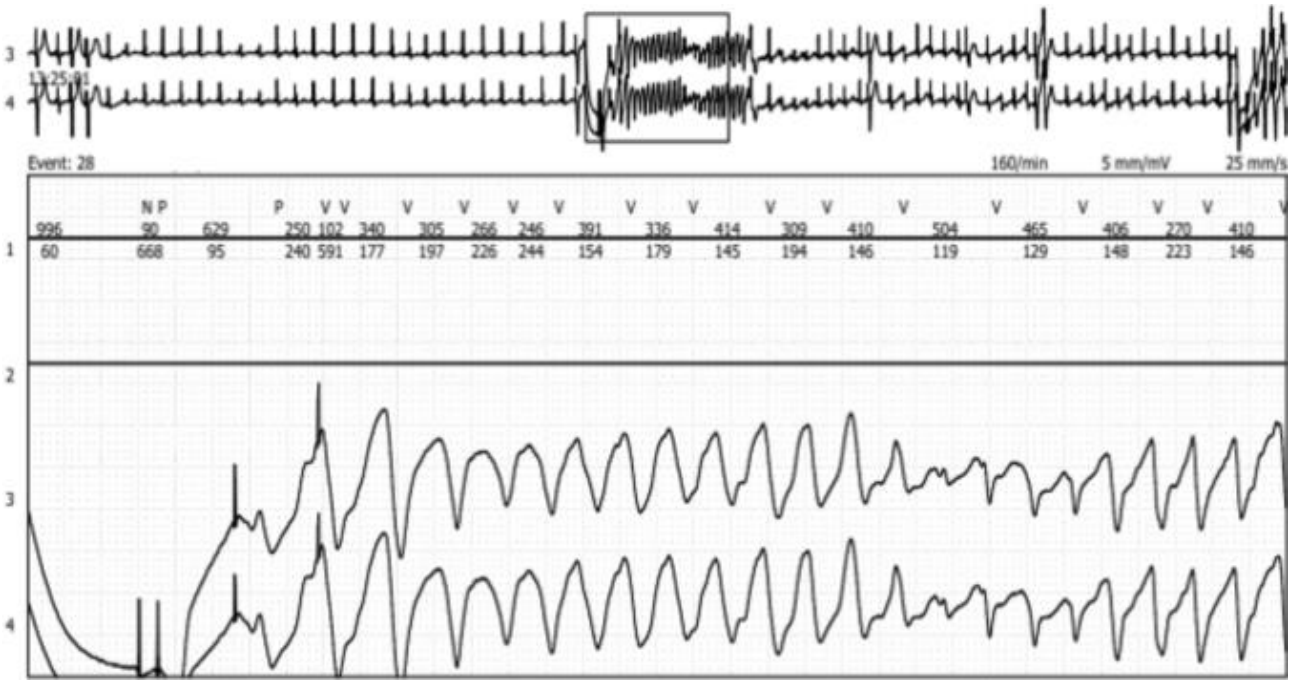

Introduction

Implantable cardioverter-defibrillators (ICDs) are indicated for the prevention of life-threatening arrhythmias, both in primary and secondary prevention, as well as in ischemic and nonischemic conditions.[1,2] Although infections are still the most frequent and dreaded complications of cardiac implantable electronic devices, lead failure is an increasingly frequent condition that results from aging of the device recipients, with consequent prolongation of "lead life."[3,4] Because inserting dual-chamber devices theoretically doubles the possibility of both infective and mechanical problems and has only a relative benefit in improved arrhythmia recognition, the use of a single-chamber system may be preferred if atrial sensing or pacing is not needed.[5] Also worth mentioning is the importance of optimal programmed stimulation in each patient, to achieve a specific goal (physiological activation vs fully paced rhythm).[6]

Learning objectives

•To make a differential diagnosis on the basis of endocavitary signals.

•To choose the best device and pacing modality in patients with cardiomyopathy.

•To think about uncommon causes of ventricular arrhythmias.

Here we describe a rare case of a young woman with a dual-chamber ICD for long-QT syndrome who was referred to our emergency department (Cardiovascular Research Centre of Aalst, Belgium) for an "arrhythmic storm" caused by atrial lead malfunction.

History of Presentation

A 41-year-old woman was referred to our institution's emergency department after receiving numerous defibrillator shocks.

Past Medical History

A dual-chamber ICD was implanted in the past for secondary prevention after aborted sudden death in the context of long QT syndrome (LQTS), genetically confirmed by identification of a potassium voltage-gated channel subfamily Q member 1 (KCNQ1) mutation. In the following years, she experienced several ventricular arrhythmia episodes that were successfully treated by the ICD. Moreover, several reprogramming sessions were performed to adapt the pacing configuration to her specific characteristics, most notably chronotropic incompetence. In particular, the dual-pacing dual-sensing dual-response (DDD) stimulation with an atrial-pacing atrial-sensing inhibited-response (AAI)-to-ventricular-pacing ventricular-sensing inhibited-response (VVI) algorithm (AAI with VVI pacing backup) with a lower rate of 50 min-1 configuration was programmed to allow for

physiological cardiac activation. As a consequence of episodes of vertigo and bradycardia for which vagal hypertonia was suspected, the lower rate was set to 65 min-1, and the AAI-to-VVI algorithm was switched off.

Differential Diagnosis

In a patient with confirmed LQTS and previous ventricular arrhythmias, the most probable diagnosis was appropriate shocks on ventricular arrhythmias.

Investigations

A quick ICD interrogation confirmed the presence of multiple ventricular arrhythmic episodes during the last 2 days, all successfully treated by the ICD. For management of the ongoing arrhythmic storm, the patient was admitted to the critical care unit for monitoring. During her subsequent hospitalization, the patient experienced numerous consecutive ventricular episodes, always correctly detected and appropriately treated by the ICD. Cardiac telemetry showed that unexpected ventricular paced (VP) beats during sinus rhythm preceded the ventricular arrhythmias (Figure 1).

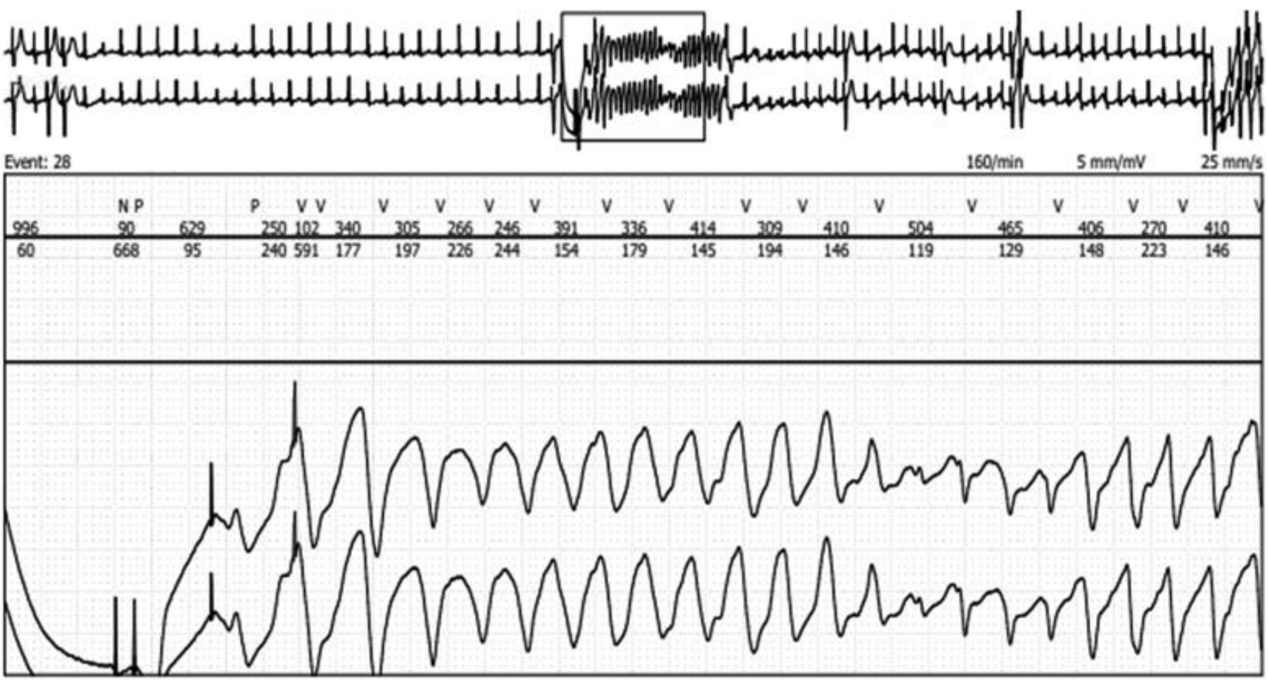

Figure 1

Telemetry Trace

Induction of ventricular tachycardia from 2 ventricular paced beats.

The ICD was ulteriorly interrogated in the electrophysiology unit. Surprisingly, it was observed that ventricular arrhythmias were always anticipated by episodes of noise on electrograms (EGMs) recorded from the atrial lead, probably resulting from atrial lead fracture. Episodes of noises were tracked and followed by double VP beats with delays of 363 milliseconds (165 beats/min) representing the maximal tracking rate. This sequence of "short-long-short intervals" induced ventricular arrhythmia (Figure 2). Device interrogation showed normal parameters of the right ventricular coil lead (sensing, 9.8 mV; pace impedance, 300 Ω; threshold, 1.6 V at 0.4 milliseconds; shock impedance, 62 Ω). Regarding the atrial lead, sensing of the A-wave and pacing threshold were normal (4 mV and 0.9 V at 0.4 milliseconds, respectively); pacing impedance, however, displayed an abrupt increase (>3,000 Ω). Fluoroscopy investigation ruled out macrofractures of any lead.

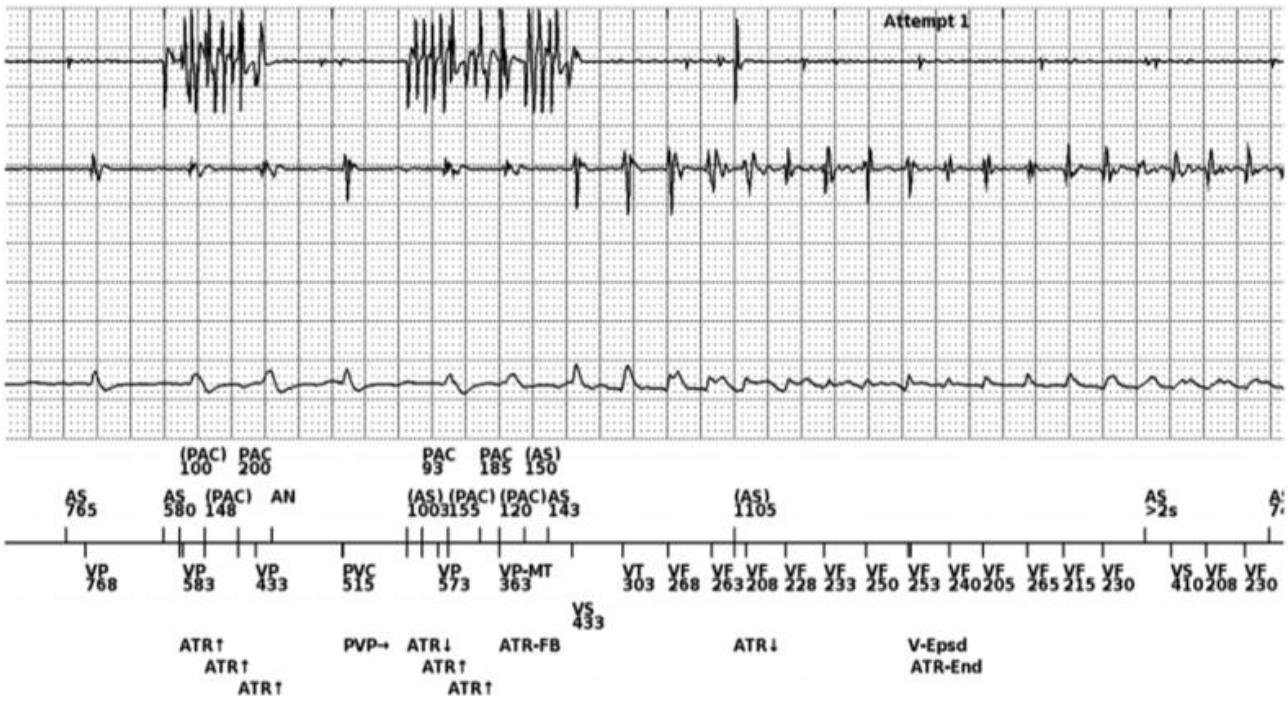

Figure 2

Endocavitary Signals and Shock Electrogram at the Onset of the Ventricular Arrhythmia

On the atrial channel (first channel), it is possible to recognize 2 short episodes of noise misinterpreted as premature atrial contractions (PACs) because of undersensing (note also undersensing of the atrial signal between the 2 episodes of noise). On the ventricular channel (second channel), during the second episode of atrial noise, there are 2 ventricular paced (VP) beats with a delay of 363 milliseconds (VP-VP-MT) that represents the maximal ventricular paced tracking rate. This sequence

of “short-long-short intervals” induced ventricular arrhythmia. AN = atrial noise; AS = atrial sense; ATR = atrial tachycardia response; FB = fallback; MT = maximum tracking rate; PVP = post ventricular atrial refractory period after premature ventricular complex; V-Epsd = ventricular episode; VF = ventricular Fibrillation; VT = ventricular Tachycardia.

Management

The therapeutic decision was made not to perform lead extraction because of the risk of dislodgment or lesion of the right ventricular coil lead and the perceived futility of the atrial pacing, thus postponing this intervention until generator replacement is needed. Rather, the ICD was reprogrammed to the VVI pacing modality during hospitalization. The patient was discharged the next day.

Discussion

This case describes a very rare condition in which fracture of the atrial lead induced ventricular arrhythmias, that were—fortunately—always correctly treated by an ICD. The addition of an atrial lead in dual-chamber ICDs could theoretically reduce inappropriate shocks by improved detection capabilities, thereby allowing better identification of supraventricular arrhythmias. However, this potential benefit has not been assessed in randomized clinical trials. Moreover, a meta-analysis showed that the rates of inappropriate ICD shocks were not different between single- and dual-chamber devices.5 In addition, cardiac pacing was historically recommended as a potentially useful preventive strategy in LQTS because it was thought to prevent “pause-dependent” ventricular tachycardia induction.7 Although this is no longer a recommendation in contemporary guidelines, dual-chamber pacing is still commonly observed in patients with previously implanted ICDs. In terms of complication risk, the placement of an atrial lead requires a longer procedural time and is associated with higher rates of peri-implant complications and generator replacements.8 In the case detailed here, several factors created the perfect substrate for the development of ventricular arrhythmias. The sequence started with fracture of the atrial lead, followed by undersensing of the “extra waves” on the atrial EGM without switching from the DDD to the VVI configuration. The latter condition is caused by both undersensing and the shorter length of noise episodes. In addition, the programmed maximum tracking rate at 165 beats/min led to a coupled interval of 363 milliseconds. Finally, an arrhythmic substrate was present with a particularly long QTc interval of 517 milliseconds (Figure 3) that made the tissue especially susceptible to the induction of arrhythmias.

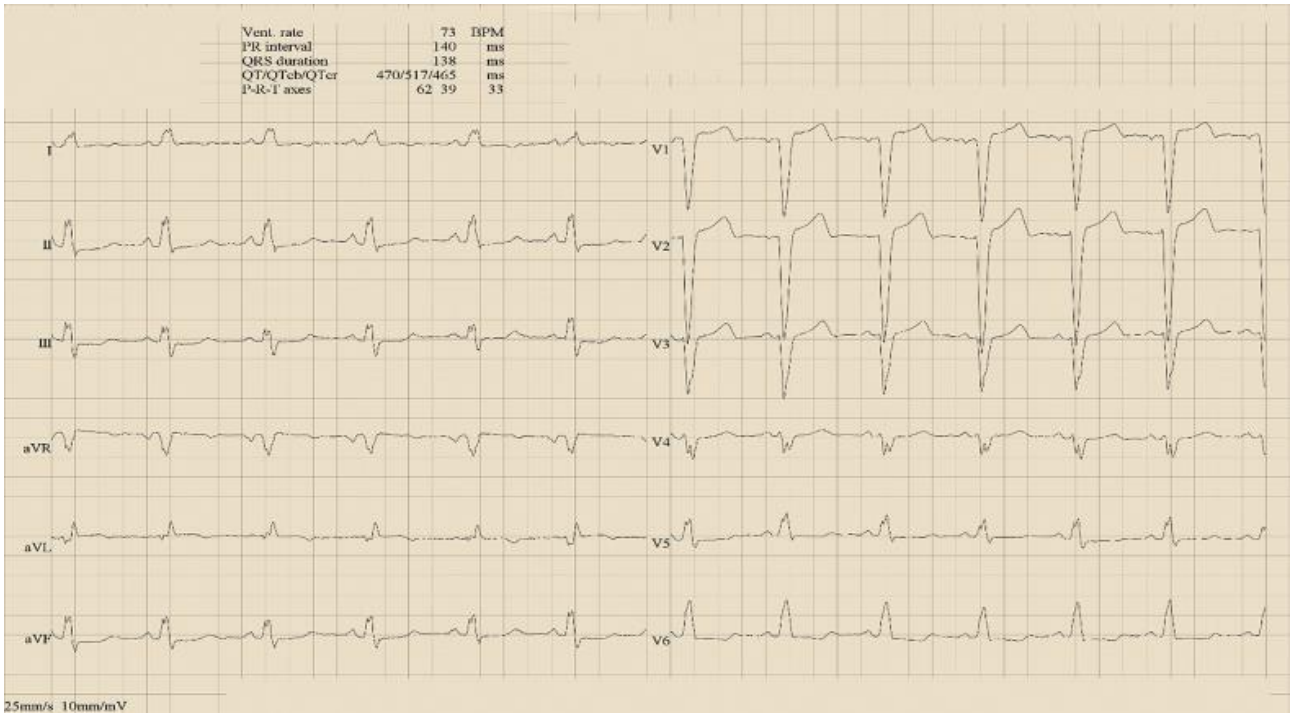

Figure 3

Electrocardiogram Intervals

Note the prolonged QTc interval of 517 milliseconds during spontaneous sinus rhythm.

Follow-Up

During subsequent follow-up, also with home monitoring, the patient did not experience any problems, and no device malfunction was observed.

Conclusions

This case report highlights the importance of a correct choice of both the type of device and the pacing modality. In retrospect, in this case, from the beginning a single-chamber device should have been selected. In addition, different types of pacing modalities (ie, AAI, DDI, VVI) or different algorithms could have avoided such a complication. Finally, in patients with LQTS with historical insertion of a bradyarrhythmia-only dual-chamber pacing system, a risk exists for induction of potentially lethal ventricular arrhythmias after atrial lead failure.

References

1. Theuns D.A.M.J., Smith T., Hunink M.G.M., et al. Effectiveness of prophylactic implantation of cardioverter-defibrillators without cardiac resynchronization therapy in patients with ischaemic or non-ischaemic heart disease: a systematic review and meta-analysis. Europace. 2010;12:1564–1570.

2. Brignole M., Auricchio A., Baron-Esquivias G., et al. 2013 ESC guidelines on cardiac pacing and cardiac resynchronization therapy. Eur Heart J. 2013;34:2281–2329.

3. Bongiorni M.G., Kennergren C., Butter C., et al. The European Lead Extraction ConTRolled (ELECTRa) study: a European Heart Rhythm Association (EHRA) registry of transvenous lead extraction outcomes. Eur Heart J. 2017;38:2995–3005.

4. Diemberger I., Mazzotti A., Biffi M., et al. From lead management to implanted patient management: systematic review and meta-analysis of the last 15 years of experience in lead extraction. Expert Rev Med Devices. 2013;10:551–573.

5. Theuns D.A.M.J., Rivero-Ayerza M., Boersma E., Jordaens L. Prevention of inappropriate therapy in implantable defibrillators: a meta-analysis of clinical trials comparing single-chamber and dual-chamber arrhythmia discrimination algorithms. Int J Cardiol. 2008;125:352–357.

6. Wilkoff B.L., Fauchier L., Stiles M.K., et al. 2015 HRS/EHRA/APHRS/SOLAECE expert consensus statement on optimal implantable cardioverter-defibrillator programming and testing. Heart Rhythm. 2016;13:e50–e86.

7. Viskin S. Cardiac pacing in the long QT syndrome: review of available data and practical recommendations. J Cardiovasc Electrophysiol. 2000;11(5):593–600.

8. Defaye P., Boveda S., Klug D., et al. Dual- vs. single-chamber defibrillators for primary prevention of sudden cardiac death: long-term follow-up of the Défibrillateur Automatique Implantable-Prévention Primaire registry. Europace. 2017;19:1478–1484.

Risk factors for Gram-negative bacterial infection of cardiovascular implantable electronic devices: multicentre observational study (CarDINe Study)

Author links open overlay panelRenato Pascale 1 2, Alice Toschi 1, Abdullah Tarik Aslan 3 4, Giulia Massaro 5 6, Angelo Maccaro 1, Davide Fabbricatore 7 8, Andrea Dell'Aquila 9, Marco Ripa 10, Mehmet Emirhan Işık 11, Yeşim Uygun Kızmaz 11, Saverio Iacopino 12, Marta Camici 13 14, Francesco Perna 15, Karolina Akinosoglou 16, Arta Karruli 17, Matthaios Papadimitriou-Olivgeris 18, Bircan Kayaaslan 19, Yeşim Aybar Bilir 19, Emin Evren Özcan 20, Oğuzhan Ekrem Turan 20, Muhammed Cihan Işık 21, María Teresa Pérez-Rodríguez 22, Belén Loeches Yagüe 23, Alejandro Martín Quirós 24, Mesut Yılmaz 25, Sabine Petersdorf 26, Tom De Potter 7, Emanuele Durante-Mangoni 17, Murat Akova 21, Antonio Curnis 9, Dino Gibertoni 27, Igor Diemberger 5 6, Luigia Scudeller 27, Pierluigi Viale 1 2, Maddalena Giannella 1 2

1 Infectious Diseases Unit, Department of Integrated Management of Infectious Risk, IRCCS Azienda Ospedaliero-Universitaria di Bologna, Bologna, Italy

2 Department of Medical and Surgical Sciences, University of Bologna, Bologna, Italy

3 Golhisar State Hospital, Department of Internal Medicine, Burdur, Turkey

4 Hacettepe University School of Medicine, Department of Internal Medicine, Ankara, Turkey

5 Department of Experimental, Diagnostic and Specialty Medicine, University of Bologna, Bologna, Italy

6 Institute of Cardiology, IRCCS Azienda Ospedaliero-Universitaria di Bologna, Bologna, Italy

7 Cardiovascular Center, Onze-Lieve-Vrouwziekenhuis Hospital, Aalst, Belgium

8 Department of Advanced Biomedical Sciences, Federico II University Hospital, Naples, Italy

9 Institute of Cardiology, Department of Medical and Surgical Specialties, Radiological Sciences, and Public Health, ASST Spedali Civili Hospital of Brescia and University of Brescia, Brescia, Italy

10 Unit of Infectious and Tropical Diseases, IRCCS San Raffaele Scientific Institute, Milan, Italy

11 University of Health Sciences Kosuyolu Training and Research Hospital, Department of Infectious Diseases and Clinical Microbiology, Istanbul, Turkey

12 Maria Cecilia Hospital, GVM Care & Research, Cotignola, Italy

13 Institute of infectious diseases, Fondazione Policlinico Universitario A. Gemelli IRCCS, Rome, Italy

14 HIV/AIDS Clinical Unit, National Institute for infectious Diseases L. Spallanzani IRCCS, Rome, Italy

15 Cardiac Arrhythmia Unit, Fondazione Policlinico Universitario A. Gemelli IRCCS, Rome, Italy

16 Internal Medicine Department, University General Hospital of Patras, Greece

17 Department of Precision Medicine, University of Campania 'L. Vanvitelli', Monaldi Hospital, Naples, Italy

18 Infectious Diseases Service, Lausanne University Hospital and University of Lausanne, Lausanne, Switzerland

19 Ankara Yıldırım Beyazıt University Faculty of Medicine, Ankara City Hospital, Department of Infectious Diseases and Clinical Microbiology, Ankara, Turkey

20 Dokuz Eylul University, Heart Rhythm Management Center, İzmir, Turkey

21 Hacettepe University School of Medicine, Department of Infectious Diseases and Clinical Microbiology, Ankara, Turkey

22 Infectious Diseases Unit, Department of Internal Medicine, Complexo Hospitalario Universitario de Vigo, Spain Instituto de Investigación Biomédica Galicia Sur, Spain

23 Infectious Diseases Unit, Hospital Universitario La Paz - IDIPAZ, Madrid, Spain

24 Emergency Department, Hospital Universitario La Paz - IDIPAZ, Madrid, Spain

25 Istanbul Medipol University Faculty of Medicine, Department of Infectious Diseases and Clinical Microbiology, Istanbul, Turkey

26 Institute of Medical Laboratory Diagnostics, HELIOS University Clinic Wuppertal, Witten/Herdecke University, Witten, Germany

27 Research and Innovation Unit, IRCCS Azienda Ospedaliero-Universitaria di Bologna, Bologna, Italy

Highlights

- Gram-negative bacteria cardiovascular implantable electronic device (GNB-CIED) infections are associated with obesity and an increased number of comorbidities
- The risk of GNB-CIED may be increased in right subclavian vein site and ventricular-pacing ventricular-sensing inhibited-response pacemaker use
- Fluorodeoxyglucose positron emission computed tomography could be a useful tool to diagnose GNB-CIED infections•
- GNB-CIED infections are associated with increased mortality risk.

Abstract

Background

Infections of cardiovascular implantable electronic devices (CIED) are mainly due to Gram-positive bacteria (GPB). Data about Gram-negative bacteria CIED (GNB-CIED) infections are limited. This study aimed to investigate risk factors, clinical and diagnostic characteristics, and outcome of patients with GNB-CIED.

Methods

A multicentre, international, retrospective, case-control-control study was performed on patients undergoing CIED implantation from 2015 to 2019 in 17 centres across Europe. For each patient diagnosed with GNB-CIED, one matching control with GPB-CIED infection and two matching controls without infection were selected.

Results

A total of 236 patients were enrolled: 59 with GNB-CIED infection, 59 with GPB-CIED infection and 118 without infection. No between-group differences were found regarding clinical presentation, diagnostic and therapeutic management. A trend toward a higher rate of fluorodeoxyglucose positron emission computed tomography (FDG PET/CT) positivity was observed among patients with GNB than in those with GPB-CIED infection (85.7% vs. 66.7%; P = 0.208). Risk factors for GNB-CIED infection were Charlson Comorbidity Index Score (relative risk reduction, RRR = 1.211; P = 0.011), obesity (RRR = 5.122; P = 0.008), ventricular-pacing ventricular-sensing inhibited-response pacemaker implantation (RRR = 3.027; P = 0.006) and right subclavian vein site of implantation (RRR = 5.014; P = 0.004). At 180-day survival analysis, GNB-CIED infection was associated with increased mortality risk (HR = 1.842; P = 0.067).

Conclusions

Obesity, high number of comorbidities and right subclavian vein implantation site were associated with increased risk of GNB-CIED infection. A prompt therapeutic intervention that may be guided using FDG PET/CT is suggested in patients with GNB-CIED infection, considering the poorer outcome observed in this group.

1. Introduction

Cardiac implantable electronic devices (CIED)—including permanent pacemakers (PM), implantable cardioverter-defibrillators (ICD) and cardiac resynchronisation therapy devices (CRTD)—have improved patients' survival and quality of life [1].

Infections are a serious complication of CIED implantation [2,3], with incidence varying from 0.5% – 10% in different studies [3,4]. Gram-positive bacteria (GPB), especially coagulase-negative Staphylococcus spp. and Staphylococcus aureus, are the most common microorganisms isolated from patients with CIED infections [5,6]. Although less frequently isolated from patients with CIED infection, Gram-negative bacteria (GNB) are currently the most common causative pathogens of healthcare-associated infections and are associated with high morbidity and mortality rates [7,8].

The literature results on CIED infections are mostly derived from cohorts of patients with GPB isolates [9], [10], [11]. Thus, data are limited about prevalence, risk factors and clinical presentation of CIED infections due to GNB (GNB-CIED) and the reliability of diagnostic tools in the management of such episodes [12,13].

To fill this gap, a multicentre, retrospective, matched case-control-control study in patients with CIED implantation was conducted to investigate the risk factors for the development of GNB-CIED infections, as well as the clinical and diagnostic characteristics and outcomes of these infections.

2. Material and methods

2.1. Study design and population

A multicentre, international, retrospective, matched, case-control-control study was performed. All adult patients with a diagnosis of CIED infection from 1 January 2015 to 31 December 2019 were screened for enrolment using local registries of implanted cardiac devices at each clinical site. Records were matched with the local microbiology databases to identify patients who developed a CIED infection within 1 year from implantation. Inclusion criteria were: i) adult age (≥ 18 years); ii) implantation with PM, ICD and/or CRTD; and iii) acceptance to participate by informed consent. Patients with CIED infection due to polymicrobial aetiology were excluded.

The included participants were classified as cases or controls according to the following definitions: i) case: a patient diagnosed with a local device infection or CIED-related infective endocarditis with isolation of a GNB (GNB-CIED infection) from the insertion site, the lead and/or blood cultures (BCs); ii) control 1: a patient diagnosed with a local device infection or CIED-related infective endocarditis with isolation of a GPB (GPB-CIED) from the wound, lead and/or BCs; iii) control 2: patients without a diagnosis of local device infection or CIED-related infective endocarditis within 1 year after CIED implantation. For each patient diagnosed with GNB-CIED, one control with GPB-CIED infection and two controls without infection were selected (ratio 1:1:2), matched by implantation period (± 1 year) and study centre. To avoid multiple stratification limiting the sample size, no other matching criteria were employed. All other variables were included as potential confounders in the multivariable multinomial logistic regression.

Hospital records and phone interviews were the sources of the follow-up data. The study was conducted according to the Declaration of Helsinki and Good Clinical Practice guidelines and approved by the ethics committee of the coordinating centre (EM487 2021_117/2021/Oss/AOUBo) and by ethics committees of all participating centres. During the study period, indications for CIED implantation and patient management were determined by the discretion of the attending physicians at each centre.

2.2. Setting

This study was endorsed by the Study Group for Implant-Associated Infections of the European Society of Clinical Microbiology and Infectious Diseases (ESGIAI), the European Society of Clinical Microbiology and Infectious Diseases Study Group for Bloodstream Infections, Endocarditis and Sepsis (ESGBIES) and The Study Group for Carbapenem Resistance (SCARE). Seventeen hospitals performing CIED implantation participated in the study: six from Italy (Bologna, Cotignola, Milan, Rome, Brescia, Naples); five from Turkey (two in Istanbul, two in Ankara, one in Izmir); two from Spain (Madrid and Vigo); one from Germany (Wuppertal); one from Switzerland (Lausanne); one from Belgium (Aalst); and one from Greece (Patras) (Supplementary Table 1 and Figure 1).

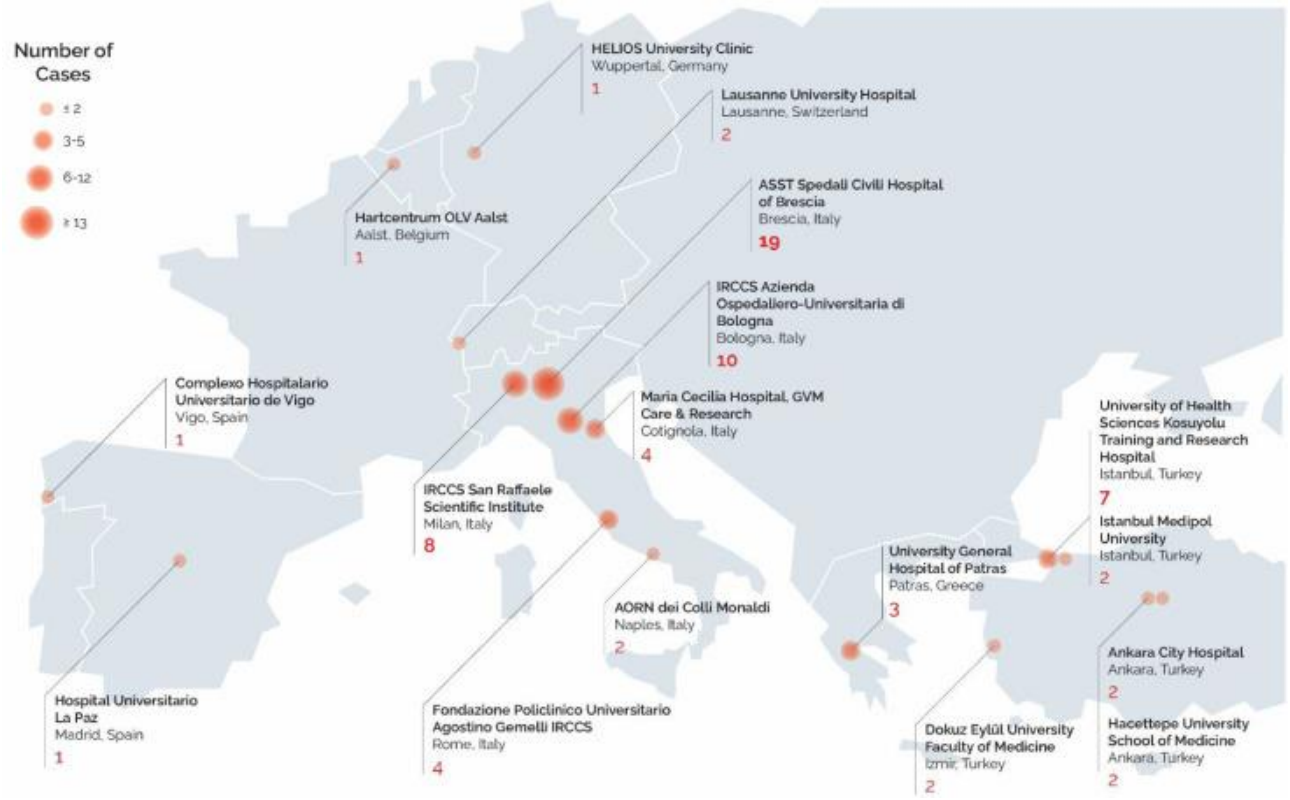

Figure 1. Participating centres.

2.3. Variables and definitions

Study variables were collected using a dedicated REDCap electronic case report form (eCRF) hosted by IRCCS Azienda Ospedaliero-Universitaria di Bologna [14]. Of note, patients were considered once at the time of their first episode of CIED infection.

The primary endpoint was the diagnosis of CIED infection, defined as local infection or CIED-related infective endocarditis according to ESC guidelines [15] and the last European Heart Rhythm Association (EHRA) international consensus document available during protocol design [16]. Secondary endpoints included: persistence of infection/failure, all-cause mortality, and recurrence at 30, 90 and 180 days from the diagnosis of CIED infection (day of drawing index positive samples). Infection persistence/failure was defined as the persistence of signs and/or symptoms of local or systemic infection at the end of appropriate management according to vital signs, clinical evolution of SOFA score [17] and laboratory data. Recurrence of infection was defined as infection of a newly implanted device after appropriate management of the index CIED infection with isolation of the same microorganism.

Other data included: demographics (age and sex); date of hospital admission and discharge; ward of management; and risk factors classified as:

patient-related: comorbidity according to Charlson Comorbidity Index Score (CCIS) [18]; immunosuppression including neutropenia (absolute neutrophil count < 500/mm3); solid organ transplantation; haematopoietic stem cell transplantation; corticosteroid therapy at a dosage ≥ to prednisone 16 mg/day during at least 15 days; uncontrolled HIV infection (< 200 CD4/mm3); oral anticoagulant use; heparin bridging; aetiology of cardiac disease and indication for cardiac device implantation; and a previous history of CIED implantation/extraction.

procedure-related: characteristics of implanted device (type, site); procedure duration; haematoma; temporary pacing; device replacement/revision/upgrade; generator change; and type of antibiotic prophylaxis.

device-related: epicardial leads; abdominal pocket; two or more leads; and dual chamber device.

The CIED infections were classified according to the timing of implantation into episodes diagnosed before or after 90 days from implantation. Isolates were classified according to the criteria of Magiorakos et al. as multidrug-resistant or extensively drug-resistant [19]. For therapeutic management source control, follow-up BCs, empiric and definitive antibiotic therapy, and treatment duration were analysed. Source control was defined as removal of a generator plus leads. Time from diagnosis to source control was collected. Positive follow-up BCs were defined as those drawn within 2 – 7 days and positive for the same pathogen recovered from the index BCs in bacteraemic CIED infection episodes. Empiric antibiotic therapy was defined as antibiotic administration before the susceptibility report was available, and it was appropriate when at least one in vitro active antibiotic was administered. Treatment duration was defined as the time elapsed from the first to the last day of an appropriate antibiotic regimen.

2.4. Statistical analysis

Demographic and clinical characteristics of patients were compared across the three groups using $\chi 2$ test or Fisher's exact test, or one-way ANOVA with Scheffé post-hoc comparison, according to the distributional properties of variables. To assess differences in the therapeutic management and outcome, patients with GNB infections were compared with those with GPB infections using $\chi 2$ test or Fisher's exact test, and Mann-Whitney U test.

Multivariable, multinomial logistic regression was performed to identify factors associated with GPB and GNB infection, using non-infected patients as the reference group. An initial model was created including all variables associated with infection at bivariate analysis with $P < 0.100$ as predictor. The final model was obtained by backward trimming non-significant covariates until all variables retained in the model were associated with at least one of the outcome categories. From this model, predictive margins were calculated and graphically displayed to represent the model-adjusted estimated relationship between significant predictors and the infection outcome.

Mortality at 180 days from infection onset for patients with CIED infection and from CIED implantation for patients without CIED infection was investigated with survival analysis, by means of log-rank test and Cox multivariable regression, in which the type of bacterial infection was imposed as the risk factor of interest and the main known predictors of mortality were added as potential confounders. Patients were censored at death or 1-year follow-up, whichever occurred first.

In both multivariable analyses, robust standard errors were obtained to account for patients' grouping in centres. The analysis was carried out with SPSS 21.0 and Stata v.17.0, and P-values < 0.05 were considered statistically significant.

3. Results

Over the study period, 294 patients undergoing CIED implantation were enrolled. Of them, 71 had GNB-CIED infection, 74 had GPB-CIED infection and 149 patients did not develop infection. The yearly prevalence of Gram-negative CIED infections per 1000 CIED in the participating centres ranged between 1.2 – 1.6 during the study period (Supplementary Figure).

After matching, 58 patients were excluded and 236 participants were analysed: 59 with GNB-CIED infection, 59 with GPB-CIED infection and 118 without infection (Figure 2). The characteristics of the study population are shown in Table 1. Among the 236 analysed participants, 174 (73.7%) were male, with mean age of 69.1 ± 12.8 years and CCIS of 5.03 ± 2.34 (Table 1). Among participants with GNB-CIED infection, 41 (69.5%) were male, with a mean age of 71.5 years (SD ± 12.5) and CCIS of 5.69 ± 2.24. The most frequent underlying cardiac diseases requiring CIED implantation in patients developing GNB-CIED infection were bradyarrhythmia (28, 47.5%), heart failure (18, 30.5%) and primary prevention (12, 20.3%) (Table 1).

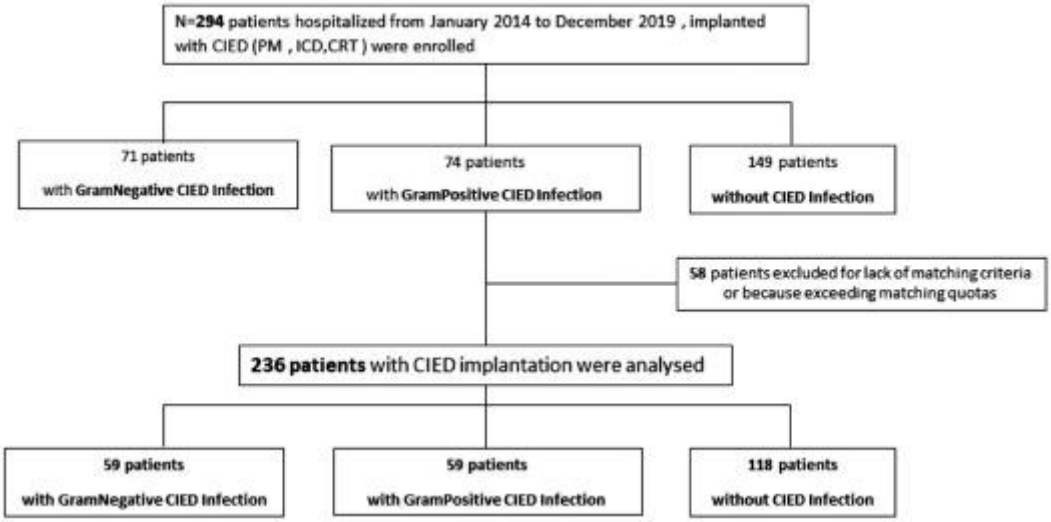

Figure 2. Study flow chart.

Table 1. Characteristics of the study population.

Empty Cell	**Total *n* = 236**	**Gram-negative *n* = 59**	**Gram-positive *n* = 59**	**Not infected *n* = 118**	***P*-value**	**Post-hoc comparisons**
Males	174 (73.7)	41 (69.5)	53 (89.8)	80 (67.8)	0.005	
Age at CIED implantation (mean ± SD)	69.1 ± 12.8	71.5 ± 12.5	69.3 ± 12.8	67.7 ± 12.0	0.149	-
Comorbidity						
Charlson Comorbidity Index (mean ± SD)	5.03 ± 2.34	5.69 ± 2.24	5.03 ± 2.34	4.29 ± 2.25	< 0.001	NI < GN
Shariff score (mean ± SD)	1.73 ± 1.17	2.00 ± 1.19	2.14 ± 1.25	1.40 ± 1.02	< 0.001	NI < GN, GP
Solid tumour	11 (4.6)	5 (8.4)	4 (6.7)	2 (1.6)	0.201	

Empty Cell	**Total *n* = 236**	**Gram-negative *n* = 59**	**Gram-positive *n* = 59**	**Not infected *n* = 118**	***P*-value**	**Post-hoc comparisons**
Obesity	19 (8.1)	11(18.6)	3 (5.1)	5 (4.2)	0.005	
Diabetes mellitus	58 (31)	22 (40)	16 (34)	20 (23.5)	0.105	
Underlying cardiac disease						
• Bradyarrhythmia	115 (48.7)	28 (47.5)	23 (39)	64 (54.2)	0.156	
• Primary prevention	71 (30.1)	12 (20.3)	22 (37.3)	37 (31.4)	0.122	
• Secondary prevention	18 (7.6)	6 (10.2)	6 (10.2)	6 (5.1)	0.339	
• Heart failure	65 (27.5)	18 (30.5)	23 (39)	24 (20.3)	0.027	
Ejection fraction						
• > 50%	104 (44.1)	26 (44.1)	21 (35.6)	57 (48.3)	0.275	
• 40% – 50%	26 (11)	9 (15.3)	7 (11.9)	10 (8.5)	0.386	
• < 40%	99 (41.9)	23 (39)	29 (49.2)	47 (39.8)	0.430	
Anticoagulation therapy						
• Warfarin	53 (22.5)	12 (20.3)	19 (32.2)	22 (18.6)	0.113	
• NOAC	33 (14)	5 (8.5)	12 (20.3)	16 (13.6)	0.175	
• Heparin	8 (3.4)	3 (5.1)	2 (3.4)	3 (2.5)	0.678	
Site of implantation (*n* = 232)					0.033	
• left subclavian vein	207 (89.2)	47 (79.7%)	53 (93.0%)	107 (92.2%)		

Empty Cell	**Total *n* = 236**	**Gram-negative *n* = 59**	**Gram-positive *n* = 59**	**Not infected *n* = 118**	***P*-value**	**Post-hoc comparisons**
• right subclavian vein	21 (9.1)	11 (18.6%)	4 (7.0%)	6 (5.2%)		
• subcutaneous vein	4 (1.7)	1 (1.7%)	0 (0)	3 (2.6%)		
Antibacterial envelope (*n* = 203)	20 (9.9)	7 (13.7%)	5 (10.2%)	8 (7.8%)	0.479	
Previous CIED implantation (*n* = 233)	67 (28.8)	19 (32.8)	22 (37.3)	26 (22.4)	0.089	
Previous device extraction	19 (29.7)	5 (27.8)	8 (38.1)	6 (24)	0.568	
Reason for previous device extraction						
• Infection	6 (31.5)	1 (20)	4 (50)	1 (16)	0.055	
• Malfunction	6 (31.5)	0 (0)	2 (25)	4 (66)	0.358	
• Other reason (vascular issue, tricuspid regurgitation)	7 (36.8)	4 (80)	2 (25)	1 (16)	0.088	
Infection episode 90 days prior implantation (*n* = 110)	16 (14.5)	10 (18.2)	6 (10.9)	/	0.279	
Type of infection						
• UTI	3 (18.7)	2 (20)	1 (16.6)			
• IAI	1 (6.25)	1 (10)	0 (0)			
• SSTI	1 (6.25)	0 (0)	1 (16.6)			
• LRTI	4 (25)	2 (20)	2 (33)			
• BSI	10 (62.5)	6 (60)	4 (66.6)			
Type of implanted CIED						

Empty Cell	**Total *n* = 236**	**Gram-negative *n* = 59**	**Gram-positive *n* = 59**	**Not infected *n* = 118**	***P*-value**	**Post-hoc comparisons**
PM-VVI	26 (11)	10 (16.9)	8 (13.6)	8 (6.8)	0.097	
PM-DDD	86 (36.4)	18 (30.5)	14 (23.7)	54 (45.8)	0.009	
CRT-P	7 (3)	2 (3.4)	1 (1.7)	4 (3.4)	0.802	
CRT-D	56 (23.7)	13 (22)	22 (37.3)	21 (17.8)	0.015	
ICD-VVI	25 (10.6)	5 (8.5)	7 (11.9)	13 (11)	0.818	
ICD-DDD	36 (15.3)	11 (18.6)	7 (11.9)	18 (15.3)	0.592	
ICD Subcutaneous	1 (0.4)	0	0	1 (0.8)	0.605	

Abbreviations: CIED, cardiac implantable electronic devices; CRT, cardiac resynchronisation therapy; CRT-D, cardiac resynchronisation therapy defibrillator; CRT-P, cardiac resynchronisation therapy pacemaker; ICD-DDD, dual chamber - implantable cardioverter-defibrillator; ICD-VVI, ventricular-pacing ventricular-sensing inhibited-response implantable cardioverter-defibrillator; IAI, intra-abdominal infection; ICD, implantable cardioverter-defibrillator; LRTI, lower respiratory tract infection; NOAC, new oral anticoagulants; PM, pacemaker; PM-DDD, dual chamber pacing pacemaker; PM-VVI, ventricular-pacing ventricular-sensing inhibited-response pacemaker; SD, standard deviation; SSTI, skin and soft tissue infection; UTI, urinary tract infection.

Infection characteristics and management are summarised in Table 2. Infectious endocarditis accounted for 61.9% of the CIED infection, with no difference in incidence between GPB or GNB aetiology. The remaining subjects had localised device pocket infection. The microorganisms responsible of CIED infection and their susceptibility profiles are reported in Supplementary Table 2. Coagulase-negative Staphylococcus spp. (32, 54.2%) and Staphylococcus aureus (23, 39.0%) were the most frequent GPB isolates. The most common isolate among GNB infections was Pseudomonas aeruginosa (17, 28.8%).

Table 2. Infection characteristics, management, and outcome.

Empty Cell	**Total *n* = 118**	**Gram-negative *n* = 59**	**Gram-positive *n* = 59**	***P*-value**
Type of infection and clinical presentation				

Empty Cell	**Total *n* = 118**	**Gram-negative *n* = 59**	**Gram-positive *n* = 59**	***P*-value**
Local device infection	45 (38.1)	23 (39.0)	22 (37.3)	0.757
Endocarditis	73 (61.9)	36 (61.0)	37 (62.7)	0.850
Septic embolism	6 (5.1)	3 (5.1)	3 (5.2)	0.983
• *Pulmonary*	4 (66.7)	1 (33)	3 (100)	0.083
• *Central nervous system*	1 (16.7)	1 (33)	0 (0)	0.195
• *Spleen*	1 (16.7)	1 (33)	0 (0)	0.195
SOFA (median, IQR)	1 (0 – 2)	1 (0 – 2)	1 (0 – 2)	0.168
Septic shock	3 (2.7)	0 (0)	3 (5.2)	0.087
Time from CIED implantation to infection diagnosis in months (median, IQR)	10.4 (2.1 – 27.3)	11.0 (1.5 – 31.3)	10.0 (4.0 – 25.0)	0.899
Days from last CIED procedure to infection diagnosis				0.025
• < *90 days*	31 (26.5)	21 (35.6)	10 (17.2)	
• > *90 days*	86 (73.5)	38 (64.4)	48 (82.8)	
Instrumental execution				
Echocardiography execution	114 (96.6)	57 (96.6)	57 (96.6)	1.000
Positive echocardiography (vegetations)	44 (37.2)	20 (33.9)	24 (40.7)	0.232
• *Transthoracic*	11 (25)	3 (15)	8 (33)	0.119
• *Transoesophageal*	33 (75)	17 (85)	16 (66)	0.944
Site of vegetations (both ETT/EET)				
• *Lead*	36 (31.6)	17 (29.8)	19 (33.3)	0.689
• *Valve*	3 (2.6)	/	3 (5.2)	0.244

Empty Cell	**Total *n* = 118**	**Gram-negative *n* = 59**	**Gram-positive *n* = 59**	***P*-value**
FDG PET/CT execution	23 (9.7)	14 (23.7)	9 (15.3)	0.245
Positive FDG PET/CT	18 (78.3)	12 (85.7)	6 (66.7)	0.280
Site of hypercaptation				
• *Lead*	9 (39)	7 (50)	2 (22)	0.083
• *Generator*	15 (65)	9 (64)	6 (66)	0.407
• *Skin and soft tissue*	3 (13)	3 (21)	0 (0)	0.079
Microbiological diagnosis				
Type of sample				
Swab of pocket	56 (47.5)	31 (52.5)	25 (42.4)	0.269
Generator	25 (21.2)	13 (22)	12 (20.3)	0.822
Leads	53 (44.9)	24 (40.7)	29 (49.2)	0.355
Blood	43 (36.4)	24 (40.7)	19 (32.2)	0.326
Follow-up blood cultures	26 (70.3)	16 (61.5)	10 (90.9)	0.074
• *Positive FU BCs*	10 (38.4)	8 (50)	2 (20)	0.134
Management				
Appropriate empiric antibiotic therapy	39 (57.4)	14 (28.6)	25 (46.3)	0.007
Duration of antibiotic therapy (days) (median IQR)	15 (8 – 25)	16 (9 – 22)	14 (8 – 32)	0.202
Device extraction	107 (90.7)	52 (88.1)	55 (93.2)	0.342
Type of extraction				
• TLE	94 (79.7)	45 (76.3)	49 (83.1)	0.369
• Surgical lead extraction	12 (10.2)	6 (10.2)	6 (10.2)	1

Empty Cell	**Total *n* = 118**	**Gram-negative *n* = 59**	**Gram-positive *n* = 59**	***P*-value**
Days from infection diagnosis to extraction (median, IQR)	9 (3 – 27)	15 (4 – 28)	9 (2 – 23)	0.338
Outcome				
Persistent infection/failure				
• 30 days	11 (9.3)	6 (10.2)	5 (8.5)	0.532
• 90 days	3 (2.6)	2 (3.4)	1 (1.7)	0.695
• 180 days	2 (1.7)	1 (1.7)	1 (1.7)	0.231
Recurrence				
• 30 days	1 (0.8)	1 (1.7)	0 (0)	0.532
• 90 days	1 (0.8)	1 (1.7)	0 (0)	0.695
• 180 days	0 (0)	0 (0)	0 (0)	0.231
All-cause mortality (*n* = 134)				
• 30 days	5(4.2)	3 (5.1)	2(3.4)	0.679 (F)
• 90 days	10 (8.5)	7(11.9)	3 (5.1)	0.398 (F)
• 180 days	12 (10.2)	9 (15.2)	3 (5.1)	0.145 (F)

Abbreviations: : CIED, cardiac implantable electronic devices; ETT, trans-thoracic echocardiography; EET, transoesophageal echocardiography; FDG PET/CT, fluorodeoxyglucose positron emission computed tomography; FU BCs, follow-up blood cultures; IQR, interquartile range; SOFA, sequential organ failure assessment score; TLE, transvenous lead extraction; (F), Fisher's exact test.

The diagnosis of CIED infection was made after a median time of 11 months (IQR = 1.5 – 31.3) from implantation in case of GNB aetiology and 10 months for GPB aetiology (IQR = 4 – 25) (P = 0.899).

Echocardiography was performed in 114 (96.6%) patients, yielding CIED endocarditis in 44 of them (37.2%) (Table 2); the rate of positive echocardiography was similar between GNB and GPB CIED infections (P = 0.232). Fluorodeoxyglucose positron emission computed tomography (FDG PET/CT) was performed in 23 patients, yielding CIED infection in 18 of them (78.3%). The FDG

PET positivity rate was higher among GNB than GPB infection but did not reach statistical significance (85.7% vs. 66.7%; P = 0.208).

Empiric antibiotic treatment was initiated in most patients (87.3%). As expected, appropriate empiric treatment was less frequent in GNB-CIED infection due to the uncommon aetiology (GNB 28.6% vs. GPB 46.3%; P = 0.007). The median full course of appropriate antibiotic therapy was 15 days (IQR 8 – 25), which was similar in both groups (Table 2). In a subgroup analysis of patients with a diagnosis of endocarditis, the median time of antibiotic therapy after device removal was 17 days (IQR 12 – 31).

Device extraction was performed in most patients (90.7%), mainly through transvenous lead extraction and without differences between GNB and GPB-CIED infection. Multinomial logistic regression (Table 3) showed that ventricular-pacing ventricular-sensing inhibited-response pacemakers (PM-VVI) were the only variable that was significantly associated with a higher risk of both GNB (relative risk reduction, RRR = 3.027, 95% CI 1.372 – 6.680; P = 0.006) and GPB infections (RRR = 3.032, 95% CI 1.058 – 8.691; P = 0.039). Among the other variables, CCIS (RRR = 1.211, 95% CI 1.045 – 1.404; P = 0.011), obesity (RRR = 5.122, 95% CI 1.536 – 17.085; P = 0.008) and right subclavian site of implantation (RRR = 5.014, 95% CI 1.665 – 15.101; P = 0.004) predicted a higher risk of GNB infection, while male sex (RRR = 3.617, 95% CI 1.576 – 8.301; P = 0.002), age at device implantation (RRR = 1.031, 95% CI 1.001 – 1.063; P = 0.041), CRT-D (RRR = 2.692, 95% CI 1.706 – 4.249; P < 0.001) and Shariff score (RRR = 1.682, 95% CI 1.234 – 2.293; P = 0.001) were associated with a higher risk of GPB infection. Figure 3 shows that patients without PM-VVI had a low risk of both GPB and GNB infections, and that the risk of both infections was higher in patients with PM-VVI at approximately the same magnitude. The risk of a GNB infection clearly increased with obesity and at higher values of CCIS. The opposite trend was estimated for Shariff score, whose higher values predicted a higher risk of GPB infection.

Table 3. Multinomial logistic regression of infection development (not infected = base outcome).

Gram-negative CIED infection risk	**RRR**	**95% CI**	***P*-value**
Males	0.869	0.425 – 1.776	0.700
Age at device implantation	1.015	0.987 – 1.044	0.303
Charlson Index Score	1.211	1.045 – 1.404	0.011
Obesity	5.122	1.536 – 17.085	0.008
PM-VVI	3.027	1.372 – 6.680	0.006
CRT-D	1.267	0.408 – 3.936	0.682
Right subclavian vein site of implantation	5.014	1.665 – 15.101	0.004
Shariff score	1.270	0.882 – 1.830	0.199
constant	0.315	0.170 – 0.585	< 0.001

Gram-negative CIED infection risk	**RRR**	**95% CI**	***P*-value**
Gram-positive CIED infection risk			
Males	3.617	1.576 – 8.301	0.002
Age at device implantation	1.031	1.001 – 1.063	0.041
Charlson Index Score	0.920	0.819 – 1.033	0.159
Obesity	0.987	0.301 – 3.240	0.983
PM-VVI	3.032	1.058 – 8.691	0.039
CRT-D	2.692	1.706 – 4.249	< 0.001
Right subclavian vein site of implantation	1.435	0.448 – 4.601	0.543
Shariff score	1.682	1.234 – 2.293	0.001
constant	0.112	0.050 – 0.250	< 0.001

Abbreviations: CIED, cardiac implantable electronic devices; CRT-D, cardiac resynchronisation therapy devices; RRR, relative risk ratio; PM-VVI, ventricular-pacing ventricular-sensing inhibited-response pacemaker.

RRR for constant was estimated with respect to all covariates at their reference value

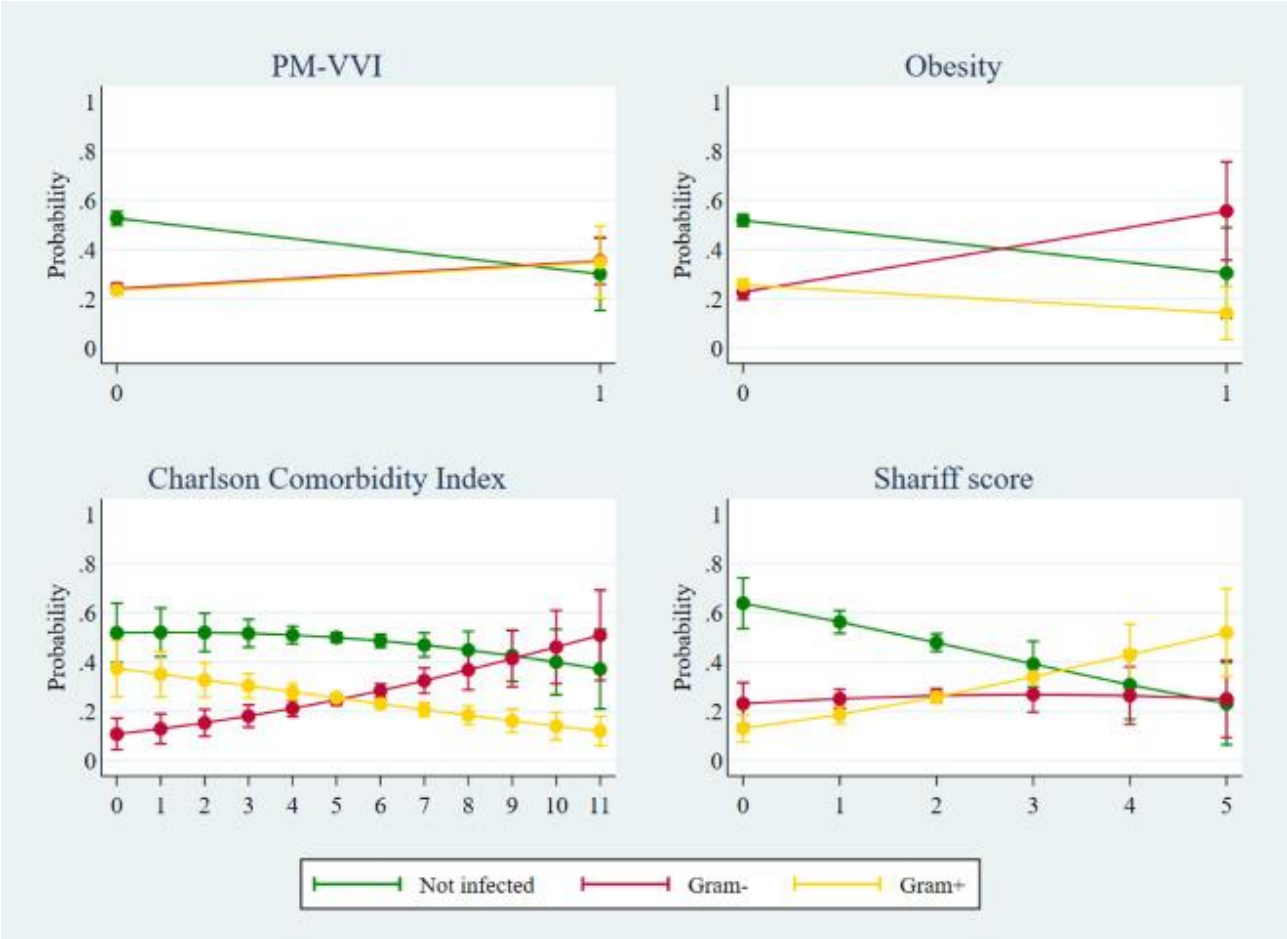

Figure 3: Predictive margins. Abbreviations: PM-VVI, ventricular-pacing ventricular-sensing inhibited-response pacemaker.

Regarding the outcomes, persistence of infection was observed in 11, three and two patients at 30, 90 and 180 days of follow-up. No between-group differences were observed. Recurrence was observed at 30 and 90 days of follow-up in two patients, both with GNB-CIED infection. All-cause mortality occurred only among infected patients in five (2.1%), 10 (4.2%) and 12 (5.1%) patients, at 30, 90 and 180 days, respectively. The all-cause mortality rates at any time of follow-up were higher for patients with GNB-CIED infection compared with those with GPB-CIED infection, although non-significantly (Table 2).

Since there were no mortality events in uninfected patients, regardless of matching, a 180-day survival analysis was performed in all patients with infection (n = 136). The Cox regression model provided the best fit to the data. The type of bacterial infection (GNB vs. GPB) was assumed as the main risk factor, with GNB-CIED showing a marginally significantly higher risk after the first 2 months of follow-up (Figure 4), which was confirmed at Cox regression analysis (HR = 1.842, 95% CI 0.958 – 3.541; P = 0.067), adjusted for endocarditis (HR = 3.983, 95% CI 1.320 – 12.014; P = 0.014) and device extraction (HR = 0.085, 95% CI 0.014 – 0.533; P = 0.008). Age at diagnosis, time from implantation to infection (transformed as natural logarithm) and CCIS were included in

the initial model and then removed because they were non-significant (all had P > 0.300) (Table 4).

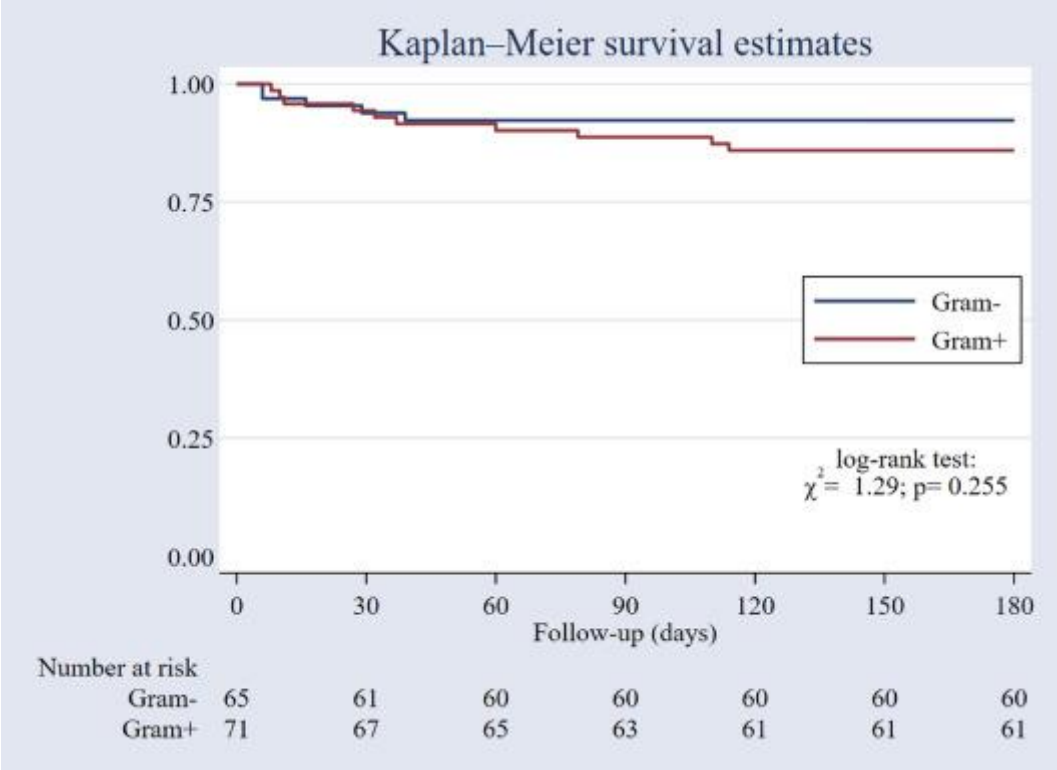

Figure 4: All-cause mortality at 180-days follow-up between patients with Gram-negative and Gram-positive cardiac implantable electronic devices infection.

Table 4. Cox multivariable regression of mortality at 180 days (patients with GNB- or GPB-CIED infection, *n* = 136).

	Initial model			**Final model**		
Empty Cell	**HR**	**95% CI**	***P*-value**	**HR**	**95% CI**	***P*-value**
Gram-negative infection	1.828	0.977 – 3.423	0.059	1.842	0.958 – 3.541	0.067
Age at diagnosis of infection (years)	0.974	0.927 – 1.023	0.293			
Time from device implantation to infection (log years)	1.188	0.811 – 1.739	0.377			
Charlson Comorbidity Index Score	1.191	0.936 – 1.516	0.155			
Endocarditis	2.975	0.898 – 9.850	0.074	3.983	1.320 – 12.014	0.014

	Initial model			Final model		
Empty Cell	**HR**	**95% CI**	***P*-value**	**HR**	**95% CI**	***P*-value**
Device extraction	0.076	0.009 – 0.668	0.020	0.085	0.014 – 0.533	0.008

Abbreviations: HR, hazard ratio; CIED, cardiac implantable electronic devices; GNB, Gram-negative bacteria; GPB, Gram-positive bacteria.

4. Discussion

It is believed that this is the largest series of patients with GNB-CIED infections, collected from 17 centres across Europe over a 5-year period, providing a comparison with GPB-CIED infections and uninfected patients. There was no significant difference between the GNB and GPB groups in terms of clinical presentation, diagnostic and therapeutic issues. The FDG PET/CT seemed to be very useful in diagnosing GNB-CIED endocarditis and GPB-CIED endocarditis (85.7% vs. 66.7%). Risk factors associated with the development of GNB-CIED infection were different from those associated with GPB-CIED infection. Finally, survival probabilities were lower among patients with GNB-CIED infection than those with GPB-CIED infection.

Gram-negative bacteria are relatively infrequent but important pathogens responsible for CIED infections. Knowledge about this type of infection is limited to case reports and case series [12,[20], [21], [22]]. The largest experience reported to date is that of Esquer Garrigos et al., who analysed a single-centre cohort of 31 GNB-CIED infections collected over a 23-year period [12]. The low prevalence of this kind of infections is confirmed by the current study and others in the literature [6].

Regarding clinical presentation of GNB-CIED infection, it was more frequently associated with pocket infection compared with GPB-CIED infection in previous studies [12]. Although these data do not appear to be confirmed in the current study, there are limited studies of this kind of infection and further investigation is required to clarify this aspect.

The FDG PET/CT is a diagnostic tool in several infectious diseases such as prosthetic joint infections, vascular prosthesis infection, vertebral osteomyelitis, septic thrombophlebitis or complicated bloodstream infections with septic metastases [23], [24], [25]. Specifically for cardiac infection, FDG PET/CT may provide advantages over echocardiography in patients with foreign bodies [26], [27], [28]. The FDG PET/CT was introduced in the 2015 ESC Criteria for the diagnosis of possible endocarditis associated with prosthetic valves [15] and for CIED infections [16,26,29]. According to the current data, the yield of FDG PET/CT seems higher for GNB- than for GPB-CIED infection diagnosis. It is worth mentioning that Chesdachai et al. [22] have recently reported 126 patients with CIED and concomitant GNB bacteraemia, finding that 3% of patients had definite CIED infection. Among imaging tools used for CIED diagnosis, echocardiography was the most frequently used. Conversely, FDG PET/CT was performed in two patients. It can be speculated that the rate of GN-CIED infection in this cohort and in general practice may have been underestimated due to the low diagnostic efficiency of traditional assays.

The Shariff score is known to be an indicator of the risk of GPB-CIED infection development in the months following device implantation [30], [31], [32]. The Shariff score confirmed its predictive

value in the current cohort of patients with GPB-CIED infection; however, its efficacy was not confirmed in the group of patients with GNB-CIED infection.

Two peri-procedural factors appeared to be related to GNB-CIED infection in the current study. The first was implantation in the right subclavian vein. This could have been due to a relatively longer duration of manoeuvres in the right side, which is usually not the first choice for implantation. Due to the retrospective nature of this study, the duration of the procedures was not accurately collected in this population; therefore, this currently remains a speculative observation. The second risk factor for GNB-CIED infection was implantation of PM-VVI. Compared with more complicated procedures, such as biventricular PM/ICD, PM-VVI implantation appears to be related to GNB-CIED infection. A possible explanation of this finding is that patients implanted with PM-VVI are usually older than those implanted with other CIED and with more comorbidities [33]. Consistent with the other findings, this observation could explain the increased risk of GNB-CIED infection in this subgroup of patients; however, further studies are needed to investigate and confirm this finding.

Implantation of cardiac resynchronisation therapy devices (CRT-D) beyond PM-VVI appears to be related to GPB-CIED infection. These findings were already reported from previous studies as risk factors for infection development [4,34], confirming the reliability of the data from the current cohort.

This study found GNB-CIED infection to be associated, with marginal statistical significance, with a higher all-cause mortality rate at 6 months, confirming prior literature data on mortality rates ranging between 2% – 10% [12,20]. At multivariable analysis, infective endocarditis was the only independent risk factor for mortality. Conversely, removal of the device was protective. Recurrence of CIED infection was observed in two patients, both with GNB aetiology. A possible explanation of this finding could be the less frequently appropriate empiric treatment administered in GNB-CIED infection. However, due to the limited number of cases, further investigations are needed to confirm this observation.

Finally, the current patients with a diagnosis of CIED endocarditis received a median 17 days of antibiotic treatment after device removal. The data may support indications from the last EHRA consensus document [16] suggesting that 2 weeks of therapy may be sufficient after device removal in patients with documented negative follow-up blood culture, absence of echocardiographic signs of valve vegetation or pulmonary abscesses and reporting early clinical improvement.

This study had several limitations. Although this is the largest cohort of patients with GNB-CIED infections currently available in the literature, the limited sample size and number of events may have affected statistical power. However, the comparison of patients with GPB-CIED infections and without CIED infections could have improved the relevance of the results identifying differences between infection aetiologies and the risk factors for GN infection in all patients needing CIED implantation. The retrospective design of the study could have reduced the accuracy and completeness of data collection. However, it was attempted to reduce this limitation by thorough data quality control, creating queries to identify and correct missing and incongruent data. Finally, heterogeneity in local management may have existed - this was unavoidable. Due to the scarcity of available data on GNB-CIED infections, multicentric studies are necessary. Statistical tools were applied with the aim of reducing the effect of heterogeneity on estimates.

In conclusion, despite these limitations, there are some novel key messages from this study. Patients with a high number of comorbidities who undergo right subclavian vein implantation may be

patients at high risk of developing a GNB-CIED infection. The higher mortality associated with GNB-CIED infection makes it necessary to suspect and make an early diagnosis of this type of infection. The FDG PET/CT seems to be useful in this framework; however, further studies are needed to confirm this hypothesis.

References

1. Choi AJ, Thomas SS, Singh JP. Cardiac resynchronization therapy and implantable cardioverter defibrillator therapy in advanced heart failure. Heart Fail Clin 2016;12(3):423–36.

2. Rundström H, Kennergren C, Andersson R, Alestig K, Hogevik H. Pacemaker endocarditis during 18 years in Göteborg. Scand J Infect Dis 2004;36(9):674–9.

3. Johansen JB, Jørgensen OD, Møller M, Arnsbo P, Mortensen PT, Nielsen JC. Infection after pacemaker implantation: infection rates and risk factors associated with infection in a population-based cohort study of 46299 consecutive patients. Eur Heart J 2011;32(8):991–8.

4. Sohail MR, Henrikson CA, Braid-Forbes MJ, Forbes KF, Lerner DJ. Mortality and cost associated with cardiovascular implantable electronic device infections. Arch Intern Med 2011;171(20):1821–8.

5. Hussein AA, Baghdy Y, Wazni OM, Brunner MP, Kabbach G, Shao M, et al. Microbiology of cardiac implantable electronic device infections. JACC Clin Electrophysiol 2016;2(4):498–505.

6. Bongiorni MG, Tascini C, Tagliaferri E, Di Cori A, Soldati E, Leonildi A, et al. Microbiology of cardiac implantable electronic device infections. Europace 2012;14(9):1334–9.

7. Diekema DJ, Beekmann SE, Chapin KC, Morel KA, Munson E, Doern GV. Epidemiology and outcome of nosocomial and community-onset bloodstream infection. J Clin Microbiol 2003;41(8):3655–60.

8. Gaynes R, Edwards JR, System NNIS. Overview of nosocomial infections caused by gram-negative bacilli. Clin Infect Dis 2005;41(6):848–54.

9. Sohail MR, Uslan DZ, Khan AH, Friedman PA, Hayes DL, Wilson WR, et al. Risk factor analysis of permanent pacemaker infection. Clin Infect Dis 2007;45(2):166–73.

10. Bloom H, Heeke B, Leon A, Mera F, Delurgio D, Beshai J, et al. Renal insufficiency and the risk of infection from pacemaker or defibrillator surgery. Pacing Clin Electrophysiol 2006;29(2):142–5.

11. Lekkerkerker JC, van Nieuwkoop C, Trines SA, van der Bom JG, Bernards A, van de Velde ET, et al. Risk factors and time delay associated with cardiac device infections: Leiden device registry. Heart 2009;95(9):715–20.

12. Esquer Garrigos Z, George MP, Vijayvargiya P, Tan EM, Farid S, Abu Saleh OM, et al. Clinical presentation, management, and outcomes of cardiovascular implantable electronic device infections due to gram-negative versus gram-positive bacteria. Mayo Clin Proc 2019;94(7):1268–77.

13. Klug D, Lacroix D, Savoye C, Goullard L, Grandmougin D, Hennequin JL, et al. Systemic infection related to endocarditis on pacemaker leads: clinical presentation and management. Circulation 1997;95(8):2098–107.

14. Harris PA, Taylor R, Minor BL, Elliott V, Fernandez M, O'Neal L, et al. The REDCap consortium: Building an international community of software platform partners. J Biomed Inform 2019;95:103208.

15. Habib G, Lancellotti P, Antunes MJ, Bongiorni MG, Casalta JP, Del Zotti F, et al. 2015 ESC Guidelines for the management of infective endocarditis: The Task Force for the Management of Infective Endocarditis of the European Society of Cardiology (ESC). Endorsed by: European Association for Cardio-Thoracic Surgery (EACTS), the European Association of Nuclear Medicine (EANM). Eur Heart J 2015;36(44):3075–128.

16. Blomström-Lundqvist C, Traykov V, Erba PA, Burri H, Nielsen JC, Bongiorni MG, et al. European Heart Rhythm Association (EHRA) international consensus document on how to prevent, diagnose, and treat cardiac implantable electronic device infections-endorsed by the Heart Rhythm Society (HRS), the Asia Pacific Heart Rhythm Society (APHRS), the Latin American Heart Rhythm Society (LAHRS), International Society for Cardiovascular Infectious Diseases (ISCVID) and the European Society of Clinical Microbiology and Infectious Diseases (ESCMID) in collaboration with the European Association for Cardio-Thoracic Surgery (EACTS). Eur J Cardiothorac Surg 2020;57(1):e1–e31.

17. Singer M, Deutschman CS, Seymour CW, Shankar-Hari M, Annane D, Bauer M, et al. The Third International Consensus Definitions for Sepsis and Septic Shock (Sepsis-3). JAMA 2016;315(8):801–10.

18. Charlson ME, Pompei P, Ales KL, MacKenzie CR. A new method of classifying prognostic comorbidity in longitudinal studies: development and validation. J Chronic Dis 1987;40(5):373–83.

19. Magiorakos AP, Srinivasan A, Carey RB, Carmeli Y, Falagas ME, Giske CG, et al. Multidrug-resistant, extensively drugresistant and pandrug-resistant bacteria: an international expert proposal for interim standard definitions for acquired resistance. Clin Microbiol Infect 2012;18:268–81.

20. Falcone M, Tiseo G, Durante-Mangoni E, Ravasio V, Barbaro F, Ursi MP, et al. Risk Factors and Outcomes of Endocarditis Due to Non-HACEK Gram-Negative Bacilli: Data from the Prospective Multicenter Italian Endocarditis Study Cohort. Antimicrob Agents Chemother 2018;62(4).

21. Fogelson B, Livesay J, Rohrer M, Edwards M, Hirsh JB. cardiac implantable electronic device related endocarditis. IDCases 2022;28:e01499.

22. Chesdachai S, Baddour LM, Sohail MR, Palraj BR, Madhavan M, Tabaja H, et al. Risk of cardiovascular implantable electronic device infection in patients presenting with gram-negative bacteremia. Open Forum Infect Dis 2022;9(9):ofac444.

23. Bleeker-Rovers CP, Vos FJ, Wanten GJ, van der Meer JW, Corstens FH, Kullberg BJ, et al. 18F-FDG PET in detecting metastatic infectious disease. J Nucl Med 2005;46(12):2014–19.

24. Vos FJ, Bleeker-Rovers CP, Sturm PD, Krabbe PF, van Dijk AP, Cuijpers ML, et al. 18F-FDG PET/CT for detection of metastatic infection in gram-positive bacteremia. J Nucl Med 2010;51(8):1234–40.

25. Yamanaka K, Matsueda T, Miyahara S, Nomura Y, Sakamoto T, Morimoto N, et al. Surgical strategy for aortic prosthetic graft infection with (18)F-fluorodeoxyglucose positron emission tomography/computed tomography. Gen Thorac Cardiovasc Surg 2016;64(9):549–51.

26. Graziosi M, Nanni C, Lorenzini M, Diemberger I, Bonfiglioli R, Pasquale F, et al. Role of [1] 8F-FDG PET/CT in the diagnosis of infective endocarditis in patients with an implanted cardiac device: a prospective study. Eur J Nucl Med Mol Imaging 2014;41(8):1617–23.

27. Ghanem-Zoubi N. FDG PET/CT in Cardiac Infection: Does It Matter? A Narrative Review. Infect Dis Ther 2022.

28. Saby L, Laas O, Habib G, Cammilleri S, Mancini J, Tessonnier L, et al. Positron emission tomography/computed tomography for diagnosis of prosthetic valve endocarditis: increased valvular 18F-fluorodeoxyglucose uptake as a novel major criterion. J Am Coll Cardiol 2013;61(23):2374– 2382.

29. Jerónimo A, Olmos C, Vilacosta I, Ortega-Candil A, Rodríguez-Rey C, Pérez– Castejón MJ, et al. Accuracy of18F-FDG PET/CT in patients with the suspicion of cardiac implantable electronic device infections. J Nucl Cardiol 2022;29(2):594–608.

30. Shariff N, Eby E, Adelstein E, Jain S, Shalaby A, Saba S, et al. Health and economic outcomes associated with use of an antimicrobial envelope as a standard of care for cardiac implantable electronic device implantation. J Cardiovasc Electrophysiol 2015;26(7):783–9.

31. Diemberger I, Migliore F, Biffi M, Cipriani A, Bertaglia E, Lorenzetti S, et al. The "Subtle" connection between development of cardiac implantable electrical device infection and survival after complete system removal: An observational prospective multicenter study. Int J Cardiol 2018;250:146– 149.

32. Balla C, Brieda A, Righetto A, Vitali F, Malagù M, Cultrera R, et al. Predictors of infection after "de novo" cardiac electronic device implantation. Eur J Intern Med 2020;77:73–8.

33. Greenspon AJ, Patel JD, Lau E, Ochoa JA, Frisch DR, Ho RT, et al. Trends in permanent pacemaker implantation in the United States from 1993 to 2009: increasing complexity of patients and procedures. J Am Coll Cardiol 2012;60(16):1540–5.

34. Olsen T, Jørgensen OD, Nielsen JC, Thøgersen AM, Philbert BT, Johansen JB. Incidence of device-related infection in 97 750 patients: clinical data from the complete Danish device-cohort (1982-2018). Eur Heart J 2019;40(23):1862– 1869.

Chapter 4

This chapter provides a concise overview of the papers authored or co-authored by the candidate during their PhD period, presented in reverse chronological order from the most recent to the earliest.

1. “Role of BIOmarkers as predictors of effectiveness of the lesion during Pulmonary Vein Isolation procedures: a prospective observational cohort study – The BIO-PVI Study. (pending publication)

2. Correlation between Bipolar and Unipolar Electrograms with a High-Density Grid catheter and MRI-Identified Scar in Patients Undergoing VT Ablation (pending publication)

Davide Fabbricatore, Michael Waight, Anthony Li, Magdi Saba.

3. Validation of an automated artificial intelligence system for 12-lead ECG interpretation.

Herman R, Demolder A, Vavrik B, Martonak M, Boza V, Kresnakova V, Iring A, Palus T, Bahyl J, Nelis O, Beles M, Fabbricatore D, Perl L, Bartunek J, Hatala R.

J Electrocardiol. 2024 Jan-Feb;82:147-154. doi: 10.1016/j.jelectrocard.2023.12.009. Epub 2023 Dec 23.

PMID: 38154405

4. Coronary Microvascular Dysfunction in Patients With Heart Failure: Characterization of Patterns in HFrEF Versus HFpEF.

Paolisso P, Gallinoro E, Belmonte M, Bertolone DT, Bermpeis K, De Colle C, Shumkova M, Leone A, Caglioni S, Esposito G, Fabbricatore D, Moya A, Delrue L, Penicka M, De Bruyne B, Barbato E, Bartunek J, Vanderheyden M.

Circ Heart Fail. 2024 Jan;17(1):e010805. doi: 10.1161/CIRCHEARTFAILURE.123.010805. Epub 2023 Dec 18.

PMID: 38108151

5. High efficiency single-catheter workflow for radiofrequency atrial fibrillation ablation in the QDOT catheter era.

Valeriano C, Buytaert D, Fabbricatore D, De Schouwer K, Addeo L, De Braekeleer L, Geelen P, De Potter T.

J Interv Card Electrophysiol. 2023 Dec 14. doi: 10.1007/s10840-023-01709-3. Online ahead of print.

PMID: 38092999

6. Association of Mild-to-Moderate Aortic Regurgitation With Outcomes in Heart Failure With Preserved Ejection Fraction.

De Colle C, Paolisso P, Gallinoro E, Bertolone DT, Mileva N, Fabbricatore D, Valeriano C, Herman R, Beles M, De Oliveira EK, Mancusi C, Heggermont W, Collet C, Vanderheyden M, De Luca N, Van Camp G, Barbato E, Bartunek J, Penicka M.

Mayo Clin Proc. 2023 Oct;98(10):1469-1481. doi: 10.1016/j.mayocp.2023.06.017.

PMID: 37793725

7. Innovative Device-Based Strategies for Managing Acute Decompensated Heart Failure.

Bertolone DT, Paolisso P, Gallinoro E, Belmonte M, Bermpeis K, De Colle C, Esposito G, Caglioni S, Fabbricatore D, Leone A, Valeriano C, Shumkova M, Storozhenko T, Viscusi MM, Botti G, Verstreken S, Morisco C, Barbato E, Bartunek J, Vanderheyden M.

Curr Probl Cardiol. 2023 Dec;48(12):102023. doi: 10.1016/j.cpcardiol.2023.102023. Epub 2023 Aug 7.

PMID: 37553060

8. Pre-cath Laboratory Planning for Left Atrial Appendage Occlusion - Optional or Essential?

Devgun J, De Potter T, Fabbricatore D, Wang DD.

Card Electrophysiol Clin. 2023 Jun;15(2):141-150. doi: 10.1016/j.ccep.2023.01.009.

PMID: 37076226

9. Diagnostic and Prognostic Role of Cardiac Magnetic Resonance in MINOCA: Systematic Review and Meta-Analysis.

Mileva N, Paolisso P, Gallinoro E, Fabbricatore D, Munhoz D, Bergamaschi L, Belmonte M, Panayotov P, Pizzi C, Barbato E, Penicka M, Andreini D, Vassilev D.

JACC Cardiovasc Imaging. 2023 Mar;16(3):376-389. doi: 10.1016/j.jcmg.2022.12.029.

PMID: 36889851

10. Ambulatory pulmonary vein isolation workflow using the Perclose ProglideTM suture-mediated vascular closure device: the PRO-PVI study.

Fabbricatore D, Buytaert D, Valeriano C, Mileva N, Paolisso P, Nagumo S, Munhoz D, Collet C, De Potter T.

Europace. 2023 Apr 15;25(4):1361-1368. doi: 10.1093/europace/euad022.

PMID: 36793243

11. Risk factors for Gram-negative bacterial infection of cardiovascular implantable electronic devices: multicentre observational study (CarDINe Study).

Pascale R, Toschi A, Aslan AT, Massaro G, Maccaro A, Fabbricatore D, Dell'Aquila A, Ripa M, Işık ME, Kızmaz YU, Iacopino S, Camici M, Perna F, Akinosoglou K, Karruli A, Papadimitriou-Olivgeris M, Kayaaslan B, Bilir YA, Evren Özcan E, Turan OE, Işık MC, Pérez-Rodríguez MT,

Yagüe BL, Quirós AM, Yılmaz M, Petersdorf S, De Potter T, Durante-Mangoni E, Akova M, Curnis A, Gibertoni D, Diemberger I, Scudeller L, Viale P, Giannella M; CarDINe Study Group.

Int J Antimicrob Agents. 2023 Mar;61(3):106734. doi: 10.1016/j.ijantimicag.2023.106734. Epub 2023 Jan 21.

12. Safety of Right and Left Ventricular Endomyocardial Biopsy in Heart Transplantation and Cardiomyopathy Patients.

Bermpeis K, Esposito G, Gallinoro E, Paolisso P, Bertolone DT, Fabbricatore D, Mileva N, Munhoz D, Buckley J, Wyffels E, Sonck J, Collet C, Barbato E, De Bruyne B, Bartunek J, Vanderheyden M.

JACC Heart Fail. 2022 Dec;10(12):963-973. doi: 10.1016/j.jchf.2022.08.005. Epub 2022 Oct 12.

PMID: 36456070

13. Deferral of Coronary Revascularization in Patients With Reduced Ejection Fraction Based on Physiological Assessment: Impact on Long-Term Survival.

Gallinoro E, Paolisso P, Di Gioia G, Bermpeis K, Fernandez-Peregrina E, Candreva A, Esposito G, Fabbricatore D, Bertolone DT, Bartunek J, Vanderheyden M, Wyffels E, Sonck J, Collet C, De Bruyne B, Barbato E.

J Am Heart Assoc. 2022 Oct 4;11(19):e026656. doi: 10.1161/JAHA.122.026656. Epub 2022 Sep 21.

PMID: 36129045

14. Absolute coronary flow and microvascular resistance reserve in patients with severe aortic stenosis.

Paolisso P, Gallinoro E, Vanderheyden M, Esposito G, Bertolone DT, Belmonte M, Mileva N, Bermpeis K, De Colle C, Fabbricatore D, Candreva A, Munhoz D, Degrieck I, Casselman F, Penicka M, Collet C, Sonck J, Mangiacapra F, de Bruyne B, Barbato E.

Heart. 2022 Dec 13;109(1):47-54. doi: 10.1136/heartjnl-2022-321348.

PMID: 35977812

15. Arrhythmic Storm Due to ICD Atrial Lead Malfunction.

Fabbricatore D, Heggermont W, Buytaert D, Van Bockstal K, De Potter T.

JACC Case Rep. 2022 Apr 6;4(7):438-442. doi: 10.1016/j.jaccas.2021.12.013. eCollection 2022 Apr 6.

PMID: 35693896

16. Pre-cath Laboratory Planning for Left Atrial Appendage Occlusion - Optional or Essential?

Devgun J, De Potter T, Fabbricatore D, Wang DD.

Interv Cardiol Clin. 2022 Apr;11(2):143-152. doi: 10.1016/j.iccl.2021.11.003. Epub 2022 Mar 10.

PMID: 35361459

17. Prospective evaluation of the learning curve and diagnostic accuracy for Pre-TAVI cardiac computed tomography analysis by cardiologists in training: The LEARN-CT study.

Paolisso P, Gallinoro E, Andreini D, Mileva N, Esposito G, Bermpeis K, Bertolone DT, Munhoz D, Belmonte M, Fabbricatore D, Sonck J, Collet C, Penicka M, De Bruyne B, Vanderheyden M, Barbato E.

J Cardiovasc Comput Tomogr. 2022 Sep-Oct;16(5):404-411. doi: 10.1016/j.jcct.2022.03.002. Epub 2022 Mar 12.

PMID: 35337770

18. Contemporary Management of Stable Coronary Artery Disease.

Bertolone DT, Gallinoro E, Esposito G, Paolisso P, Bermpeis K, De Colle C, Fabbricatore D, Mileva N, Valeriano C, Munhoz D, Belmonte M, Vanderheyden M, Bartunek J, Sonck J, Wyffels E, Collet C, Mancusi C, Morisco C, De Luca N, De Bruyne B, Barbato E.

High Blood Press Cardiovasc Prev. 2022 May;29(3):207-219. doi: 10.1007/s40292-021-00497-z. Epub 2022 Feb 11.

PMID: 35147890

19. Performance of non-invasive myocardial work to predict the first hospitalization for de novo heart failure with preserved ejection fraction.

Paolisso P, Gallinoro E, Mileva N, Moya A, Fabbricatore D, Esposito G, De Colle C, Beles M, Spapen J, Heggermont W, Collet C, Van Camp G, Vanderheyden M, Barbato E, Bartunek J, Penicka M.

ESC Heart Fail. 2022 Feb;9(1):373-384. doi: 10.1002/ehf2.13740. Epub 2021 Nov 24.

PMID: 34821061

20. Microvascular Dysfunction in Patients With Type II Diabetes Mellitus: Invasive Assessment of Absolute Coronary Blood Flow and Microvascular Resistance Reserve.

Gallinoro E, Paolisso P, Candreva A, Bermpeis K, Fabbricatore D, Esposito G, Bertolone D, Fernandez Peregrina E, Munhoz D, Mileva N, Penicka M, Bartunek J, Vanderheyden M, Wyffels E, Sonck J, Collet C, De Bruyne B, Barbato E.

Front Cardiovasc Med. 2021 Oct 19;8:765071. doi: 10.3389/fcvm.2021.765071. eCollection 2021.

PMID: 34738020

21. Ultralow temperature cryoablation using near-critical nitrogen for cavotricuspid isthmus-ablation, first-in-human results.

Klaver MN, De Potter TJR, Iliodromitis K, Babkin A, Cabrita D, Fabbricatore D, Boersma LVA.

J Cardiovasc Electrophysiol. 2021 Aug;32(8):2025-2032. doi: 10.1111/jce.15142. Epub 2021 Jul 9.

PMID: 34196991

22. Could Home Monitoring parameters provide information about the impact of the pandemic period on CIED patients? A comparison between 2019 and 2020.

Bontempi L, Aboelhassan M, Cerini M, Salghetti F, Fabbricatore D, Maiolo V, Freda L, Giacopelli D, Curnis A.

J Cardiovasc Med (Hagerstown). 2021 Jul 1;22(7):606-608. doi: 10.2459/JCM.0000000000001193.

PMID: 34076608

23. Cardiogenic Shock due to COVID-19-Related Myocarditis in a 19-Year-Old Autistic Patient.

Pascariello G, Cimino G, Calvi E, Bernardi N, Grigolato M, Garyfallidis P, Fabbricatore D, Pezzola E, Lombardi CM, Metra M, Vizzardi E.

J Med Cases. 2020 Jul;11(7):207-210. doi: 10.14740/jmc3517. Epub 2020 Jun 29.

PMID: 33984092

24. Transvenous lead extraction in patients with persistent left superior vena cava.

Curnis A, Aboelhassan M, Cerini M, Salghetti F, Fabbricatore D, Maiolo V, Arabia G, Giacopelli D, Fouad DA, Bontempi L.

J Cardiovasc Electrophysiol. 2021 May;32(5):1407-1410. doi: 10.1111/jce.15021. Epub 2021 Apr 16.

PMID: 33783892

25. Use of a novel implantable cardioverter-defibrillator multisensor algorithm for heart failure monitoring in a COVID-19 patient: A case report.

Bontempi L, Cerini M, Salghetti F, Fabbricatore D, Nozza C, Campari M, Valsecchi S, Curnis A.

Clin Case Rep. 2021 Jan 28;9(3):1178-1182. doi: 10.1002/ccr3.3721. eCollection 2021 Mar.

PMID: 33768806

26. Clinical Characteristics and Outcomes of Patients with COVID-19 Infection: The Results of the SARS-RAS Study of the Italian Society of Hypertension.

Mancusi C, Grassi G, Borghi C, Ferri C, Muiesan ML, Volpe M, Iaccarino G; SARS-RAS Investigator Group.

High Blood Press Cardiovasc Prev. 2021 Jan;28(1):5-11. doi: 10.1007/s40292-020-00429-3. Epub 2021 Jan 20.

PMID: 33471297

27. Leadless pacemaker: State of the art and incoming developments to broaden indications.

Curnis A, Salghetti F, Cerini M, Fabbricatore D, Ghizzoni G, Arrigoni L, Generati G, Arabia G, Maiolo V, Aboelhassan M, Bontempi L.

Pacing Clin Electrophysiol. 2020 Dec;43(12):1428-1437. doi: 10.1111/pace.14097. Epub 2020 Nov 29.

PMID: 33089526